

AD\_\_\_\_\_

Award Number: W81XWH-12-1-0600

TITLE: A Combination Therapy of JO-1 and Chemotherapy in Ovarian Cancer Models

PRINCIPAL INVESTIGATOR: Andre Lieber

CONTRACTING ORGANIZATION: University of Washington  
Seattle, WA 98195

REPORT DATE: December 2014

TYPE OF REPORT: Final

PREPARED FOR: U.S. Army Medical Research and Materiel Command  
Fort Detrick, Maryland 21702-5012

DISTRIBUTION STATEMENT: Approved for Public Release;  
Distribution Unlimited

The views, opinions and/or findings contained in this report are those of the author(s) and should not be construed as an official Department of the Army position, policy or decision unless so designated by other documentation.

REPORT DOCUMENTATION PAGE				Form Approved OMB No. 0704-0188	
Public reporting burden for this collection of information is estimated to average 1 hour per response, including the time for reviewing instructions, searching existing data sources, gathering and maintaining the data needed, and completing and reviewing this collection of information. Send comments regarding this burden estimate or any other aspect of this collection of information, including suggestions for reducing this burden to Department of Defense, Washington Headquarters Services, Directorate for Information Operations and Reports (0704-0188), 1215 Jefferson Davis Highway, Suite 1204, Arlington, VA 22202-4302. Respondents should be aware that notwithstanding any other provision of law, no person shall be subject to any penalty for failing to comply with a collection of information if it does not display a currently valid OMB control number. PLEASE DO NOT RETURN YOUR FORM TO THE ABOVE ADDRESS.					
1. REPORT DATE December 2014		2. REPORT TYPE Final		3. DATES COVERED 30 Sep 2012 - 29 Sep 2014	
4. TITLE AND SUBTITLE A Combination Therapy of JO-1 and Chemotherapy in Ovarian Cancer Models				5a. CONTRACT NUMBER	
				5b. GRANT NUMBER W81XWH-12-1-0600	
				5c. PROGRAM ELEMENT NUMBER	
6. AUTHOR(S) Andre Lieber  E-Mail: lieber00@u.washington.edu				5d. PROJECT NUMBER	
				5e. TASK NUMBER	
				5f. WORK UNIT NUMBER	
7. PERFORMING ORGANIZATION NAME(S) AND ADDRESS(ES)  University of Washington Seattle, WA 98195				8. PERFORMING ORGANIZATION REPORT NUMBER	
9. SPONSORING / MONITORING AGENCY NAME(S) AND ADDRESS(ES)  U.S. Army Medical Research and Materiel Command Fort Detrick, Maryland 21702-5012				10. SPONSOR/MONITOR'S ACRONYM(S)	
				11. SPONSOR/MONITOR'S REPORT NUMBER(S)	
12. DISTRIBUTION / AVAILABILITY STATEMENT  Approved for Public Release; Distribution Unlimited					
13. SUPPLEMENTARY NOTES					
14. ABSTRACT <ul style="list-style-type: none"> <li>- A manufacturing protocol for JO-1 with and without His-tag at large scale has been established.</li> <li>- There were no adverse effects after intravenous injection of JO-1 in DSG2 transgenic mice.</li> <li>- JO-1 has favorable pharmacokinetics parameters.</li> <li>- The effect of JO-1 on normal tissues is minimal because DSG2 is trapped in epithelial junctions in normal tissues and not accessible to intravenously injected JO-1.</li> <li>- JO-1 enhances Doxil chemotherapy in xenograft models of ovarian cancer and in mouse models with syngeneic tumors.</li> <li>- JO-1 continues to be effective after multiple treatment cycles even in the presence of detectable antibodies.</li> <li>- JO-1 facilitates pre-existing anti-tumor T-cell responses.</li> <li>- An affinity-enhanced version of JO-1 (called JO-4) was produced.</li> <li>- JO-4 co-therapy allows for reduction of effective Doxil dose in a xenograft model of ovarian cancer.</li> <li>- JO-4 increases the therapeutic effect of Doxil on lymphogenic metastases.</li> <li>- Combined treatment with JO-4 and Doxil is safe in non-human primates</li> </ul>					
15. SUBJECT TERMS adenovirus, desmoglein 2, epithelial junctions, ovarian cancer, doxorubicine, liposomal, clinical trial					
16. SECURITY CLASSIFICATION OF:			17. LIMITATION OF ABSTRACT	18. NUMBER OF PAGES	19a. NAME OF RESPONSIBLE PERSON
a. REPORT	b. ABSTRACT	c. THIS PAGE			USAMRMC
Unclassified	Unclassified	Unclassified	Unclassified	104	19b. TELEPHONE NUMBER (include area code)

## Table of Contents

	<u>Page</u>
<b>1. Introduction.....</b>	<b>1</b>
<b>2. Keywords.....</b>	<b>1</b>
<b>3. Overall Project Summary.....</b>	<b>1</b>
<b>4. Key Research Accomplishments.....</b>	<b>1</b>
<b>5. Conclusion.....</b>	<b>7</b>
<b>6. Publications, Abstracts, and Presentations.....</b>	<b>9</b>
<b>7. Inventions, Patents and Licenses.....</b>	<b>10</b>
<b>8. Reportable Outcomes.....</b>	<b>9</b>
<b>9. Other Achievements.....</b>	<b>8</b>
<b>10. References.....</b>	<b>12</b>
<b>11. Appendices.....</b>	<b>14</b>

## 1. INTRODUCTION

The goal of this Translational Pilot Award proposal is to create the basis for a clinical trial for our recombinant junction opener in combination with chemotherapy in patients with progressive ovarian cancer. Toward this goal we will *i)* perform detailed safety studies in DSG2 transgenic mice, *ii)* study the effect of JO-1 in ovarian cancer models, and *iii)* test combinations of JO-1 with major chemotherapy drugs.

## 2. KEYWORDS

adenovirus, desmoglein 2, epithelial junctions, ovarian cancer, doxorubicine, liposomal, clinical trial

## 3. ACCOMPLISHMENTS

### What were the major goals of the project?

1. Generate preclinical safety and pharmacokinetic data for intravenous JO-1 injection in DSG2 transgenic mice. *i)* GLP manufacturing of JO-1, *ii)* Toxicology studies in DSG2 transgenic mice
2. Study biodistribution of JO-1 and JO-1 monotherapy in a syngeneic ovarian cancer model. *i)* Investigate JO-1 biodistribution and in vivo kinetics of JO-1 accumulation in ID8-DSG2 tumors. *ii)* Test whether JO-1 can facilitate existing immune responses in DSG2 transgenic mice bearing ID8-DSG2 tumors.
3. Test combinations of JO-1 with major chemotherapy drugs. *i)* Test the co-therapies in xenograft tumor models. *ii)* Test lower doses of chemotherapeutics. *iii)* Test the co-therapies in immunocompetent DSG2 mice with ID8-DSG2 cells.

### What was accomplished under these goals?

**Task 1.1: GLP manufacturing of JO-1.** A manufacturing protocol for JO-1 at large scale has been established. The generation and characterization of a master *E.coli* cell bank has been completed. A pilot lot of JO-1 for toxicity and efficacy studies (Tasks 1.2., 2 and 3) and has been produced under GLP conditions by the FHCRC Biologics Manufacturing Core Laboratory. This lot met cGMP quality control standards defined by the FDA in a pre-IND meeting. We demonstrated that after 9 months of storage at -80°C, JO-1 did not lose activity (test ongoing). After consultation with the FDA, the following potency assays of the cGMP product were established: DSG2 binding assay: The clinical function of the product is to bind to DSG2 triggering intracellular signaling. Binding of JO-1 to DSG2 was measured by ELISA. Rabbit polyclonal antibodies against DSG2 were used for capture followed by recombinant DSG2, the cGMP JO-1 lot/reference sample, mouse mAb against the Ad3 fiber knob, and anti-mouse IgG-HRP. PEG permeability assay: A total of  $5 \times 10^5$  T84 cells were seeded on 12 mm transwell inserts and cultured for 20 days until the transepithelial electrical resistance (TEER) remained constant, i.e. tight junctions have formed. The cells were exposed to JO-1 for 15 min at room temperature. 1  $\mu$ Ci of [ $^{14}$ C] polyethylene glycol-4000 (MW: 4,000Da) was added to the inner chamber. Medium aliquots were harvested from the inner and outer chambers and measured by a scintillation counter. Permeability was calculated as described elsewhere (19). JO-1 preparations are considered to be functionally potent if they increase PEG permeability >3-fold within 30 min. More recently, we have also established and optimized a fermentation and purification protocol for an affinity-enhanced JO-1 version that lacks the 6xHis tag. We plan perform our clinical trial with this product.

**Task 1.2: Toxicology studies in DSG2 transgenic mice.** Because JO-1 does not bind to mouse cells (15), we generated human DSG2 (hDSG2) transgenic mice that expressed human DSG2 at a level and in a pattern seen in humans (15). Furthermore, we established syngeneic tumor cell lines (ID8, TC1, MMC (11)) with ectopic hDSG2 expression at levels seen in human tumors (1). In epithelial tissues of hDSG2 transgenic mice, hDSG2 is specifically localized to junctions (15). Furthermore, JO-1 triggers junction opening in hDSG2-expressing epithelial mouse tumor cells indicating that hDSG2 interacts with mouse signaling and cytoskeletal proteins thus overriding a potential function of mouse DSG2 in maintenance of junctions in transgenic mice. (Notably, there are no mouse DSG2-specific antibodies available.)

There were no adverse effects or critical abnormalities found in hematologic and serum chemistry parameters or histopathological studies of tissues after intravenous injection of JO-1 (2 to 10 mg/kg) into hDSG2 transgenic mice (with or without pre-existing anti JO-1 antibodies. We observed a mild lymphocytopenia and intestinal inflammation that subsided by day 3 after injection. We speculate that the favorable safety profile of JO-1 is due to the fact that hDSG2 in tissues other than the tumor and a subset of epithelial cells in the intestine/colon is not accessible to intravenously injected JO-1.

**Task 2.1: JO-1 biodistribution in DSG2 transgenic mice.** The hDSG2 transgenic mouse model was also used to obtain biodistribution and pharmacokinetics data for JO-1. These studies showed a serum half-life of 6 hours and hDSG2-dependent accumulation of JO-1 in epithelial cells of the small intestine and colon (1). We

also found hDSG2 dependent binding of JO-1 to peripheral blood lymphocytes and hDSG2-independent uptake by liver, spleen and lymph node macrophages.

**Task 2.2.: Kinetics of JO-1 and QD-labeled IgG accumulation in tumors.** Instead of using quantum dot labeled IgG we studied the effect of JO-1 mediated junction opening in epithelial tumors and tissues of hDSG2 transgenic mice by measuring the uptake of PEG-modified gold nanoparticles (AuNP) with defined diameters of 35 and 120nm (Fig.1A). Notably, the average diameter of most encapsulated chemotherapy drugs is 100nm. We produced Au-NP and confirmed their size by dynamic light scattering. The biodistribution of AuNPs in tissue samples was quantified by inductively coupled plasma mass spectrometry (ICP-MS) at the Environmental Health Laboratory at the University of Washington (Seattle, WA). This method is more sensitive than the imaging of QD-labeled proteins. So far, we have measured the Au-NP amount in tumors (Figs.1B and C). Studies on other tissues are ongoing. In tumors, we found that the accumulation of 120nm Au-NP is at least 3 orders of magnitude less efficient than the accumulation of 35nm particles. The amount of 120nm AuNP per gram tumor tissue increased >10-fold when mice were pre-injected with JO-1. We are currently analyzing the AuNP penetration on tumor sections using transmission electron microscopy. We expect that the studies with AuNP will further corroborate that epithelial junctions represent a barrier to intratumoral accumulation of larger drugs ) and that this can in part be overcome by JO-1.

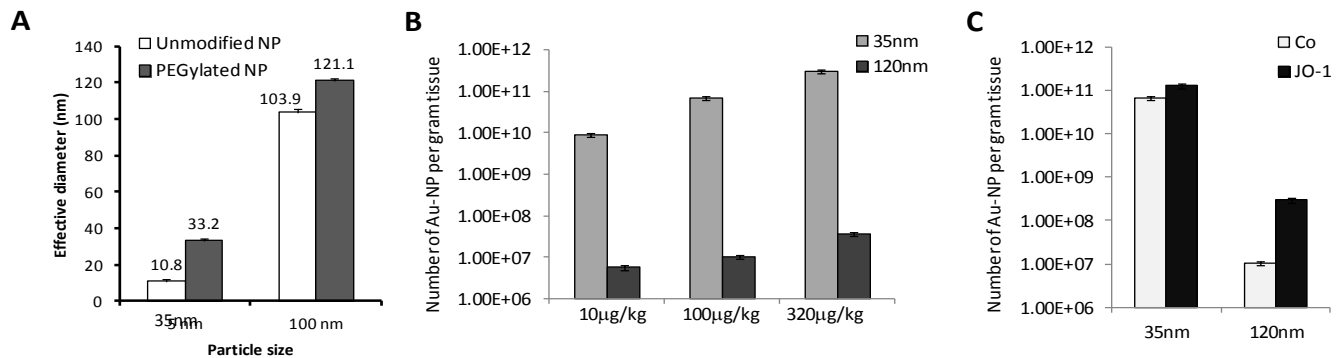


**Figure 1. Accumulation of differently sized PEGylated gold-nanoparticles (Au-NP) in tumors. A)** Particle sizing of gold nanoparticles by dynamic light scattering (DLS) before and after modification with mPEG<sub>5000</sub>-SH. Data are presented as mean ± standard deviation, N = 6. 5 nm were from Ted Pella, Redding, CA. 100nm particles were from Nanopartz, Inc., Loveland, CO. **B)** hDSG2 transgenic mice with syngeneic mammary fat pad MMC-hDSG2 tumors (800-1000mm<sup>3</sup>) were intravenously injected with Au-NP at different doses. Six hours later blood was flushed from the circulation and tumors were harvested. Shown are the numbers of Au-NP particles per gram tumor. N=3. **C)** hDSG2 transgenic mice with established tumors were intravenously injected with PBS (Co) or JO-1 (2mg/kg) followed by an intravenous injection of Au-P at a dose of 100ug/kg. Tumors were harvested 6 hours later. N=3

**Task 2.3. Study mechanism of junction opening.** Binding of JO-1 to DSG2 triggers shedding of the DSG2 extracellular domain and activation of pathways that are reminiscent of an epithelial to mesenchymal transition (EMT), including the phosphorylation of MAP kinases and the downregulation of junction proteins (2, 15, 17). Both mechanisms result in transient opening of epithelial junctions. Furthermore, we have recently shown that during Ad3 replication, viral protein complexes (PtDd) similar to JO-1 are released from infected cells, open the junctions between neighboring cells and thus allow *de novo* produced virus to spread in epithelial tumors (10). A similar positive feed-forward mechanism should work for JO-1 penetration in tumors. To better understand DSG2 shedding, we analyzed phospho kinase activation upon JO-1 incubation using proteome arrays. The data show that JO-1 activates MAPK pathways (Fig.2A). As a potential downstream effect of MAPK activation we studied MMP-mediated DSG2 shedding of the DSG2 extracellular domain (ECD). We found that JO-1 increases shedding and that this process is decreased by the membrane metalloprotease (MMP) inhibitor TAPI-0 (Fig.2B). We therefore conclude that JO-1 activates MAPK signaling, which in turn activates MMPs and subsequent cleavage of the DSG2 ECD.

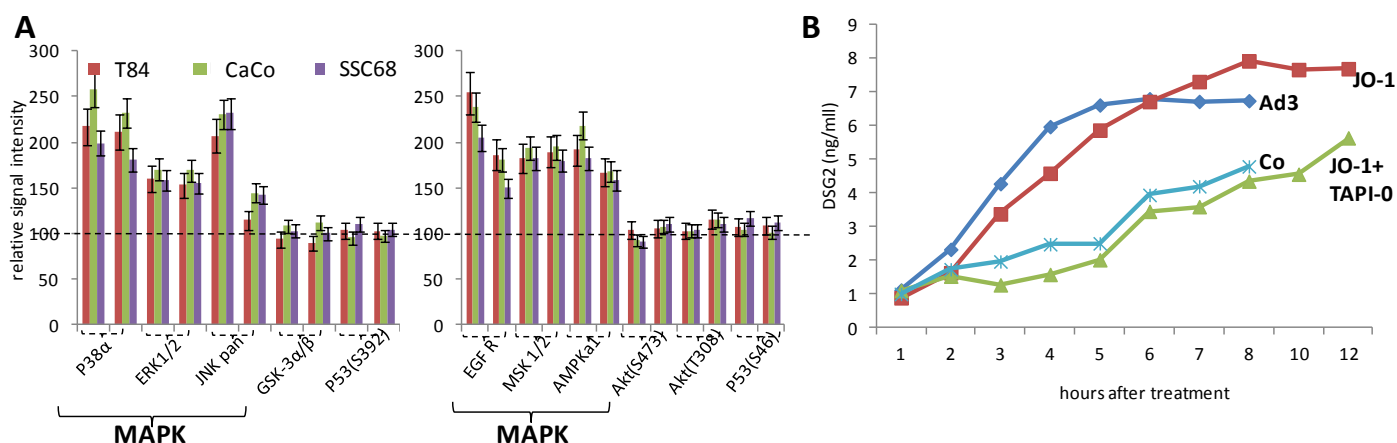


**Figure 2. JO-1 triggered intracellular signaling. A)** Human phosphokinase array. Human colon cancer epithelial cells (T84, CaCo, SSC68) were incubated with JO-1 (1ug/ml) or with JO-1 dialysis for 4 hours at 37°C. Cell lysates were subjected to hybridization on filters containing antibodies that are able to detect relative levels of phosphorylation of 43 different kinase phosphorylation sites (Proteome Profiler antibody array from R&D Systems). Signals were quantitated and plotted taking the signals from dialysis buffer as 100%. N=3 **B)** Shedding of DSG2 ECD into culture supernatant, Human epithelial cancer (A549) cells were incubated with Ad3 virus (300pfu/cell), JO-1 (1ug/ml), or JO-1 plus MMP inhibitor (50uM TAPI-0). Supernatant samples were collected at the indicated time points and DSG2 ECD concentrations were measured by ELISA.

### Task 2.3. Test whether JO-1 can facilitate existing immune responses in DSG2 transgenic mice bearing syngeneic tumors.

Using an immunocompetent hDSG2-transgenic mouse tumor model, we showed that JO-1 injection reduced the number of intratumoral Tregs, which in turn allowed pre-existing anti-tumor CD8 T-cells to control tumor growth (Fig.2). We used hDSG2 transgenic mice and syngeneic TC1 cells that expressed human DSG2. TC1 cells express HPV E6 and E7 and trigger E7-specific T-cells in C57Bl/6 mice. However, these tumor-specific T-cells are unable to control tumor growth and 100% of tumor-bearing animals reached the study endpoint by day 20. Two injections of JO-1 into tumor-bearing mice at days 6 and 14 resulted in complete tumor regression in 60% of mice (Fig.2A). This effect was due to an increased number of E7-specific T-cells (Fig.2B) and could be blocked by systemic depletion of CD8 cells. Importantly, we also found in flow cytometry analyses of tumor-infiltrating leukocytes that the number of Tregs (CD25+/FoxP3+) was about 6-fold less in JO-1 treated animal tumors compared to PBS injected animals (Fig.2C).

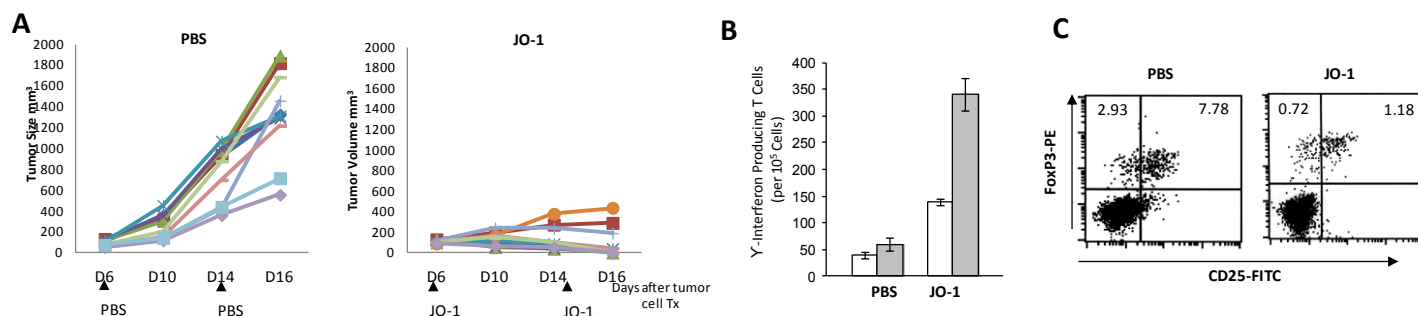


**Figure 2. JO-1 facilitates anti-tumor T-cell responses. A)** hDSG2 transgenic mice with established subcutaneous syngeneic TC1-hDSG2 tumors were intravenously injected with PBS or JO-1 (2mg/kg) at days 6 and 14 after tumor cell transplantation and tumor volumes were measured. Each line represents an individual animal. N=10. **B)** Analysis of frequencies of IFN $\gamma$ -producing E7 specific T-cells in the spleen 4 days after PBS or JO-1 injection. Shown are the frequencies of IFN $\gamma$  producing T-cells specific to the HPV16 E749-57 carrying the H-2Db restricted peptide (RAHYNIVTF) (grey bars) or an unrelated control peptide (white bars). N=3 animals per group. The differences in the JO-1 group are significant ( $p<0.05$ ). **C)** Analysis of intratumoral (FoxP3+) Tregs 4 days after PBS or JO-1 injection. Shown are representative flow cytometry data.

We then studied whether JO-1 monotherapy in combination with Treg depletion has a therapeutic effect in a syngeneic DSG2 transgenic mouse model (Fig.3). The study was performed in rat neu/ human DSG2 transgenic mouse model with syngeneic MMC-DSG2 tumors. It showed that Treg depletion by low-dose cyclophosphamide significantly enhanced JO-1 therapy.

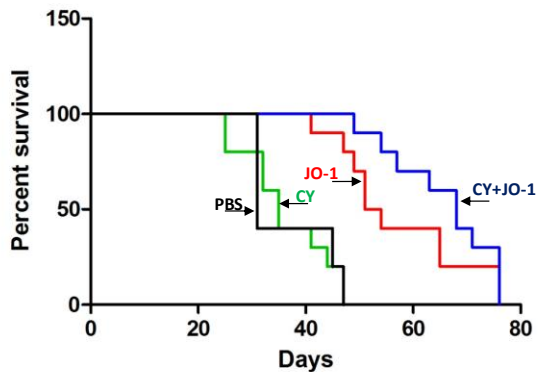


**Figure 3.** hDSG2 transgenic mice with mammary fat pad-localized MMC-hDSG2 tumors were injected weekly with JO-1 (2mg/kg) and/or cyclophosphamide (CY) 75mg/kg). This CY dose is not cytotoxic to tumor cells *in vivo* however efficiently depletes Tregs (14). Shown is animal survival. N=10

### Task 3.1. Test the co-therapies in xenograft tumor models.

We evaluated PEGylated liposomal doxorubicin (PLD/Doxil<sup>TM</sup>) in xenograft models with ovarian cancer cells (ovc316). Ovc316 cells are derived from a patient and closely model the heterogeneity and plasticity seen in tumors *in situ* (12). Mice with pre-established ovc316 tumors were intravenously injected with JO-1, followed one hour later by an intravenous injection of Doxil. The ability of JO-1 to open up intercellular junctions increased the penetration and amount of Doxil in tumors. Immunofluorescence analysis of tumor sections from JO-1/PLD treated animals showed PLD distributed over a greater distance from blood vessels (Fig.4A). More than 10-fold higher amounts of Doxil per gram tumor tissues were measured by ELISA when Doxil was combined with JO-1. The enhancing effect of JO-1 on Doxil therapy was shown in an orthotopic model with intraperitoneal ovc316 tumors (Fig.4B). While all mice treated with Doxil alone died by day 80 after tumor inoculation, the combination of JO-1 and Doxil resulted in long-term survival (>160 days) of ~80% of animals.

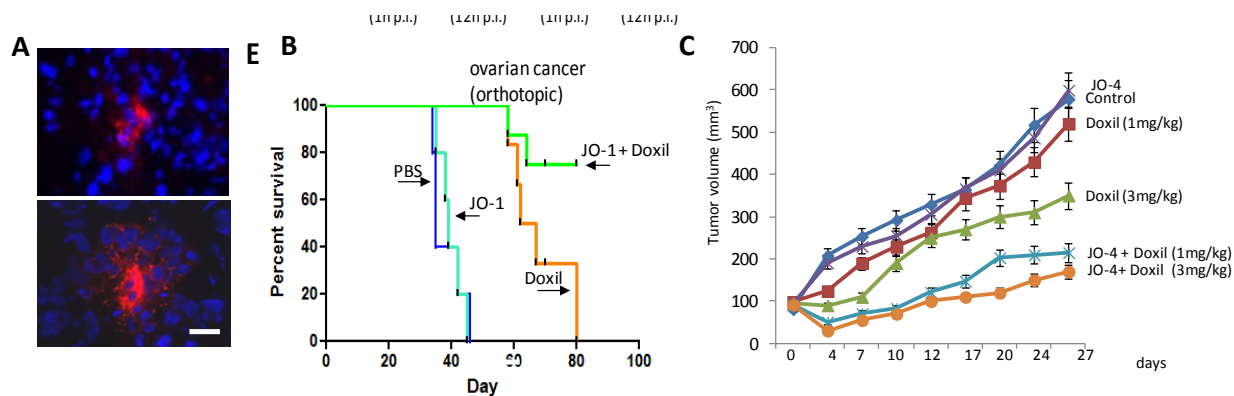


**Figure 4. JO-1 enhances PLD therapy in an ovarian cancer xenograft models. A)** Better penetration and accumulation of Doxil in tumors. Immunofluorescence analysis of tumor sections 2 hours after intravenous Doxil or JO-1/PLD injection. Doxil is stained red using antibodies that specifically bind to PEG in nanoparticles. The scale bars are 20  $\mu$ m. **B)** Survival study/intraperitoneal model. CB17-SCID/beige mice with intraperitoneal tumors derived from primary human ovarian cancer cells ovc316. Treatment was started at day 25 after tumor cell implantation and repeated weekly. Mice were injected intravenously with 2 mg/kg JO-1 or PBS, followed by an intravenous injection of Doxil (1 mg/kg) or PBS one hour later. Onset of ascites was taken as the endpoint in therapy studies. Shown is the survival of animals in a Kaplan Meier graph. n=10.  $p < 0.001$  for Doxil vs JO-1 + Doxil. **C)** Efficacy study in mammary fat pad tumor model using primary ovarian cancer (ovc316) cells. Treatment was started when tumors reached a volume of 100 mm<sup>3</sup>. Mice were injected intravenously with Doxil (1 mg/kg or 3mg/kg) alone or in combination with 2 mg/kg JO-4. Treatment was repeated weekly. N=10.



**Task 3.2. Test lower doses of chemotherapeutics.** In the majority of cancer patients, the dose of Doxil has to be reduced from 50mg/m<sup>2</sup> to less than 30mg/m<sup>2</sup> due to toxicity. One of our clinical objectives is to test whether a junction opener can salvage the therapeutic effect of a lower dose of Doxil. We performed a study in mice with xenograft tumors derived from primary ovarian cancer ovc316 cells. In this study we used an affinity-enhanced version of JO-1 called JO-4 (18) (Richter, M et al submitted (see Appendix). Mice with pre-established, mammary fat pad-localized ovc316 tumors were weekly intravenously injected with JO-4 at a dose of 2mg/kg, followed one hour later by an intravenous injection of Doxil at a therapeutic dose of 3 mg/kg or a subtherapeutic "low" dose of 1 mg/kg (Fig.4C). This study shows higher anti-tumor efficacy of JO-4 plus "low"-dose Doxil (1 mg/kg), compared to "high" dose Doxil alone (3 mg/kg), indicating that it is possible to lower the effective dose of Doxil when combined with JO-4. Note that

**Task 3.3. test whether JO-4 acts increases the therapeutic effect of Doxil on lymphogenic metastases.** In order to metastasize, epithelial cancer cells acquire mesenchymal features through EMT. There is strong support that, once metastatic cells homed to other tissues, they regain epithelial features, including epithelial junctions (6, 9). To corroborate this, we employed a model of epithelial breast cancer that forms spontaneous metastases. The model is based on MDA-MB-231-luc-D3H2LN cells which allow for *in vivo* imaging of tumor growth based on luciferase expression. If the primary tumor is not removed, it invades the peritoneum and forms metastases in mesenteric lymph nodes that are clearly distinguishable from the primary tumor by *in vivo* imaging (Fig. 5A). Immunofluorescence analysis of sections showed membrane-localized DSG2 in the primary tumor and metastatic lesions (Fig. 5B). The amount of DSG2, as assessed by Western blot analysis, was comparable in the primary and secondary tumors (Fig. 5C). To address the question whether JO-4 can also act on metastases, we performed a therapy study in the model with invasive tumors that form lymphogenic metastases in mesenteric lymph nodes. Treatment (PBS, Doxil (1mg/kg) alone, JO-4 (2 mg/kg) + Doxil) was started when metastases were clearly detectable by *in vivo* luciferase imaging. Luminescence signals for the primary and secondary lesions were recorded separately the day before treatment and at day 5 after treatment and expressed as a ratio to show tumor progression (Fig. 5D,E). In most untreated mice, both primary tumor and metastases grew. Regression of the metastatic lesions was observed in one out of five Doxil-treated mice. Tumors in the remaining four animals did not respond to Doxil. In contrast, all primary tumors and three out of four metastatic lesions shrank when mice were treated with the combination of JO-4 and Doxil. This suggests that in this model, JO-4 can open epithelial junctions in metastases.

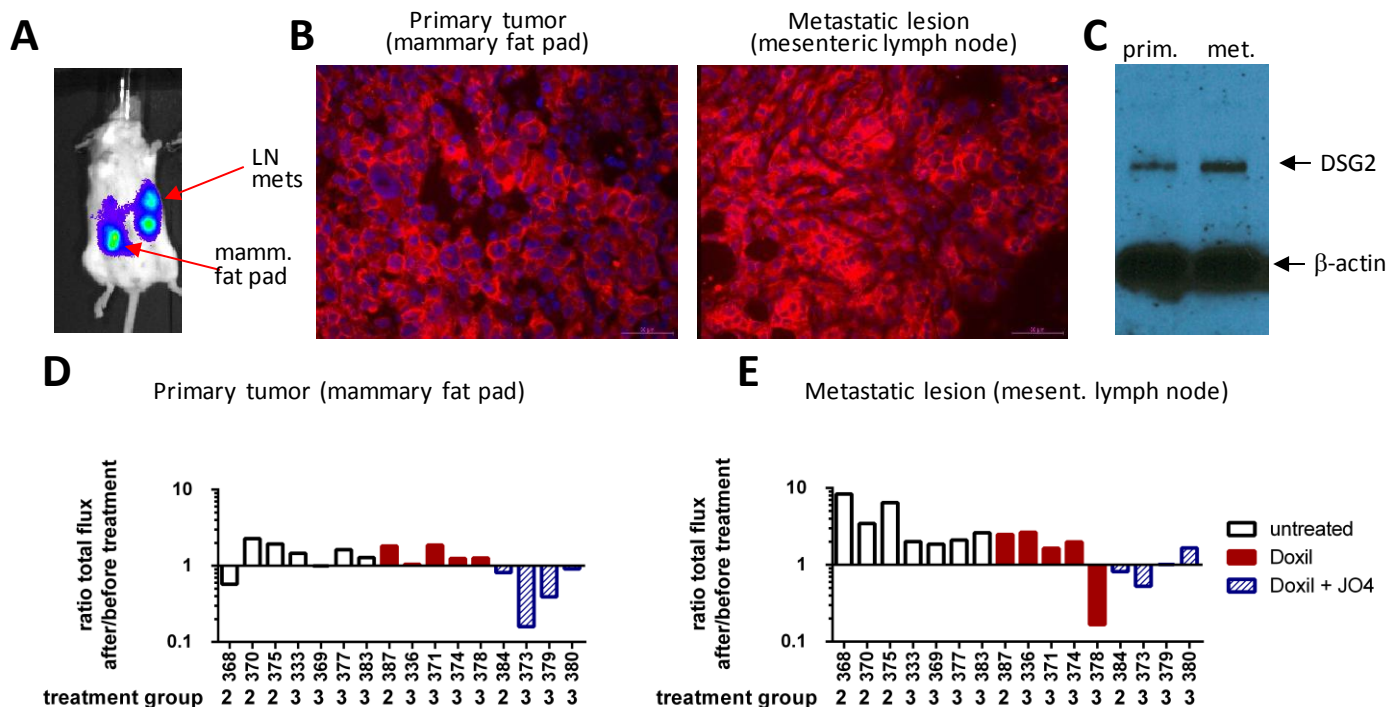


**Figure 5 Studies in the spontaneous metastasis model based on MDA-MB-231-luc-D3H2LN cells. A)** *in vivo* luciferase imaging of a representative animal. The primary tumor in the mammary fat pad forms metastasis in regional lymph nodes (LN) e.g. pancreatic and mesenteric lymph nodes. **B)** DSG2 immunofluorescence analysis of sections from



the primary tumor and mesenteric lymph node metastases. DSG2 appears in red in cell membranes. Nuclei are stained in blue. **C)** Western blot analysis of primary tumor and metastases with DSG2 antibodies.  $\beta$ -actin is used as a loading control. A representative animal is shown. **D, E)** Comparison of *in vivo* luciferase signal in the primary tumor (e) and metastasis (f) one day before and 5 days after treatment with Doxil or JO-4 + Doxil. Shown is the total flux of the primary tumor or metastasis ROI after treatment divided by the ROI before treatment. Shown are averages of imaging sequences of five images each.

### Task 3.4. Test the co-therapies in immunocompetent DSG2 transgenic mice with syngeneic tumors

**Tumor-specificity of JO-1 action:** Using hDSG2 transgenic mice, we demonstrated that JO-1 predominantly accumulates in tumors (1). A number of factors could account for this finding, including: *i)* overexpression of hDSG2 by tumor cells, *ii)* better accessibility of hDSG2 on tumor cells, due to a lack of strict cell polarization compared to hDSG2-expressing normal epithelial cells, and *iii)* a high degree of vascularization and vascular permeability in tumors. Because of its preferential binding to and action on epithelial junctions of tumors, JO-1 appears to create a “sink” for therapeutic drugs in tumors, which decreases the levels and exposure of these drugs in normal tissues. A low level of hDSG2-specific JO-1 accumulation was also detected in the small and large intestine, specifically in intestinal epithelial cells that underwent cell division which potentially allowed for access to DSG2 (15).

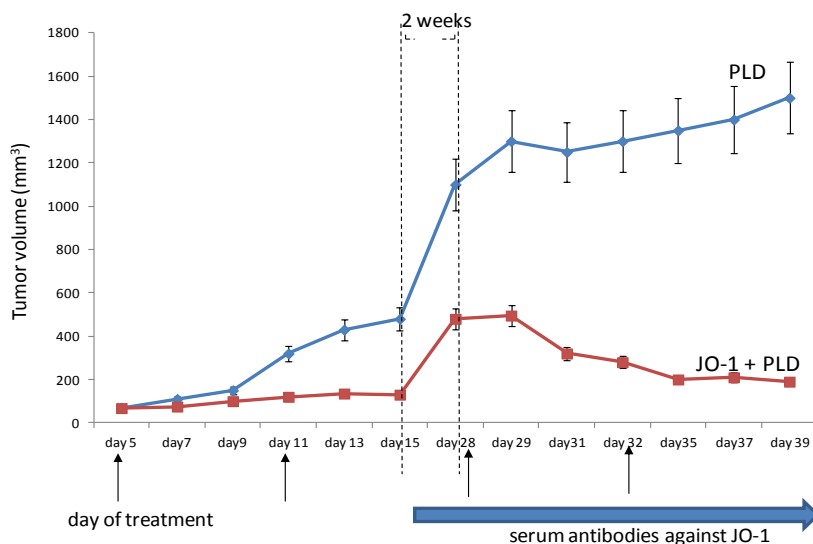


**Figure 6. JO-1/PLD(Doxil) therapy in immunocompetent hDSG2 transgenic mice.**

A total of  $4 \times 10^6$  MMC-hDSG2 cells were injected into the mammary fat pad of hDSG2 transgenic mice. When tumors reached a volume of  $\sim 80 \text{ mm}^3$ , JO-1 (2 mg/kg) or PBS was injected intravenously followed one hour later by PLD (i.v. 1.5 mg/kg). Treatment was repeated as indicated at day 5 and 11. Tumors were then allowed to regrow for about 2 weeks. At this time, serum was analyzed for anti-JO-1 antibodies. Two more treatment cycles were performed at day 28 and day 32.  $N=5$ .

**Repeated JO-1/PLD treatment:** JO-1 is an adenovirus-derived protein and therefore potentially immunogenic. This might not be a critical issue if JO-1 is used in combination with chemotherapy, which suppresses immune responses to foreign proteins. This expectation is supported by studies with oncolytic adenovirus vectors in which immunosuppression allowed for repeated vector application (3, 4, 13). Furthermore, we have demonstrated that JO-1 remains active *in vitro* and *in vivo* even in the presence of anti-JO-1 antibodies generated by JO-1 vaccination of mice (1). This may be due to the fact that JO-1 binds to DSG2 with a very high avidity thus disrupting potential complexes between JO-1 and anti-JO-1 antibodies. (Notably, JO-1 is a dimer of a trimeric fiber knob, which contributes to the picomolar avidity to DSG2 (16).) To test the potential for anti-JO-1 antibody responses to adversely affect the therapeutic effects of JO-1, we performed repeated injections of JO-1 in an immunocompetent hDSG2 mouse tumor model (Fig.6). After two treatment cycles of JO-1 and PLD, treatment was stopped and tumors were allowed to re-grow. The third and fourth treatment cycles were started on days 28 and 32, respectively. At the time of the third cycle, serum anti-JO-1 antibodies were detectable by ELISA in the JO-1/PLD treated group of animals. However, the antibody levels were about  $\sim 10$ -fold lower than in the group which received JO-1 without PLD. In both the third and fourth treatment cycles JO-1 had an enhancing effect on PLD therapy, demonstrating that JO-1 continues to be effective after multiple treatment cycles even in the presence of detectable antibodies.

**JO-1 efficacy in an hDSG2 transgenic mouse model with spontaneous tumors.** Transplanted tumors might differ phenotypically from tumors that arise spontaneously. We have therefore cross-bred hDSG2 transgenic mice with *neu*-transgenic (*neu*-tg) mice for 7 generations. Neu-transgenic mice overexpress the rat proto-oncogene *Neu* and develop spontaneous mammary tumors between 4 and 8 months of age (7, 8). The onset of tumor development was similar in double hDSG2/*neu* transgenic mice. The histology of spontaneous tumors in these mice reflects the main features seen in human breast cancer, specifically strong hDSG2

immunoreactivity in junctions between malignant cells (Fig.7A). As seen in the transplantable tumor models, JO-1 increased the efficacy of PLD treatment (Fig.7B).

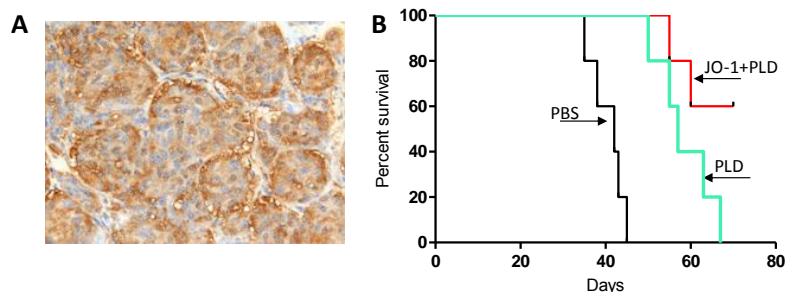


**Figure 7. JO-1/PLD therapy in hDSG2/neu transgenic mice with spontaneous tumors.** **A)** DSG2 expression in spontaneous mammary tumors. **B)** Therapy study. As soon as mammary tumors were palpable, JO-1/PLD injection was started. Treatment was repeated weekly. The endpoint in the survival study was >20% loss in body weight due to cancer-related cachexia. N=4

**Safety of JO-4/Doxil cotherapy in non-human primates:** While not part of the DoD proposal we performed safety studies in macaques. The results are described in our paper that was submitted to *Molecular Therapy - Methods&Clinical Development* (see Appendix). Below is a short summary of the data: We first confirmed that the intravenous injection of JO-4 was safe in hDSG2 transgenic mice. Next we tested JO-4 as a single agent in *M.fascicularis* at a relatively low dose (0.6 mg/kg) that we determined based on allometric scaling of the therapeutic dose used in mouse experiments. We followed the animals three days and performed a full necropsy to assess toxic side effects on normal tissues. In this study, we did not find critical JO-4 related abnormalities. In a second NHP study we combined JO-4 with Doxil. JO-4 was used at a dose that was effective in mouse tumor models (2 mg/kg). Doxil was injected at a dose that will be used in the clinical trial (40 mg/m<sup>2</sup>). Analysis of clinical symptoms and blood parameters did not show remarkable signs of toxicity. Upon necropsy, performed at 6 hours after the second injection cycle, no treatment-related abnormalities in gross examination of organs and histological analysis of tissue sections were observed. Therefore, the combination of JO-4 and Doxil was safe in an adequate animal model. Blood and tissue samples from the second study were also used to study JO-4 and Doxil blood clearance and tissue biodistribution. Despite the limitations of the study (N=1), a series of cautious conclusions can be made: *i)* The concentration of shed DSG2 in the serum did not increase after JO-4 injection, indicating minimal interaction with DSG2 on normal tissues. (In contrast, in mouse tumor models, JO-4 triggered the cleavage and shedding of DSG2 in xenograft tumors, because in tumors, not all DSG2 is trapped in junctions (2)). *ii)* As expected, serum IgG antibodies against JO-4 developed after one week. However the concentration of anti-JO-4 antibodies was at a level that was completely saturated after the second JO-4 injection (no detectable anti-JO-4 antibodies at 4 hours after the second injection). Serum antibodies had no effect on the pharmacokinetics of JO-4 after the second injection. Corresponding JO-4/anti-JO-4 IgG immune complexes were found by ELISA and immunofluorescence analysis of tissue sections in a series of lymphoid (spleen, lymph nodes) and non-lymphoid organs (adrenals, epididymis, lung, kidney, gall bladder, and pancreas). *iii)* Non-opsonized JO-4 was detected (at concentrations less than 50 ng per 100 mg tissue) in adrenals, epididymis, lung, liver, and kidneys. *iv)* JO-4 pretreatment resulted in a longer Doxil retention in the blood. Depositions of Doxil were found in the liver, adrenals, brain, bone marrow, lymph nodes and spleen. The most notable effect of JO-4 was that Doxil concentrations were higher in the liver of the JO-4 pre-treated animal, while lower Doxil concentrations in adrenals, bone marrow, heart, lymph nodes, seminal vesicle, and spleen. We speculate that JO-4 increases the liver's capacity to trap Doxil so that other tissues are less exposed. Clearly this needs to be validated in more animals.

Based on these finding, in the next IND-enabling toxicology study with clinical grade JO-4, we plan to test whether accumulative toxicity develops after 4 cycles of treatment given at an interval of 4 weeks (based in the design of the clinical trial). We will pay specific attention to adrenals and liver functions. Furthermore, to prevent opsonization of JO-4, we consider treatment with prednisolone treatment for 48 hours before JO-4 injection to suppress anti-JO-4 antibodies (5).

## Summary: KEY RESEARCH ACCOMPLISHMENTS

- A manufacturing protocol for JO-1 with and without His-tag at large scale has been established.
- There were no adverse effects after intravenous injection of JO-1 in DSG2 transgenic mice.
- JO-1 has favorable pharmacokinetics parameters.
- The effect of JO-1 on normal tissues is minimal because DSG2 is trapped in epithelial junctions in normal tissues and not accessible to intravenously injected JO-1.

- JO-1 enhances Doxil chemotherapy in xenograft models of ovarian cancer and in mouse models with syngeneic tumors.
- JO-1 continues to be effective after multiple treatment cycles even in the presence of detectable antibodies.
- JO-1 facilitates pre-existing anti-tumor T-cell responses.
- An affinity-enhanced version of JO-1 (called JO-4) was produced.
- JO-4 co-therapy allows for reduction of effective Doxil dose in a xenograft model of ovarian cancer.
- JO-4 increases the therapeutic effect of Doxil on lymphogenic metastases.
- Combined treatment with JO-4 and Doxil is safe in non-human primates

***What opportunities for training and professional development has the project provided?***

During the 2-year project period, I have presented the project to five undergraduate students that worked in his laboratory to show them an example for how basic virology research can be translated into new approaches for cancer treatment. I believe that this has motivated them to envision a career as a physician/scientist. For graduate and post-graduate fellows in my laboratory, my work on this project provided detailed insights into the complexity of designing clinical trials, preparing IND applications, interacting with the FDA, and raising money for clinical development. Based on this, it will be easier for them to avoid mistakes and make realistic plans. Finally, in the context of this project, I have trained scientists in my lab in new techniques (e.g. phospho-kinase arrays) and animal models (e.g. in vivo imaging of spontaneous metastases). In the context of JO-1/JO-4 manufacturing I became familiar with new techniques for protein purification and characterization (e.g. size exclusion chromatography, analytic ultracentrifugation).

***How were the results disseminated to communities of interest?***

In the past, the PI has participated in meetings with ovarian cancer patients and survivors and has presented the JO-1 technology there. These meetings were organized by the Pacific Ovarian Cancer Research Consortium. Also, to raise financial support for the JO-1 clinical trial, the PI has been in constant contact with private and industry sponsors trying to promote ovarian cancer research. In meetings with the FDA, the PI has explained the necessity to find new approaches for diagnosis and treatment of ovarian cancer.

***What do you plan to do during the next reporting period?***

Nothing to Report

## **4. IMPACT**

***What was the impact on the development of the principal discipline(s) of the project?***

A central treatment resistance mechanism in solid tumors is the maintenance of epithelial junctions between malignant cells that prevent drug penetration into the tumor. To overcome this physical barrier, we capitalized on a mechanism that a specific group of human adenoviruses, including serotype 3 (Ad3), have evolved to penetrate the epithelial barrier in the airway tract. We have previously reported that this involves the binding of the Ad3 particles via the fiber protein to the junction protein desmoglein 2 (DSG2), which triggers intracellular signaling resulting in the transient opening of intercellular junctions (Nat Med 17:96). We have then delineated the minimal domain within the fiber that mediates junction opening and produced it as a recombinant protein in E.coli. We have shown that intravenous injection of this junction opener increased the efficacy of monoclonal antibodies and chemotherapeutic drugs in human xenograft tumor models. We the support of this DoD grant, we generated more efficacy and safety data towards the clinical translation of the junction opener in combination with PEGylated liposomal doxorubicin (PLD) / Doxil® in patients with progressive, persistent or recurrent ovarian/fallopian tube cancer, who have previously failed to respond to standard therapies. Data generated with the support of this grant have allowed us to attract private investors to sponsor the clinical trial. cGMP manufacturing will start in January 2015. We expect to submit an IND application by July and start the trial by September 2015.

***What was the impact on other disciplines?***

While we focused on the combination of the JO-1 technology with chemotherapy drugs for the treatment of ovarian cancer, this technology can be combined with other types of cancer and other cancer treatments. For example researchers at the OHSU and at Samyang Biotech are using JO-1 in combination with their proprietary nanoparticle-based platforms for drug delivery.

### ***What was the impact on technology transfer?***

The technology has resulted in the funding of Compliment Corp ([www.complimentcorp.com/](http://www.complimentcorp.com/)). Compliment Corp has licensed the technology from the University of Washington. A co-development agreement with BRIM Biotechnology Inc. ([www.brimbiotech.com/](http://www.brimbiotech.com/)) has been signed in summer 2014. This agreement covers the funding for the clinical translation of the JO-1/JO-4-based technology as well as another technology that was developed in the PI's lab.

Furthermore, Compliment Corp has signed a sublicense agreement with Samyang Biopharmaceuticals Corporation for the use of JO-1 in combination with Samyang's nanoparticle platform for cancer drug delivery.

### ***What was the impact on society beyond science and technology?***

Nothing to Report

## **5. CHANGES AND PROBLEMS**

### ***Changes in approach and reason for change***

Last year we developed an affinity-enhanced version of JO-1 (called JO-4) that is more potent in enhancing the efficacy of chemotherapy drugs, specifically Doxil (see Appendix "submitted manuscript"). We are planning to use JO-4 in a clinical trial in ovarian cancer patients in combination with Doxil. Therefore a series of efficacy studies (see Fig. 4B and 5) and the NHP toxicity studies were performed with JO-4.

### ***Actual or anticipated problems or delays and actions or plans to resolve them***

The original version of JO-1 and JO-4 and all the studies described in this proposal were performed with His-tagged proteins which allowed for the easy purification using Ni-NTA columns. In a pre-IND meeting, the FDA did not object the use of His-tagged proteins in a clinical trial. We have however anticipated that the His tag represents an immunogenic epitope and have recently confirmed in the NHP study that most of the serum antibodies that developed against JO-4 were directed against the His tag. We have therefore generated a JO-4 version without an His tag and have developed a three-step chromatography purification process to obtain protein with >80% purity. We are currently performing efficacy, toxicity and PK bridging studies with the His-JO-4 and noHi-JO-4. If we confirm the potency and safety of noHis-JO-4 we will use it in the clinical trial.

### ***Changes that had a significant impact on expenditures***

Nothing to Report

### ***Significant changes in use or care of human subjects, vertebrate animals, biohazards, and/or select agents.***

Nothing to Report

## **6. PRODUCTS**

### **Publications, conferences papers, and presentations**

#### ***Manuscripts:***

Beyer, I., Persson, J., Song, H., Cao, H., Feng, Q., Yumul, R., van Rensburg, R., Li, ZY, Berenson, R., Carter, D., Roffler, S., Drescher, C., Lieber, A. (2012) Co-administration of epithelial junction opener JO-1 improves the efficacy and safety of chemotherapeutic drugs

*Clinical Cancer Research*, 18(12):3340-51

Wang H, Beyer I, Persson J, Song H, Li Z, Richter M, Cao H, van Rensburg R, Yao X, Hudkins K, Yumul R, Zhang XB, Yu M, Fender P, Hemminki A, Lieber A. (2012) A new human DSG2-transgenic mouse model for studying the tropism and pathology of human adenoviruses. *J Virol*. 86(11):6286-302

Lu ZZ, Wang H, Zhang Y, Cao H, Li Z, Fender P, Lieber A. (2013) Penton-dodecahedral particles trigger opening of intercellular junctions and facilitate viral spread during adenovirus serotype 3 infection of epithelial cells. *PLoS Pathog*. Oct;9(10):e1003718.

Wang H, Yumul R, Cao H, Ran L, Fan X, Richter M, Epstein F, Gralow J, Zubieta C, Fender P, Lieber A. (2013) Structural and functional studies on the interaction of adenovirus fiber knobs and desmoglein 2. J Virol., 87(21):11346-62.

Choi IK, Strauss R, Richter M, Yun CO, Lieber (2013) Strategies to increase drug penetration in solid tumors. A.Front Oncol. 2013 Jul 26;3:193.

Beyer I, van Rensburg R, Lieber A. (2013) Overcoming physical barriers in cancer therapy. Tissue Barriers. 1(1):e23647

Richter, M., Yumul, R., Wang, HJ., Saydaminova, K., Ho, M., May, D., Baldessari, A., Gough, M., Drescher, C., Urban, N., Roffler, S. Carter, D., Uckert, W., Zubieta, Z., Fender, P., Lieber A. (2014) Preclinical efficacy studies with an affinity enhanced epithelial junction opener and PEGylated liposomal doxorubicin in mice and non-human primates. Molecular Therapy-Methods & Clinical Development, submitted. (see attachment)

#### **Abstracts:**

Cao, H., Beyer, I., Lai, P-L., Disis, M., Lieber, A. 2013. Removal of physical barriers inside the tumor improves T-cell therapy. *Molecular Therapy*, 21:S5, presentation at the 16th annual meeting of the American Society of Cell and Gene Therapy

Beyer, I., Cao, H., Persson, J., Yumul, R., Lieber, A. 2013. A new epithelial junction opener for cancer therapy. *Molecular Therapy*, 21:S78, presentation at the 16th annual meeting of the American Society of Cell and Gene Therapy

Yumul, R., Cao, H., Richter, M., Gralow, J., Lieber, A. 2013. Affinity-enhanced epithelial junction openers improve cancer chemotherapy. *Molecular Therapy*, 21:S116, presentation at the 16th annual meeting of the American Society of Cell and Gene Therapy

Wang, HJ, Saydaminova, K., Fender, P., Lieber, A. (2014) Intracellular signaling triggered by DSG2 interacting adenoviruses. presentation at the 17th annual meeting of the American Society of Cell and Gene Therapy

Richter, M., Yumul, R., Ly, Z., Wang, HJ, Fender, P., Lieber, A. (2014) Species B adenovirus spread in solid tumors. 8th International Conference on Oncolytic Virus Therapeutics, Oxford, UK

#### **-Website(s) or other Internet site(s)**

[www.complimentcorp.com/](http://www.complimentcorp.com/)

[www.brimbiotech.com/](http://www.brimbiotech.com/)

#### **-technologies or techniques**

We have generated human DSG2 transgenic mice that express DSG2 in a pattern similar to humans. Furthermore, we have generated a series of cell lines that ectopically express DSG2. These mice and cell lines have been made available to other laboratories. Furthermore, we have sent out JO-1 and JO-4 to five laboratories for the use in basic and translation research.

#### **-inventions, patent applications, and/or licenses**

UW ID	Type	Patent Number	Status	Filing date
45130.01US1	US Provisional	61/353652	Converted	6/10/2010
45130.02US1	US Provisional	61/430091	Converted	1/5/2011
45130.03US1	US Provisional	61/470663	Converted	4/1/2011
45130.04WO2	PCT	PCT/US2011/040053	Nationalized	6/10/2011
45130.05US2	US nonprovisional	13/158246	Issued	6/10/2011
45130.06US1	US Provisional	61/705523	Converted	9/25/2012
45130.11WO2	PCT	PCT/US2013/061431	Pending	9/24/2013

Compliment Corp has the exclusive, worldwide license for the technology. Compliment has granted a sublicense to Samyang Biopharmaceuticals Corporation for the use of JO-1 in combination with Samyang's nanoparticle platform for cancer drug delivery.

**-other products**  
Nothing to Report

## 7. PARTICIPANTS & OTHER COLLABORATING ORGANIZATIONS

**What individuals have worked on the project?**

Name	Roma Yumul
Project Role	Research Technician
UW ID	859-007-033
Nearest person per month worked	5
Contributions to Project	Breeding and genotyping of transgenic mice, tumor cell and drug injection, monitoring of tumor growth, production of JO-1 and JO-4
Funding Support	DoD, NIH

Name	Hua Cao
Project Role	Research Scientist
UW ID	872-001-727
Nearest person per month worked	3
Contributions to Project	Tissue analyses, T-cell assays, toxicity studies in mice
Funding Support	DoD, NIH

Name	Hongjie Wang
Project Role	Research Scientist
UW ID	864-005-822
Nearest person per month worked	0.5
Contributions to Project	Manufacturing and purification of JO1 and JO4
Funding Support	NIH, DoD

Name	Andre Lieber
Project Role	PI
UW ID	
Nearest person per month worked	1.5
Contributions to Project	establishment of collaborations and administration of the grant, planned the experiments and performed data analysis.
Funding Support	NIH, DoD

### **Has there been a change in the active other support of the PI since the last reporting period**

All active grants for PI Lieber have ended and, at this point, none of the pending applications has received a fundable score. Because of this, most of the PI's lab member will have to be laid-off by April 2015.

### **OTHER SUPPORT: LIEBER**

#### **Active:**

SBIR R44CA162582, phase II (Lieber Co-PI) 10/01/13-09/30/15  
Reducing Complement Inhibition to Treat Leukemia and Lymphoma  
(50% Lieber)

SBIR R43 CA183379-01, Phase I (Lieber Co-PI) 10/01/14-09/30/15  
Tumor Tight Junction Opener + Chemotherapy Conjugates to Treat Cancer



(50% Lieber)

**Pending:**

1R01AI117707-01 (Lieber)	12/01/15-11/30/19
An in vivo stem cell genome editing approach to protect high risk individuals from HIV infection	
1R21CA194227-01 (Lieber)	04/01/15-03/31/17
Overcoming ovarian cancer resistance to chemotherapy by interfering with cancer stem cell formation	
1R01HL128288-01 (Lieber)	07/01/15-06/30/20
In vivo hematopoietic stem cell gene therapy	
2R01CA144057-11A1 (Lieber)	03/01/05-08/31/19
Evaluations of Vectors Based on Species B Adenoviruses	
1R01CA193232-01 (Lieber)	04/01/15-03/31/20
Preclinical and clinical studies with a recombinant epithelial junction opener	
1R21CA193077-01 (Lieber)	04/01/15-03/31/17
Hematopoietic stem cell based gene therapy of breast cancer	
Life Sciences Discovery Fund (Lieber)	01/01/15-12/31/15
Pilot project	
FHCRC Ovarian Cancer SPORE PI: Urban)	
Project 3: Clinical trial with junction opener and Doxil in ovarian cancer patients	
R35: Outstanding Investigator Award	07/01/15-06/30/22
Early detection, immuno-prophylaxis, and treatment of ovarian cancer	

**What other organization were involved as partners?**

N/A

**8.SPECIAL REPORTING REQUIREMENTS**

Nothing to Report

**9. APPENDICES**

- 1) submitted manuscript:
- 2) resubmitted Project 3 of Ovarian Cancer SPORE proposal

**REFERENCES**

- 1. Beyer, I., H. Cao, J. Persson, H. Song, M. Richter, Q. Feng, R. Yumul, R. van Rensburg, Z. Li, R. Berenson, D. Carter, S. Roffler, C. Drescher, and A. Lieber. 2012. Coadministration of epithelial junction opener JO-1 improves the efficacy and safety of chemotherapeutic drugs. Clin Cancer Res **18**:3340-3351.
- 2. Beyer, I., R. van Rensburg, R. Strauss, Z. Li, H. Wang, J. Persson, R. Yumul, Q. Feng, H. Song, J. Bartek, P. Fender, and A. Lieber. 2011. Epithelial junction opener JO-1 improves monoclonal antibody therapy of cancer. Cancer Res **71**:7080-7090.

3. **Bouvet, M., B. Fang, S. Ekmekcioglu, L. Ji, C. D. Bucana, K. Hamada, E. A. Grimm, and J. A. Roth.** 1998. Suppression of the immune response to an adenovirus vector and enhancement of intratumoral transgene expression by low-dose etoposide. *Gene Ther* **5**:189-195.
4. **Dhar, D., J. F. Spencer, K. Toth, and W. S. Wold.** 2009. Pre-existing immunity and passive immunity to adenovirus 5 prevents toxicity caused by an oncolytic adenovirus vector in the Syrian hamster model. *Mol Ther* **17**:1724-1732.
5. **Dykes, A. C., I. D. Walker, G. D. Lowe, and R. C. Tait.** 2001. Combined prednisolone and intravenous immunoglobulin treatment for acquired factor VIII inhibitors: a 2-year review. *Haemophilia* **7**:160-163.
6. **Jolly, M. K., B. Huang, M. Lu, S. A. Mani, H. Levine, and E. Ben-Jacob.** 2014. Towards elucidating the connection between epithelial-mesenchymal transitions and stemness. *J R Soc Interface* **11**.
7. **Knutson, K. L., B. Almand, Y. Dang, and M. L. Disis.** 2004. Neu antigen-negative variants can be generated after neu-specific antibody therapy in neu transgenic mice. *Cancer Res* **64**:1146-1151.
8. **Lu, H., K. L. Knutson, E. Gad, and M. L. Disis.** 2006. The tumor antigen repertoire identified in tumor-bearing neu transgenic mice predicts human tumor antigens. *Cancer Res* **66**:9754-9761.
9. **Lu, M., M. K. Jolly, H. Levine, J. N. Onuchic, and E. Ben-Jacob.** 2013. MicroRNA-based regulation of epithelial-hybrid-mesenchymal fate determination. *Proc Natl Acad Sci U S A* **110**:18144-18149.
10. **Lu, Z. Z., H. Wang, Y. Zhang, H. Cao, Z. Li, P. Fender, and A. Lieber.** 2013. Penton-Dodecahedral Particles Trigger Opening of Intercellular Junctions and Facilitate Viral Spread during Adenovirus Serotype 3 Infection of Epithelial Cells. *PLoS Pathog* **9**:e1003718.
11. **Persson, J., I. Beyer, R. Yumul, Z. Li, H. P. Kiem, S. Roffler, and A. Lieber.** 2011. Immuno-therapy with anti-CTLA4 antibodies in tolerized and non-tolerized mouse tumor models. *PLoS One* **6**:e22303.
12. **Strauss, R., Z. Y. Li, Y. Liu, I. Beyer, J. Persson, P. Sova, T. Moller, S. Pesonen, A. Hemminki, P. Hamerlik, C. Drescher, N. Urban, J. Bartek, and A. Lieber.** 2011. Analysis of epithelial and mesenchymal markers in ovarian cancer reveals phenotypic heterogeneity and plasticity. *PLoS One* **6**:e16186.
13. **Thomas, M. A., J. F. Spencer, K. Toth, J. E. Sagartz, N. J. Phillips, and W. S. Wold.** 2008. Immunosuppression enhances oncolytic adenovirus replication and antitumor efficacy in the Syrian hamster model. *Mol Ther* **16**:1665-1673.
14. **Tuve, S., B. M. Chen, Y. Liu, T. L. Cheng, P. Toure, P. S. Sow, Q. Feng, N. Kiviat, R. Strauss, S. Ni, Z. Y. Li, S. R. Roffler, and A. Lieber.** 2007. Combination of tumor site-located CTL-associated antigen-4 blockade and systemic regulatory T-cell depletion induces tumor-destructive immune responses. *Cancer Res* **67**:5929-5939.
15. **Wang, H., I. Beyer, J. Persson, H. Song, Z. Li, M. Richter, H. Cao, R. van Rensburg, X. Yao, K. Hudkins, R. Yumul, X. B. Zhang, M. Yu, P. Fender, A. Hemminki, and A. Lieber.** 2012. A new human DSG2-transgenic mouse model for studying the tropism and pathology of human adenoviruses. *J Virol* **86**:6286-6302.
16. **Wang, H., Z. Li, R. Yumul, S. Lara, A. Hemminki, P. Fender, and A. Lieber.** 2011. Multimerization of adenovirus serotype 3 fiber knob domains is required for efficient binding of virus to desmoglein 2 and subsequent opening of epithelial junctions. *J Virol* **85**:6390-6402.
17. **Wang, H., Z. Y. Li, Y. Liu, J. Persson, I. Beyer, T. Moller, D. Koyuncu, M. R. Drescher, R. Strauss, X. B. Zhang, J. K. Wahl, 3rd, N. Urban, C. Drescher, A. Hemminki, P. Fender, and A. Lieber.** 2011. Desmoglein 2 is a receptor for adenovirus serotypes 3, 7, 11 and 14. *Nat Med* **17**:96-104.
18. **Wang, H., R. Yumul, H. Cao, L. Ran, X. Fan, M. Richter, F. Epstein, J. Gralow, C. Zubieta, P. Fender, and A. Lieber.** 2013. Structural and functional studies on the interaction of adenovirus fiber knobs and desmoglein 2. *J Virol* **87**:11346-11362.
19. **Yang, Z., M. Horn, J. Wang, D. D. Shen, and R. J. Ho.** 2004. Development and characterization of a recombinant madin-darby canine kidney cell line that expresses rat multidrug resistance-associated protein 1 (rMRP1). *AAPS J* **6**:77-85.

## **Appendix #1**

Paper submitted to Molecular Therapy: Methods and Clinical Development

**Preclinical safety and efficacy studies with an affinity-enhanced epithelial junction opener and PEGylated liposomal doxorubicin**

Maximilian Richter<sup>1</sup>, Roma Yumul<sup>1</sup>, Hongjie Wang<sup>1</sup>, Kamola Saydaminova<sup>1</sup>, Martin Ho<sup>1</sup>, Drew May<sup>3</sup>, Audrey Baldessari<sup>3</sup>, Michael Gough<sup>3</sup>, Charles Drescher<sup>4</sup>, Nicole Urban<sup>4</sup>, Steve Roffler<sup>5</sup>, Chloé Zubieta<sup>6</sup>, Darrick Carter<sup>1,7</sup>, Pascal Fender<sup>8</sup>, André Lieber<sup>1,2</sup>

<sup>1</sup>University of Washington, Division of Medical Genetics, Box 357720, Seattle, WA 98195

<sup>2</sup>University of Washington, Department of Pathology

<sup>3</sup>Washington National Primate Research Center, Seattle, WA 98195

<sup>4</sup>Fred Hutchinson Cancer Research Center, Seattle, WA

<sup>5</sup>Academia Sinica, Taipei, Taiwan

<sup>6</sup>European Synchrotron Radiation Facility, Grenoble, France

<sup>7</sup>Compliment Corp., Seattle, WA 98102

<sup>8</sup>Unit of Virus Host Cell Interactions, UMI3265, CNRS/EMBL/UJF, Grenoble, France

Correspondence should be addressed to A.L., University of Washington, Box 357720, Seattle, WA 98195, phone: (206) 221-3973, email: [lieber00@u.washington.edu](mailto:lieber00@u.washington.edu)

Seattle, WA

Short title: Epithelial junction opener ovarian cancer co-therapy

## **Abstract**

A central treatment resistance mechanism in solid tumors is the maintenance of epithelial junctions between malignant cells that prevent drug penetration into the tumor. We have developed a small recombinant protein (JO-1) that triggers the transient opening of intercellular junctions and thus increases the efficacy of monoclonal antibodies and chemotherapeutic drugs without causing toxicity in mouse tumor models. Here we provide data towards the clinical translation of an affinity-enhanced version of JO-1, which we call JO-4, in combination with PEGylated liposomal doxorubicin (PLD) / Doxil® for ovarian cancer therapy. We have presented X-ray crystallography data suggesting a structural basis for the higher affinity of JO-4 to DSG2. We also confirmed JO-4 efficacy in a xenograft model with primary ovarian cancer cells showing that JO-4 can salvage Doxil therapy when given at a dose that was 3-fold lower than the therapeutic dose. Furthermore, we tested the safety of intravenous JO-4 alone and in combination with Doxil in *Macaca fascicularis*, an adequate animal model for predicting toxicity in humans. Our studies did not show critical JO-4 related toxicity or an increase of Doxil-related side effects. Our efficacy and safety data will help to support an Investigational New Drug-filing for a JO-4/Doxil combination treatment.

## **Introduction**

***Epithelial phenotype of cancer:*** More than 80% of all cancer cases are carcinomas, formed by the malignant transformation of epithelial cells. One of the key features of epithelial tumors is the presence of intercellular junctions, which link cells to one another and act as barriers to the penetration of molecules with a molecular weight of >400 daltons (Da) [1-3]. One of these junction proteins, desmoglein 2 (DSG2), is upregulated in malignant cells [4, 5]. For example, in more than 60 ovarian cancer biopsies with different histological types analyzed, we consistently found higher expression levels of DSG2 in ovarian cancer cells than in the surrounding normal tissue or tumor stroma cells [6].

For most carcinomas, progression to malignancy is accompanied by a loss of epithelial differentiation and a shift towards a mesenchymal phenotype, *i.e.* epithelial to mesenchymal transition (EMT) [7]. EMT increases migration and invasiveness of many cell types and is often one of the conditions for tumor infiltration and metastasis. However, following invasion or metastasis, cells that have undergone the process of EMT can also revert to a well-differentiated epithelial phenotype [8]. In support of this, there exist numerous examples of advanced carcinomas showing that mesenchymal cells can regain characteristics of epithelial cells or undergo mesenchymal to epithelial transition (MET) [8-10]. Both EMT and MET are regulated through an intricate interplay of RNA binding protein/miRNA complexes, including LIN28/miR-let7 and miR-200/ZEB [9, 10].

***Intratumoral drug penetration and resistance:*** Potential causes of drug resistance in solid tumors include genetically and epigenetically determined factors expressed in individual cells and those related to the solid tumor environment. The latter include tumor stroma cells and proteins that form a dense matrix as well as intercellular junctions that seal the space between tumor cells [11]. To be effective, drugs have to diffuse throughout the tumor to achieve a lethal concentration in all of the tumor cells. However, most drugs, in particular those based on nanoparticles or liposomes with diameters around 100 nm, do not diffuse more than a few cell layers from blood vessels implying that more distant tumor



cells receive only sub-therapeutic drug exposure [11-13]. Furthermore, several studies have shown that the upregulation of epithelial junction proteins correlates with increased resistance to therapy, including therapy with the two major classes of cancer drugs - monoclonal antibodies and chemotherapeutics [14-16]. We therefore hypothesized that transient opening of junctions would increase the therapeutic efficacy of, and potentially, overcome resistance to chemotherapy in advanced stage epithelial cancers.

***Adenovirus serotype 3 derived junction opener (JO-1):*** We have recently reported that a group of human adenoviruses uses DSG2 as a receptor for infection [17]. Among the DSG2-targeting viruses is adenovirus serotype 3 (Ad3). Ad3 is able to efficiently breach the epithelial barrier in the airway tract and infect airway epithelial cells. This is achieved by the binding of Ad3 to DSG2 and subsequent intracellular signaling that results in transient opening of tight junctions between epithelial cells [17, 18]. We have capitalized on this mechanism and generated a recombinant protein that contains the minimal structural domains from Ad3 that are required to open the intercellular junctions in epithelial tumors. This protein is called "junction opener 1" (JO-1) [6, 19-21]). JO-1 is a small recombinant protein derived from the Ad3 fiber [21]. It contains two self-dimerizing trimeric Ad3 fiber knob. JO-1 can be easily produced in *E. coli* and purified by affinity chromatography. Binding of JO-1 to DSG2 triggers shedding of the DSG2 extracellular domain and activation of pathways that are reminiscent of an epithelial to mesenchymal transition (EMT), including the phosphorylation of MAP kinases and the downregulation of junction proteins [17, 19, 20]. Both mechanisms result in transient opening of epithelial junctions. Importantly, multimerization of the trimeric Ad3 fiber knob through a K-coil motif is required for DSG2-triggered signaling and junction opening [21].

Furthermore, we have recently shown that during Ad3 replication, viral protein complexes, so called pento-dodecahedra (PtDd), that are structurally similar to JO-1, are released from infected cells, open the junctions between neighboring cells and thus allow *de novo* produced virus to spread in epithelial tumors [18]. A similar positive feed-forward mechanism should work for JO-1 penetration in tumors.

We have shown in over 25 xenograft models that the intravenous injection of JO-1 increased the efficacy of cancer therapies, including monoclonal antibodies and chemotherapy drugs, in a broad range of epithelial tumors [6, 19]. Further studies have shown that the effective doses of chemotherapy drugs can be reduced when they are combined with JO-1 [6].

The homology between the human and mouse DSG2 gene is 77.1% and neither Ad3 nor JO-1 binds to mouse cells [20]. We therefore generated transgenic mice that contain the 90kb human DSG2 locus including all regulatory regions. These mice express human DSG2 in a pattern and at a level similar to humans [20]. Furthermore, we have shown that JO-1 triggers hDSG2-mediated signaling and opening of epithelial junctions in epithelial mouse tumor cells that ectopically express hDSG2 [20]. This indicates that human DSG2 can interact with mouse cytoskeletal proteins and kinases and implies that hDSG2 transgenic mice can be used as a model to study downstream effects of JO-1 binding to DSG2 after intravenous injection. The intravenous injection of JO-1 into hDSG2 transgenic mice was safe and well-tolerated [17, 19]. Using hDSG2 transgenic mice, we also demonstrated that JO-1 predominantly acts on junctions in tumors [6]. A number of factors could account for this finding, including: *i*) overexpression of hDSG2 by tumor cells, *ii*) better accessibility of hDSG2 on tumor cells, due to a lack of strict cell polarization compared to hDSG2-expressing normal epithelial cells, and *iii*) a high degree of vascularization and vascular permeability in tumors. Because of its preferential binding to and action on epithelial junctions of tumors, JO-1 appears to create a “sink” for therapeutic drugs in tumors, which decreases the levels and exposure of these drugs in normal tissues, at least in mouse tumor models (with a tumor weight to body weight ratio of 1:20 [20]. This “sink” effect will most likely be less pronounced in cancer patients. Furthermore, we have shown in hDSG2 transgenic mice with syngeneic tumors that JO-1 remains active in the presence of anti-JO-1 antibodies generated by JO-1 vaccination of mice [6, 22]. This may be due to the fact that JO-1 binds to DSG2 with a very high avidity thus disrupting potential complexes between JO-1 and anti-JO1 antibodies.

**Clinical trial with affinity-enhanced junction opener (JO-4):** More recently, by screening of a mutant Ad3 fiber knob library, we identified a series of (trimeric) Ad3 fiber knob mutants with increased affinity to DSG2 [22]. The highest affinity was conveyed by a specific mutation of valine residue at position 239 to an aspartic acid residue (V239D). Preliminary data showed that the dimerized form of this mutant (called JO-4) was therapeutically more potent than JO-1 in a series of cancer models [22]. Our goal is to use JO-4 in combination with Doxil, a PEGylated, liposome-encapsulated form of doxorubicin, in ovarian cancer patients. Doxil is FDA approved for treatment of advanced ovarian cancer patients that failed first line platinum therapy and is a preferred agent in this setting. When used as a monotherapy, objective response rates from 10%-26% have been reported [23-25]. At the FDA recommend dose of 50 mg/m<sup>2</sup>, monotherapy with Doxil is associated with grade 3 or worse toxicity in 30% of patients with hand-foot syndrome and stomatitis/mucositis being the most common. Doses have to be reduced to as low as 30 mg/m<sup>2</sup> in combination regimens which may be limiting efficacy.

In this study, we provide preclinical data showing in an ovarian cancer mouse model that the combination with JO-4 allows salvaging the therapeutic effect of Doxil when given at a dose three fold lower than the therapeutic dose. Furthermore, we provide preclinical data in a xenograft model that JO-4 also increases the therapeutic effect of Doxil on lymphogenic metastases. In preparation of an IND application, we have performed a toxicity and biodistribution study of combined JO-4 and Doxil treatment in *Macaca fascicularis*. This study showed that the combination therapy is safe in an adequate animal model.

## **Results**

**Structural and functional characterization of JO-4.** JO-4 is a dimeric form of the trimeric Ad3 fiber knob with each fiber knob monomer containing a V→D substitution in amino acid position 239. Valine is a small hydrophobic amino acid residue while aspartic acid is negatively charged. The mutation is localized

in the EF loop of each Ad3 knob monomer (**Fig. 1a**). X-ray crystallography of the non-dimerized, trimeric Ad3-V239D fiber knob showed that the EF loop in V239D is displaced with respect to the wild type due to the formation of a salt bridge between Asp239 and Lys275 (**Figs. 1b and c**). The Lys275 side chain rotamer adopts a different conformation in the V239D mutant compared to wild type in order to interact with Asp239. This salt bridge locks the EF loop into a new conformation, potentially explaining the increased binding affinity for the receptor. Detailed data on the analysis of Ad3 knob V236D crystals are shown in **Table 1**. We previously demonstrated that the affinity of the Ad3-V236D fiber knob is higher than the parental, non-mutated fiber knob [22]. Here we studied the interaction of the self-dimerizing Ad3-V236D fiber knob, i.e. JO-4, with DSG2 by Surface Plasmon Resonance (SPR) analysis (**Fig. 1d**). The DSG2 interaction to mobilized JO-4 had a high affinity with a  $K_D$  in the nanomolar range ( $K_D=1.4$  nM). This high affinity can be explained by both a high association rate ( $k_a= 3.3 \cdot 10^5 \text{ M}^{-1}\text{s}^{-1}$ ) and, by the very slow dissociation ( $k_d= 4.7 \cdot 10^{-4} \text{ s}^{-1}$ ). This feature is clearly seen in the sensorgrams at the end of the injection where the signal remains stable for the time of analysis.

In summary of our structural studies we concluded that the new conformation of the EF loop in JO-4 potentially explains its high affinity to DSG2.

***JO-4 co-therapy allows for reduction of effective Doxil dose in a xenograft model of ovarian cancer.*** In the majority of cancer patients, the dose of Doxil has to be reduced from 50mg/m<sup>2</sup> to less than 30mg/m<sup>2</sup> due to toxicity. One of our clinical objectives is to test whether JO-4 can salvage the therapeutic effect of a lower dose of Doxil. We performed a study in mice with xenograft tumors derived from primary ovarian cancer ovc316 cells. Ovc316 cells were obtained from a patient and closely model the heterogeneity and plasticity seen in tumors *in situ* [26]. Mice with pre-established, mammary fat pad-localized ovc316 tumors were weekly intravenously injected with JO-4 at a dose of 2mg/kg, followed one hour later by an intravenous injection of Doxil at a therapeutic dose of 3 mg/kg or a subtherapeutic

"low" dose of 1 mg/kg (**Fig.2a**). This study shows higher anti-tumor efficacy of JO-4 plus "low"-dose Doxil (1 mg/kg), compared to "high" dose Doxil alone (3 mg/kg), indicating that it is possible to lower the effective dose of Doxil when combined with JO-4.

***JO-4 increases the therapeutic effect of Doxil on lymphogenic metastases.*** As outlined above, in order to metastasize, epithelial cancer cells acquire mesenchymal features through EMT. There is strong support that, once metastatic cells homed to other tissues, they regain epithelial features, including epithelial junctions [9, 10]. To corroborate this, we employed a model of epithelial breast cancer that forms spontaneous metastases. The model is based on MDA-MB-231-luc-D3H2LN cells which allow for *in vivo* imaging of tumor growth based on luciferase expression. Tumor cells injected into the mammary fat pad formed axillary lymph node metastases if the primary tumor was removed 5 weeks after inoculation (**Suppl. Fig. 1a**). If the primary tumor is not removed, it invades the peritoneum (**Suppl.Fig. 1b**) and forms metastases in mesenteric lymph nodes that are clearly distinguishable from the primary tumor by *in vivo* imaging (**Fig. 2b**). Immunofluorescence analysis of sections showed membrane-localized DSG2 in the primary tumor and metastatic lesions (**Fig. 2c, Suppl. Fig.1b**). The amount of DSG2, as assessed by Western blot analysis, was comparable in the primary and secondary tumors (**Fig. 2d**). To address the question whether JO-4 can also act on metastases, we performed a therapy study in the model with invasive tumors that form lymphogenic metastases in mesenteric lymph nodes. Treatment (PBS, Doxil (1mg/kg) alone, JO-4 (2 mg/kg) + Doxil) was started when metastases were clearly detectable by *in vivo* luciferase imaging. Luminescence signals for the primary and secondary lesions were recorded separately the day before treatment and at day 5 after treatment and expressed as a ratio to show tumor progression (**Fig. 2e, f, Suppl. Fig. 2**). In most untreated mice, both primary tumor and metastases grew. Regression of the metastatic lesions was observed in one out of five Doxil-treated mice. Tumors in the remaining four animals did not respond to Doxil. In contrast, all primary tumors and three out four

metastatic lesions shrank when mice were treated with the combination of JO-4 and Doxil. This suggests that in this model, JO-4 can open epithelial junctions in metastases.

***JO-4 injection is safe in human DSG2 transgenic mice.*** There were no adverse effects or critical abnormalities in hematologic and serum chemistry parameters or histopathological studies of tissues after intravenous injection of JO-4 (2 and 10 mg/kg) into hDSG2 transgenic mice with or without pre-existing anti JO-4 antibodies (data not shown). After injection of 10 mg/kg, we observed a mild lymphocytopenia and intestinal inflammation that subsided by day 3 after injection.

***Intravenous JO-4 injection into non-human primates is safe (NHP study #1).*** Ad3 and Ad3 fiber knobs do not efficiently bind to mouse [20], rat, hamster, and dog PBMCs or transformed cell lines (data not shown) and the DSG2 gene homology for these species compared to human DSG2 is less than 80%. Although hDSG2 transgenic mice allow us to study a number of variables in a large number of animals, it is unclear whether the hDSG2-mouse system accurately models a homologous system with human DSG2 in human cells. Better models are non-human primates. The DSG2 gene homology between humans and macaques is 96.6%. We have shown that the DSG2 expression pattern and level in tissues of *Macaca fascicularis* is similar to humans [20]. Ad3 and Ad3 derivatives bind to monkey DSG2 and trigger junction opening at a level that is comparable to human cells [20]. This justifies the use of *Macaca fascicularis* for toxicology studies in preparation of an IND package. A preliminary study was conducted in which two animals (~5kg) were injected intravenously with a single dose of JO-4 (0.6 mg/kg) (**Fig. 3a**). This dose was chosen because, after allometric scaling, it corresponded to 2 mg/kg of JO-4 used in mice (<http://www.fda.gov/downloads/Drugs/Guidances/UCM078932.pdf>). The animals were monitored by an independent group of veterinarians and pathologists at the Washington State Northwest Primate Research Center (WaNPRC) at the University of Washington. Blood samples were taken daily. A full



necropsy was performed at day 3 after JO-4 injection (see **Suppl. Materials: "NHP study #1"**). There was no evidence of changes in health/behavior, laboratory studies or pathologies. Histological analysis revealed a mild gastro-enterocolitis, which is often observed in monkeys in this center. Analysis of hematological parameters revealed a mild lymphopenia at day 1, thrombocytopenia at days 1, 2, and 3 (**Fig. 3b**). A mild transaminitis was observed at day 1 after JO-4 injection which could be related to residual bacterial endotoxin in the JO-4 preparation. This is supported by elevated serum  $\gamma$ -interferon levels observed within hours after JO-4 injection (**Fig. 3b**), a response that can be attributed by LPS activation of tissues macrophages. We are currently working on the clinical grade production of JO-4 which will also remove all LPS from the preparation.

***Combined treatment with JO-4 and Doxil is safe in non-human primates (NHP study #2).*** A second study in male *M. fascicularis* was performed to address the question whether JO-4 increases Doxil toxicity. One animal (A-88) was injected intravenously with JO-4 at a dose of 2 mg/kg\*, i.e. at a dose that was effective in mouse models. (In a pre-IND meeting initiated after NHP study#1, the FDA recommended not to use allometric scaling for NHP dose selection in macaques.) Another animal (A-93) was injected with saline. One hour later, both animals received an intravenous injection of Doxil at a dose of 40mg/m<sup>2</sup> (1.1 mg/kg), i.e. at a dose that will be used in the clinical trial (**Fig. 4a**). Animals were monitored daily and blood samples were collected at 4, 6, and 24 hours and then at day 3, 7 and 14 after Doxil injection. At day 14, animals received a second cycle of treatment. At six hours after the second Doxil injection, animals were euthanized and a gross necropsy was performed by a certified veterinary pathologist. The rationales for the second injection cycle followed by the necropsy were *i)* to assess potential anaphylactic reactions in a treated animal with serum antibodies against JO-4, *ii)* to assess JO-4 tissue distribution, *iii)* to study the effect of JO-4 on Doxil serum clearance and tissue uptake.

*Vital symptoms:* Daily monitoring showed no abnormal changes in body weight, food intake, infusion site appearance, body temperature, posture, respiration, feces/urine, food water, recumbent, attitude, and skin. ECGs, taken before treatment and 24 hours, 3, 7, and 14 days after the first injection cycle and 6 hours after the second injection cycle, were normal.

*Pathology and histology after necropsy:* At necropsy, animals were in good health; no external lesions were observed and all body systems and organs appeared grossly unremarkable. Histology analysis of sections from 39 tissues showed mild gastroenterocolitis in both animals, a condition that is commonly seen in the colony and not related to the treatment. Histology of all other tissues was normal or interpreted as nonspecific background or incidental findings. Bone marrow cytology was unremarkable. The full pathology report can be found in the **Suppl. Materials: "NHP study #2**.

*Blood cell counts and chemistry:* CBC analysis showed mild leukocytosis starting at day 7 after treatment in both animals due to an increase in neutrophils (**Fig. 4b**). In addition, animal A-88 also showed increased lymphocyte counts at day 3 and 7 after the first treatment cycle and 6 hours after the second treatment that was most likely related to JO-4 injection. A mild lymphocytopenia was seen at day 14 after the first treatment most likely due to Doxil treatment. A transient elevation of serum aspartate aminotransferase (AST) after the treatment was observed in both animals. In the JO-4 treated animal, transiently increased serum alanine aminotransferase (ALT/SGPT) levels were detected at 24 hours after injection (**Fig. 4c**). JO-4 injection also increased the serum levels of IFN $\gamma$  up to day 3 after injection (**Fig. 4d**). Considering studies in mice, the transient elevation of IFN $\gamma$  and ALT could be due to residual amounts of bacterial LPS in the JO-4 preparation (2.2 EU/mg). Because in studies with mouse tumor models, JO-1 caused cleavage of the extracellular domain (ECD) of DSG2, we measured the concentration of soluble DSG2 ECD in serum (**Fig. 4e**). While clearly detectable, no JO-4-related effects on the kinetics of serum DSG2 concentration were observed.

Serum and tissue samples were used to measure JO-4 and Doxil concentrations as well as antibodies against JO-4.

*JO-4 serum clearance and biodistribution:* In the JO-4 injected animal A-88, serum JO-4 levels declined to undetectable levels by day 3 after injection (**Fig. 5a**). A second injection resulted in similar levels at 4 hours after injection and similar decline by 6 hours. IgG antibodies specific to JO-4 became detectable in serum at day 7 and increased by day 14 (**Fig. 5b**). After the second JO-4 injection, anti-JO-4 IgG dropped to background levels. This indicates that a fraction of the injected JO-4 forms complexes with anti-JO-4 antibodies which are then either taken up by tissues or are not detectable by ELISA due to epitope masking. Further studies with tissue samples support the first scenario (see below). JO-4 concentrations and levels of anti-JO-4 antibodies in tissue lysates were measured by ELISA (**Fig. 5c, d**). When considered together, the data suggest the following: In animal A-88, JO-4 was present in epithelial tissues such as the adrenal glands, epididymis, gall bladder, kidneys, lung, and pancreas (**Fig. 5c**). Immunofluorescence staining of the adrenals, epididymis, kidney and lungs against JO-4 showed association of signals with the membrane of epithelial cells in animal A-88 (**Figs. 6a,b**). Together with JO-4, anti-JO-4 antibodies were found in a series of organs including adrenals, epididymes, eye, lungs, colon, cecum, lymph nodes, prostate, spleen, stomach and urinary bladder suggesting opsonization of antibody-JO-4 complexes. The latter is supported by immunofluorescence studies that showed colocalization of a fraction of JO-4 with IgG. (**Fig. 6c**). In the liver, JO-4 was predominantly found in association with Kupffer cells (**Fig. 6d**). The finding that JO-4 strongly localized to adrenals was unexpected. The adrenal glands are one of the organs that have the greatest blood supply per gram of tissue and the JO-4 and JO-4 immune complex signals in this tissue might, in part, originate from residual blood.

*Doxil serum clearance and biodistribution:* Doxil concentrations were measured by ELISA using two monoclonal antibodies that recognize PEG in nanoparticles [27]. Serum clearance of Doxil after intravenous injection (**Fig. 7a**) is consistent with the expected half-life of ~80 hours in humans [28].

There was a slower decrease of serum Doxil concentrations during the first 24 hours in the animal that received JO-4 (A-88). Doxil was undetectable in both animals at day 14. A second injection resulted in higher Doxil concentrations at 4 and 6 hours in animal A-88. Doxil concentrations were also measured in tissues samples (**Fig. 7b**). The highest Doxil concentrations in animal A-93 w/o JO-4) were found in adrenals, bone marrow, brain, heart, GI tract, liver, mesenteric lymph nodes, seminal vesicle, and spleen. JO-4 injection (animal A-88) resulted in increased Doxil accumulation in the epididymes and the liver. Interestingly, Doxil concentration in A-88 were lower in the adrenals, bone marrow, heart, lymph nodes, seminal vesicle, and spleen compared to the animal that did not receive JO-4. We speculate that JO-4 increases the liver's capacity to trap Doxil so that other tissues are less exposed. Notably, transaminases were slightly higher in the JO-4 treated animal (**Fig.4c**).

In summary analysis of vital symptoms, blood parameters, and organ histology did not show remarkable signs of toxicity. Upon necropsy, no significant treatment-related abnormalities in gross examination of organs and histological analysis of tissue sections were observed. Although JO-4 accumulation was found in normal tissues, this did not appear to cause toxic effects. We therefore concluded that the combination of JO-4 and Doxil was well tolerated in a non-human primate model.

## **Discussion**

Malignant cells in epithelial ovarian cancer are linked through junctions, which inhibit drug penetration into the tumor implying that cancer cells that are farther away from blood vessels receive only sub-toxic concentrations of drugs and are not affected by chemotherapy or become prone to develop resistance [29, 30]. Epithelial junctions in particular are a barrier for tumor penetration of newer generations of chemotherapy drugs based on liposomes or nanoparticles which often have a diameter greater than 100nm [13]. We have developed a recombinant protein (JO-1) capable of transiently opening epithelial junctions and increasing intratumoral chemotherapy drug accumulation and penetrations. Our goal is to

test an affinity enhanced version of this junction opener (JO-4) in combination with Doxil in ovarian cancer patients. We therefore performed a series of preclinical safety and efficacy studies in support of an IND application.

JO-4 has a single amino acid mutation in the EF loop of the DSG2 interacting domain, the Ad3 fiber knob. This V239D substitution changes the conformation of the EF loop as determined by X-ray crystallography. Interestingly, the L240 amino acid next to the V239D mutation has been previously reported as one of the putative critical residues for the receptor interaction [31]. In the crystal structure, the position of the backbone and side chain of Leu240 is altered with respect to the wild type. Leu240 is exposed to the solvent and the backbone of the EF loop is in a more extended conformation, possibly facilitating interactions with DSG2. Theoretically, this could bring the DSG2-interacting regions in the Ad3 fiber knob (see **Fig.1a & 1b**) into closer proximity to DSG2, which, in turn could account for the higher affinity of the Ad3-V239D fiber knob mutant compared to the wildtype Ad3 fiber knob. To investigate these interactions in more detail, the atomic resolution of the Ad3 fiber and V239D mutant in complex with the DSG2 ectodomain would be required.

An important finding in our studies with an ovarian cancer xenograft model was that JO-4 allowed Doxil to remain therapeutically active when applied at lower doses together with JO-4. This is clinically relevant because in almost all patients the Doxil doses have to be lowered due to toxicity that develops after several treatment cycles. While it is now acknowledged that, after metastasis, cancer cells regain an epithelial phenotype, including epithelial junctions, which protect cancer cells from immune attacks and treatment [32], in the literature one can still find the misconception that metastatic lesions do not contain junctions, which would imply that JO-4 would not act on metastases. To address this, we employed a model of spontaneous metastasis. We showed the presence of membrane DSG2 in metastases and the ability of JO-4 to promote reduction of the primary tumor and metastatic lesions by Doxil. These data with JO-4 in mouse models together with the preclinical efficacy data that we

assembled for JO-1 give a solid basis that JO-4 has the potential to increase the therapeutic efficacy in ovarian cancer patients.

A major concern was the safety of intravenously injected JO-4. The JO-4 target receptor DSG2 is expressed in most epithelial tissues. Our histology analyses however showed that DSG2 in normal epithelial tissues, which display a strict apical basal polarization, is trapped in lateral junctions and not readily accessible to intravenously injected ligands. In contrast, in epithelial tumors this polarization is lost and DSG2 can be found on all membrane sides of tumor cells [20]. Safety of JO-4 is in part predicted by studies with Ad3 or Ad3 fiber knob containing vectors in humans. For more than a decade, Ad5 vectors that possess Ad3 fibers (Ad5/3), which also infect cells through DSG2 [21], have been used for cancer therapy in animal models and humans with a very good safety profile after intravenous injection [33, 34]. A recent phase I trial demonstrated safety of an intraperitoneally applied Ad5/3-based oncolytic vector in recurrent ovarian cancer patients [35]. Last year, we performed a study with an oncolytic vector based on Ad3 [36]. In this study, twenty-five patients with chemotherapy refractory cancer were treated intravenously with a fully serotype 3-based oncolytic adenovirus Ad3-hTERT-E1A. The only grade 3 adverse reactions observed were self-limiting cytopenias. Neutralizing antibodies against Ad3 increased in all patients. Signs of possible efficacy were seen in 11/15 (73%) patients evaluable for tumor markers. Particularly promising results were seen in breast cancer patients and especially those receiving concomitant trastuzumab. The latter might suggest that Ad3 acts in a similar way to JO-1 on tumor junctions and increases drug penetration.

We first confirmed that the intravenous injection of JO-4 was safe in hDSG2 transgenic mice. Next we tested JO-4 as a single agent in *M. fascicularis* at a relatively low dose (0.6 mg/kg) that we determined based on allometric scaling of the therapeutic dose used in mouse experiments. We followed the animals three days and performed a full necropsy to assess toxic side effects on normal tissues. In this study, we did not find critical JO-4 related abnormalities. In a second NHP study we combined JO-4 with



Doxil. JO-4 was used at a dose that was effective in mouse tumor models (2 mg/kg). Doxil was injected at a dose that will be used in the clinical trial (40 mg/m<sup>2</sup>). Analysis of clinical symptoms and blood parameters did not show remarkable signs of toxicity. Upon necropsy, performed at 6 hours after the second injection cycle, no treatment-related abnormalities in gross examination of organs and histological analysis of tissue sections were observed. Therefore, the combination of JO-4 and Doxil was safe in an adequate animal model. Blood and tissue samples from the second study were also used to study JO-4 and Doxil blood clearance and tissue biodistribution. Despite the limitations of the study (N=1), a series of cautious conclusions can be made: *i)* The concentration of shed DSG2 in the serum did not increase after JO-4 injection, indicating minimal interaction with DSG2 on normal tissues. (In contrast, in mouse tumor models, JO-4 triggered the cleavage and shedding of DSG2 in xenograft tumors, because in tumors, not all DSG2 is trapped in junctions [19]). *ii)* As expected, serum IgG antibodies against JO-4 developed after one week. However the concentration of anti-JO-4 antibodies was at a level that was completely saturated after the second JO-4 injection (no detectable anti-JO-4 antibodies at 4 hours after the second injection). Serum antibodies had no effect on the pharmacokinetics of JO-4 after the second injection. Corresponding JO-4/anti-JO-4 IgG immune complexes were found by ELISA and immunofluorescence analysis of tissue sections in a series of lymphoid (spleen, lymph nodes) and non-lymphoid organs (adrenals, epididymis, lung, kidney, gall bladder, and pancreas). *iii)* Non-opsonized JO-4 was detected (at concentrations less than 50 ng per 100 mg tissue) in adrenals, epididymis, lung, liver, and kidneys. *iv)* JO-4 pretreatment resulted in a longer Doxil retention in the blood. Depositions of Doxil were found in the liver, adrenals, brain, bone marrow, lymph nodes and spleen. The most notable effect of JO-4 was that Doxil concentrations were higher in the liver of the JO-4 pre-treated animal, while lower Doxil concentrations in adrenals, bone marrow, heart, lymph nodes, seminal vesicle, and spleen. We speculate that JO-4 increases the liver's capacity to trap Doxil so that other tissues are less exposed. Clearly this needs to be validated in more animals.

Based on these findings, in the next IND-enabling toxicology study with clinical grade JO-4, we plan to test whether accumulative toxicity develops after 4 cycles of treatment given at an interval of 4 weeks (based in the design of the clinical trial). We will pay specific attention to adrenals and liver functions. Furthermore, to prevent opsonization of JO-4, we consider treatment with prednisolone treatment for 48 hours before JO-4 injection to suppress anti-JO-4 antibodies [37].

In summary, our studies in DSG2 transgenic mice and non-human primates did not show critical JO-4-related toxicity. These data together with favorable FDA comments to a recently submitted pre-IND application create a basis for a successful clinical application of the JO-4 technology. Our current efforts are focused on the cGMP production of a JO-4 protein in which the His tag has been removed and a large scale GLP-toxicology study in NHPs.

## **Material and Methods**

**Proteins.** Recombinant human DSG2 protein was from Leinco Technologies, Inc. (St. Louis, MO). JO-4 was produced in *E. coli* with an N-terminal 6-His tags, using the pQE30 expression vector (Qiagen, Valencia, CA) and purified by Ni-NTA agarose chromatography as described elsewhere [38]. JO-4 preparations used in animals were depleted of bacterial endotoxin using Endotrap blue 1/1 columns (Hyglos GmbH, Bernried, Germany).

**Cell lines.** Ovc316 cells are Her2/neu positive epithelial tumor cells derived from an ovarian cancer biopsy [39]. Ovc316 cells were cultured in MEGM (Lonza, Mapleton, IL), containing 3 µg/l hEGF, 5 µg/l insulin, 5 mg/l hydrocortisone, 26 mg/l bovine pituitary extract, 25 mg/l amphotericin B and supplemented with 1% FBS, 100 I.U. penicillin, 100 µg/l streptomycin, 10 mg/l ciprofloxacin. MDA-MB-231-luc-D3H2LN cells (Caliper Life Sciences, Hopkinton, MA), a triple-negative breast cancer cell line,

were cultured in Leibovitz's L-15 medium supplemented with 10% FBS, 100 I.U. penicillin, 100 µg/l streptomycin.

**Surface Plasmon Resonance:** *Surface Plasmon Resonance:* Acquisitions were done on a BIAcore 3000 instrument. HBS-P (GE-Healthcare, Pittsburgh, PA) supplemented with 2 mM CaCl<sub>2</sub> was used as running buffer at a flow rate of 15 µl/min. Immobilization on CM5 sensorchip (BIAcore) was performed using JO-4 at 10 µg/ml diluted in 10 mM Acetate buffer pH 4.5 injected for 10 minutes on ethyl(dimethylaminopropyl) carbodiimide (EDC)/N-Hydroxysuccinimide (NHS) activated flow-cell (7.500 RU). A control flow-cell was activated by (EDC/NHS) and inactivated by ethanolamine. Different concentrations of DSG2 (12.5 to 200nM) were injected for 3 minutes of association followed by 2.5 minutes of dissociation time, and the signal was automatically subtracted from the background of the ethanolamine deactivated EDC-NHS flow cell. Regeneration was done by a two-time injection of EDTA 10mM for 2 minutes. Kinetic and affinity constants were calculated using the BIAeval software.

**Crystallography:** Crystallization conditions for Ad3 fiber knob mutant V239D were screened using the service of the High Throughput Screening Lab at Hauptman Woodward Medical Research Institute. For diffraction studies, V239D mutant protein was crystallized using the hanging drop method. Crystals were grown using a reservoir solution of 1.75M MgSO<sub>4</sub>(7H<sub>2</sub>O) in TAPS buffer 0.1M pH9.0 and a protein solution of 8mg/ml. Crystals were frozen using a cryoprotectant composed of 85% reservoir and 15% glycerol (v/v). Data collection was performed at 100K on an ID23-2 [40] of the ESRF using the EDNA pipeline [41]. Data were indexed and scaled using XDS/XSCALE [42, 43] and the structure solved by molecular replacement (PDB 1H7Z) with the program PHASER [44]. The model was built and refined using COOT [45] and BUSTER [46], respectively. The entry "Structure of the adenovirus 3 knob domain V239D mutant" has been assigned the PDB ID code 4WYJ.

**Animal studies:** All experiments involving animals were conducted in accordance with the institutional guidelines set forth by the University of Washington.

**Mice:** Mice were housed in specific-pathogen-free facilities. Immunodeficient (CB17) mice [strain name: NOD.CB17-Prkdc<sup>scid</sup>/J] were obtained from the Jackson Laboratory. Human DSG2 transgenic mice contain 90kb of the human DSG2 locus and express hDSG2 at a level and in a pattern similar to humans [20]. MDA-MB-231-luc-D3H2LN and ovc316 xenograft tumors were established by injection of the corresponding tumor cells into the mammary fat pad (1:1 with Matrigel) of CB17 mice. JO-4 was intravenously injected one hour before the application of PEGylated liposomal doxorubicin/Doxil<sup>TM</sup> (Be Venue Laboratories, Inc., Bedford, OH), Tumor volumes were measured three times a week. Each treatment group consisted of a minimum of 5 mice. Animals were sacrificed and the experiment terminated when tumors in one of the groups reached a volume of 800 mm<sup>3</sup> or tumors displayed ulceration.

**In vivo imaging:** *In vivo* luciferase imaging was performed on a IVIS Lumina Series II (PerkinElmer Inc., Waltham, MA). Mice with subcutaneous MDA-MB-231-luc-D3H2LN tumors were imaged as follows: Animals were injected i.p. with 15 mg/ml Luciferin in PBS at 150 mg/kg. Five minutes later animals were transferred to anesthesia induction chamber and animals were induced for 3 minutes. Animals were then transferred to the IVIS imaging chamber. 10 minutes after substrate injection, the imaging procedure was started. Two sequences of 5 X 1 min exposures were recorded at small binning and F-stop of 1. For the first sequence the primary tumor site was shielded, for the second sequence the shielding was removed. For analysis, regions of interest (ROIs) were put over the primary tumor site and the metastatic site (remainder of the mouse body) and the total flux (photons per second summed over the area of the ROI) of the ROIs was measured using Living Image 4.0 Software (PerkinElmer Inc.).

**Human DSG2 Western blot.** Primary tumors and mesenteric metastatic lesions were collected and homogenized in PBS with protease inhibitors (Roche, Mannheim, Germany) with a QIAGEN TissueRuptor (Qiagen, Valencia, CA). Homogenates were sonicated on ice for 30 s and then spun down at 4 °C at maximum speed in a table top centrifuge for 20 minutes. Samples in reducing Laemmli buffer were

separated via SDS-PAGE and blots were incubated with primary anti-human DSG2 (Santa Cruz Biotech, 6D8, 1:1000) and anti-human beta actin (Sigma) (1:3000) antibodies and a HRP-linked secondary anti-mouse IgG antibody (1:2000).

***Macaques:*** All studies were performed by the Washington State Northwest Primate Research Center (WaNPRC) at the University of Washington. JO-4 and Doxil<sup>TM</sup> (Ben Venue Laboratories, Bedford, OH) were infused intravenously at a rate of 2 ml/min. Blood samples were drawn at the time points indicated. At the end of the observation period, a complete necropsy was performed on selected animals.

***Preparation of tissues for ELISA:*** 100 mg of tissues in PBS-0.05%Tween20 were homogenized using the TissueRuptor system (Qiagen, Valencia, CA), sonicated for 20 seconds, and subjected to three freeze/thaw cycles. Cell debris was spun down and supernatants from lysed tissues were used in the JO-4 and Doxil ELISA at 1:5, 1:20, and 1:100 dilutions. Two independent tissue samples were used.

***DSG2 ELISA:*** ELISA was performed using the goat polyclonal anti-DSG2 antibody AF947 (R&D Systems, Minneapolis, MN) and the mouse monoclonal antibody 6D8 directed against ECD3 (AbD Serotec, Raleigh, NC). The detection limit of the DSG2 ELISA was 0.5 ng/ml. The antibodies cross-react with macaque DSG2.

***JO-4 ELISA:*** The ELISA consisted of a polyclonal rabbit antibody directed against the Ad3 fiber knob as capture antibody and a mouse monoclonal anti-Ad3 fiber knob antibody (clone 2-1) as detection antibody. The sensitivity of the ELISA was 0.5 ng/ml.

***Anti-JO-4 antibody ELISA:*** Polyclonal Ad3 fiber antibody was absorbed on ELISA plates followed by JO-4 protein at a saturating concentration. Dilutions of monkey serum (1:10, 1:100, 1000) were added and binding was detected with either goat-anti monkey IgG+IgA+IgM-HRP (MyBioSource, San Diego, CA).

***Doxil ELISA:*** To measure liposomal doxorubicin/Doxil concentrations, mice were sacrificed and blood was flushed from the circulation with 10 mL PBS. Tissues were homogenized in PBS/0.1% Tween 20/protease inhibitors. Anti-PEG (PEG, polyethylene glycol) antibody AGP4 was used as a capture

antibody [27]. Binding was detected with anti-PEG antibody 3.3.-biotin followed by a streptavidin–HRP conjugate.

***IFN $\gamma$  ELISA:*** Serum interferon  $\gamma$  levels were measured using an ELISA kit from Invitrogen (Grand Island, NY).

***DSG2 Immunofluorescence:*** The following antibodies were used on 4% para-formaldehyde-fixed OCT sections: anti-PEG mAb-AGP3-biotin [27]; anti-Ad3 fiber knob mAb- clone 2-1; goat- $\alpha$ -human DSG2 (R&D Systems); anti-monkey IgG-FITC, Non-human Primate Reagent Resource Cat#: 1B3-FITC.

### **Conflict of Interests**

AL and DC are co-owners of Compliment Corp., a start-up company that is involved in the clinical development of the JO-4 technology.

### **Acknowledgments**

The work was supported by NIH grants R01 CA080192 (AL), R01 HLA078836 (AL), and the Pacific Ovarian Cancer Research Consortium/Specialized Program of Research Excellence in Ovarian Cancer Grant P50 CA83636 (NU), a grant from Department of Defense (W81XWH-12-1-0600) (AL), a grant from BRIM Biotechnology, Inc and a grant from Samyang Biopharmaceuticals Corporation. The NHP studies were supported by the National Primate Research Center at the University of Washington, NIH grant RR00166 and the National Center for Research Resources and the Office of Research Infrastructure Programs (ORIP) of the National Institutes of Health through Grant Number OD 010425. M.R. is a recipient of a fellowship award from the Deutscher Akademischer Austauschdienst (DAAD). We would like to acknowledge the beam line staff on 23-2 at European Synchrotron Radiation Facility (ESRF). We thank Alexandra Sova for help with organizing the NHP data.

### **Supplementary Material**

**Suppl. Fig.1 Mouse model with invasive cancer and spontaneous metastases.** Mammary fat pad tumor derived from MDA-MB-231-luc-D3H2LN were established. **a)** The primary tumor invades and penetrates the peritoneum. **b)** primary tumors were removed when they reached a volume of ~200mm and before they became attached to the peritoneum. 5 weeks later axillary metastases were observed by *in vivo* luciferase imaging. The image also shows residual primary tumor that re-grew. Right panel: DSG2 immunofluorescence analysis of sections from the primary tumor and axillary lymph node metastases. DSG2 appears in red in cell membranes. The images are representative for the other animals.

**Suppl. Fig.2 Monitoring of therapeutic effect of JO-4+Doxil by *in vivo* imaging.** Shown are a representative control untreated (CTRL, top) and treated animal (bottom). Treatment was started at day 31.

**Suppl. Material: Pathology report for NHP-study #1**

**Suppl. Material: Pathology report for NHP-study #2**

## References

1. Lipinski CA, Lombardo F, Dominy BW, Feeney PJ (2001). Experimental and computational approaches to estimate solubility and permeability in drug discovery and development settings. *Adv Drug Deliv Rev* **46**: 3-26.
2. Lavin SR, McWhorter TJ, Karasov WH (2007). Mechanistic bases for differences in passive absorption. *J Exp Biol* **210**: 2754-2764.
3. Green SK, Karlsson MC, Ravetch JV, Kerbel RS (2002). Disruption of cell-cell adhesion enhances antibody-dependent cellular cytotoxicity: implications for antibody-based therapeutics of cancer. *Cancer Res* **62**: 6891-6900.
4. Biedermann K, et al. (2005). Desmoglein 2 is expressed abnormally rather than mutated in familial and sporadic gastric cancer. *J Pathol* **207**: 199-206.
5. Harada H, Iwatsuki K, Ohtsuka M, Han GW, Kaneko F (1996). Abnormal desmoglein expression by squamous cell carcinoma cells. *Acta Derm Venereol* **76**: 417-420.
6. Beyer I, et al. (2012). Coadministration of epithelial junction opener JO-1 improves the efficacy and safety of chemotherapeutic drugs. *Clin Cancer Res* **18**: 3340-3351.
7. Turley EA, Veisoh M, Radisky DC, Bissell MJ (2008). Mechanisms of disease: epithelial-mesenchymal transition--does cellular plasticity fuel neoplastic progression? *Nat Clin Pract Oncol* **5**: 280-290.
8. Christiansen JJ, Rajasekaran AK (2006). Reassessing epithelial to mesenchymal transition as a prerequisite for carcinoma invasion and metastasis. *Cancer Res* **66**: 8319-8326.
9. Jolly MK, Huang B, Lu M, Mani SA, Levine H, Ben-Jacob E (2014). Towards elucidating the connection between epithelial-mesenchymal transitions and stemness. *J R Soc Interface* **11**.
10. Lu M, Jolly MK, Levine H, Onuchic JN, Ben-Jacob E (2013). MicroRNA-based regulation of epithelial-hybrid-mesenchymal fate determination. *Proc Natl Acad Sci U S A* **110**: 18144-18149.
11. Choi IK, Strauss R, Richter M, Yun CO, Lieber A (2013). Strategies to increase drug penetration in solid tumors. *Front Oncol* **3**: 193.
12. Tannock IF, Lee CM, Tunggal JK, Cowan DS, Egorin MJ (2002). Limited penetration of anticancer drugs through tumor tissue: a potential cause of resistance of solid tumors to chemotherapy. *Clin Cancer Res* **8**: 878-884.
13. Minchinton AI, Tannock IF (2006). Drug penetration in solid tumours. *Nat Rev Cancer* **6**: 583-592.
14. Fessler SP, Wotkowicz MT, Mahanta SK, Bamdad C (2009). MUC1\* is a determinant of trastuzumab (Herceptin) resistance in breast cancer cells. *Breast Cancer Res Treat* **118**: 113-124.
15. Oliveras-Ferraro C, et al. (2011). Stem cell property epithelial-to-mesenchymal transition is a core transcriptional network for predicting cetuximab (Erbix) efficacy in KRAS wild-type tumor cells. *J Cell Biochem* **112**: 10-29.
16. Lee CM, Tannock IF (2010). The distribution of the therapeutic monoclonal antibodies cetuximab and trastuzumab within solid tumors. *BMC Cancer* **10**: 255.
17. Wang H, et al. (2011). Desmoglein 2 is a receptor for adenovirus serotypes 3, 7, 11 and 14. *Nat Med* **17**: 96-104.
18. Lu ZZ, et al. (2013). Penton-Dodecahedral Particles Trigger Opening of Intercellular Junctions and Facilitate Viral Spread during Adenovirus Serotype 3 Infection of Epithelial Cells. *PLoS Pathog* **9**: e1003718.
19. Beyer I, et al. (2011). Epithelial junction opener JO-1 improves monoclonal antibody therapy of cancer. *Cancer Res* **71**: 7080-7090.
20. Wang H, et al. (2012). A new human DSG2-transgenic mouse model for studying the tropism and pathology of human adenoviruses. *J Virol* **86**: 6286-6302.



21. Wang H, *et al.* (2011). Multimerization of adenovirus serotype 3 fiber knob domains is required for efficient binding of virus to desmoglein 2 and subsequent opening of epithelial junctions. *J Virol* **85**: 6390-6402.
22. Wang H, *et al.* (2013). Structural and functional studies on the interaction of adenovirus fiber knobs and desmoglein 2. *J Virol* **87**: 11346-11362.
23. Gordon AN, *et al.* (2000). Phase II study of liposomal doxorubicin in platinum- and paclitaxel-refractory epithelial ovarian cancer. *J Clin Oncol* **18**: 3093-3100.
24. Muggia FM, *et al.* (1997). Phase II study of liposomal doxorubicin in refractory ovarian cancer: antitumor activity and toxicity modification by liposomal encapsulation. *J Clin Oncol* **15**: 987-993.
25. Markman M, Kennedy A, Webster K, Peterson G, Kulp B, Belinson J (2000). Phase 2 trial of liposomal doxorubicin (40 mg/m<sup>2</sup>) in platinum/paclitaxel-refractory ovarian and fallopian tube cancers and primary carcinoma of the peritoneum. *Gynecol Oncol* **78**: 369-372.
26. Strauss R, *et al.* (2011). Analysis of epithelial and mesenchymal markers in ovarian cancer reveals phenotypic heterogeneity and plasticity. *PLoS One* **6**: e16186.
27. Su YC, Chen BM, Chuang KH, Cheng TL, Roffler SR (2010). Sensitive quantification of PEGylated compounds by second-generation anti-poly(ethylene glycol) monoclonal antibodies. *Bioconjug Chem* **21**: 1264-1270.
28. Gusella M, *et al.* (2014). Age affects pegylated liposomal doxorubicin elimination and tolerability in patients over 70 years old. *Cancer Chemother Pharmacol* **73**: 517-524.
29. Latifi A, *et al.* (2011). Cisplatin treatment of primary and metastatic epithelial ovarian carcinomas generates residual cells with mesenchymal stem cell-like profile. *J Cell Biochem* **112**: 2850-2864.
30. Baribeau S, Chaudhry P, Parent S, Asselin E (2014). Resveratrol inhibits cisplatin-induced epithelial-to-mesenchymal transition in ovarian cancer cell lines. *PLoS One* **9**: e86987.
31. Durmort C, *et al.* (2001). Structure of the fiber head of Ad3, a non-CAR-binding serotype of adenovirus. *Virology* **285**: 302-312.
32. Scheel C, Weinberg RA (2012). Cancer stem cells and epithelial-mesenchymal transition: concepts and molecular links. *Semin Cancer Biol* **22**: 396-403.
33. Pesonen S, *et al.* (2010). Prolonged systemic circulation of chimeric oncolytic adenovirus Ad5/3-Cox2L-D24 in patients with metastatic and refractory solid tumors. *Gene Ther* **17**: 892-904.
34. Koski A, *et al.* (2010). Treatment of cancer patients with a serotype 5/3 chimeric oncolytic adenovirus expressing GMCSF. *Mol Ther* **18**: 1874-1884.
35. Kim KH, *et al.* (2012). A phase I clinical trial of Ad5.SSTR/TK.RGD, a novel infectivity-enhanced bicistronic adenovirus, in patients with recurrent gynecologic cancer. *Clin Cancer Res* **18**: 3440-3451.
36. Hemminki O, *et al.* (2012). Ad3-hTERT-E1A, a Fully Serotype 3 Oncolytic Adenovirus, in Patients With Chemotherapy Refractory Cancer. *Mol Ther* **20**: 1821-1830.
37. Dykes AC, Walker ID, Lowe GD, Tait RC (2001). Combined prednisolone and intravenous immunoglobulin treatment for acquired factor VIII inhibitors: a 2-year review. *Haemophilia* **7**: 160-163.
38. Wang H, *et al.* (2007). Identification of CD46 binding sites within the adenovirus serotype 35 fiber knob. *J Virol* **81**: 12785-12792.
39. Strauss R, *et al.* (2009). Epithelial phenotype of ovarian cancer mediates resistance to oncolytic adenoviruses. *Cancer Research* **15**: 5115-5125.
40. Flot D, *et al.* (2010). The ID23-2 structural biology microfocus beamline at the ESRF. *J Synchrotron Radiat* **17**: 107-118.

41. Incardona MF, Bourenkov GP, Levik K, Pieritz RA, Popov AN, Svensson O (2009). EDNA: a framework for plugin-based applications applied to X-ray experiment online data analysis. *J Synchrotron Radiat* **16**: 872-879.
42. Kabsch W (2010). Integration, scaling, space-group assignment and post-refinement. *Acta Crystallogr D Biol Crystallogr* **66**: 133-144.
43. Kabsch W (2010). Xds. *Acta Crystallogr D Biol Crystallogr* **66**: 125-132.
44. McCoy AJ, Grosse-Kunstleve RW, Adams PD, Winn MD, Storoni LC, Read RJ (2007). Phaser crystallographic software. *J Appl Crystallogr* **40**: 658-674.
45. Emsley P, Lohkamp B, Scott WG, Cowtan K (2010). Features and development of Coot. *Acta Crystallogr D Biol Crystallogr* **66**: 486-501.
46. Bricogne G. BE, Brandl M., Flensburg C., Keller P., Paciorek W., Roversi P., Sharff A., Smart O.S., Vonrhein C., Womack T.O. (2011). BUSTER version 2.10.0. *Cambridge, United Kingdom: Global Phasing Ltd.*

**Table 1. Collection and refinement statistics**

<b>Data collection</b>	
Space group	P41212
Cell dimensions	
<i>a</i> , <i>b</i> , <i>c</i> (Å)	137.6, 137.6, 108.9
$\alpha$ , $\beta$ , $\gamma$ (°)	90, 90, 90
Resolution (Å)	44-2.65 (2.74-2.65) *
<i>R</i> <sub>sym</sub> or <i>R</i> <sub>merge</sub>	0.105(1.43)
<i>I</i> / $\sigma$ <i>I</i>	18.9(1.43)
Completeness (%)	99.0(90.3)
Redundancy	8.9(8.6)
<b>Refinement</b>	
Resolution (Å)	44.-2.65 (2.74-2.65)
No. reflections	30618 (2704)
<i>R</i> <sub>work</sub> / <i>R</i> <sub>free</sub>	0.176/0.205 (0.242/0.2835)
No. atoms	
Protein	4442
Ligand/ion	295
Water	245
B-factors	
Protein	70.
Ligand/ion	135.
Water	70.
R.m.s deviations	
Bond lengths (Å)	0.01
Bond angles (°)	1.17

\*Highest resolution shell is shown in parenthesis.

## Figure legends

**Fig. 1. Structural and functional studies with JO-4.** **a)** Ad3 fiber knob amino acid sequence with beta sheets A to J indicated by a line. JO-4 contains Ad3 fiber knobs with a valine to aspartic acid substitution in position 239 of the Ad3 fiber knob. Regions that have previously been found to be involved in DSG2 binding are boxed [22]. **b)** 3D-structure superimposition of the trimeric (wild type) Ad3 fiber knob and the V239D mutated fiber knob. The common structure appears in grey, the EF loops of wild-type and mutant Ad3 knob monomers are labelled in blue and green, respectively. **c)** Shown is the interactions between D239 and K275 in the mutant and the new position of the L240 residue. Residue labels are colored green for the mutant and gray for wt. H-bonds between D239 and K275 are shown in dashes. **d)** Affinity of JO-4 to DSG2 measured by Surface Plasmon Resonance. JO-4 was immobilized on sensorchips, and background was automatically subtracted from the control flow cell. DSG2 were injected for 3 minutes at a concentration range from 12.5 to 200 nM and kinetics and affinity parameters were evaluated using the BIAeval software ( $k_a = 3.3 \cdot 10^5 \text{ M}^{-1}\text{s}^{-1}$ ;  $k_d = 4.7 \cdot 10^{-4} \text{ s}^{-1}$ ;  $K_D = 1,4 \text{ nM}$ ).

**Fig.2. Efficacy studies with JO-4 and Doxil in mouse models.** **a)** Efficacy study in mammary fat tumor pad model using primary ovarian cancer (ovc316) cells. Treatment was started when tumors reached a volume of  $100 \text{ mm}^3$ . Mice were injected intravenously with Doxil (1 mg/kg or 3mg/kg) alone or in combination with 2 mg/kg JO-4. Treatment was repeated weekly. N=10. **b-f)** Studies in the spontaneous metastasis model based on MDA-MB-231-luc-D3H2LN cells. **b)** *in vivo* luciferase imaging of a representative animal. The primary tumor in the mammary fat pad forms metastasis in regional lymph nodes (LN) e.g. pancreatic and mesenteric lymph nodes. **c)** DSG2 immunofluorescence analysis of sections from the primary tumor and mesenteric lymph node metastases. DSG2 appears in red in cell membranes. Nuclei are stained in blue **d)** Western blot analysis of primary tumor and metastases with DSG2 antibodies.  $\beta$ -actin is used as a loading control. A representative animal is shown. **e, f)** Comparison

of *in vivo* luciferase signal in the primary tumor (e) and metastasis (f) one day before and 5 days after treatment with Doxil or JO-4 + Doxil. Shown is the total flux of the primary tumor or metastasis ROI after treatment divided by the ROI before treatment. Shown are averages of imaging sequences of five images each.

**Fig.3. NHP study #1 (JO-4 alone): Three day toxicity study in macaques injected intravenously with 0.6 mg/kg of JO-4. a)** Experimental design. Two sedated *M. fascicularis*, A10271 (A-71) (age 4y8m, weight 5.5kg) and A10272 (A-72) (age 5y, weight 6.96kg) were injected through the saphenous vein with 5 ml of JO-4 at a dose of 0.6 mg/kg at an infusion rate of 2 ml/min). Blood samples were collected daily. A full necropsy was performed at day 3. **b)** Shown are hematological parameters that were different from normal. The normal range is marked by the grey shaded area.

**Fig.4. NHP study #2 (JO-4+Doxil): Blood analysis. a)** Experimental design: Two sedated *M. fascicularis*, A11288 (A-88) (age 4y11m, weight 5.0 kg) and A11293 (A-93) (age 5y10m, weight 6.1 kg) were injected through the saphenous vein with 5ml of saline (A-93) or 5ml of JO-4 at a dose of 2 mg/kg (A-88) at an infusion rate of 2 ml/min). One hour later both animals received an intravenous injection of 20 ml of Doxil at a dose of 40 mg/m<sup>2</sup> (1.1 mg/kg). Blood was collected at the indicated time points. **b)** One set of blood samples was submitted to the UW Clinical Laboratory for CBC and blood chemistry analysis. A second set of plasma samples was used for measuring the concentrations of JO-4, anti-JO-4 antibodies, Doxil, DSG2, and pro-inflammatory cytokines. Blood cell counts: Treatment related changes were observed for white blood cells, neutrophils, and lymphocytes. All other hematological parameters including red blood cell, platelet, monocyte, eosinophil, basophil counts were normal. **c)** Blood chemistry. Treatment related changes were observed for AST and ALT. Sodium, potassium, chloride, glucose, blood urea nitrogen, creatinine, total protein, albumin, globulin, A:G ratio, total bilirubin,

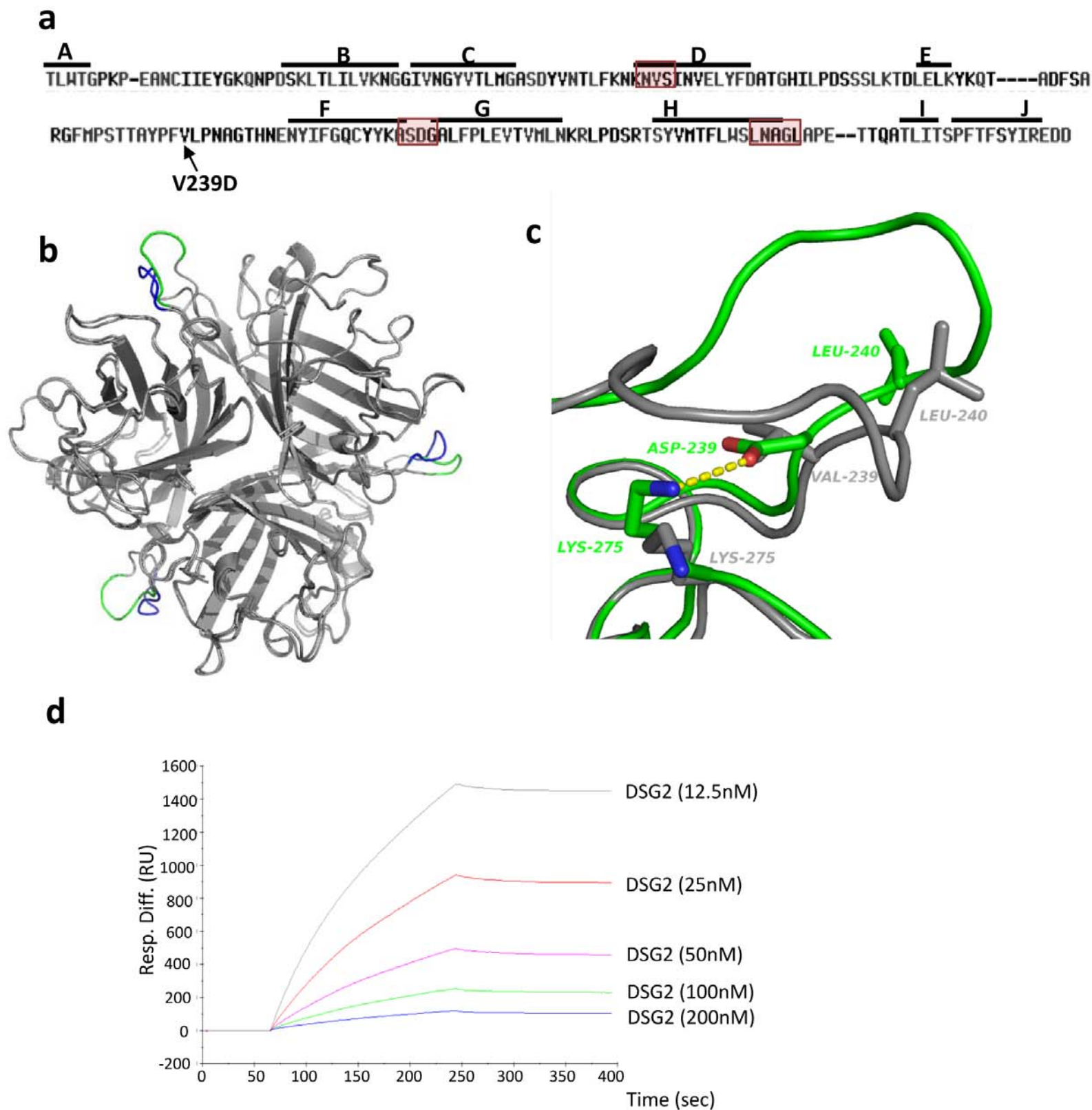
calcium, magnesium, phosphate, cholesterol, alkaline phosphatase, and GGT levels were unremarkable.

**d)** Serum interferon- $\gamma$  levels were measured by ELISA. For all analyzed serum proteins, at least two serum dilutions in duplicates were analyzed in two independent ELISAs. **e)** Serum DSG2 (sDSG2) ECD concentrations.

**Fig.5. NHP study #2 (JO-4+Doxil): JO-4 analysis.** **a)** JO-4 concentrations were measured by ELISA. In animal A-88, there was no JO-4 detectable before injection. Animal A-93 did not show detectable JO-4 signals at all. **b)** anti-JO-4 serum antibodies. Polyclonal Ad3 fiber antibody was absorbed on ELISA plates followed by JO-4 protein at a saturating concentration. Dilutions of monkey serum (1:10, 1:100, 1:1000) were added and binding was detected with either goat-anti monkey IgG+IgA+IgM-HRP or goat anti-monkey IgG-HRP (MyBioSource). There were no significant differences in OD450 values for both conjugates indicating that most of the anti-JO-4 antibodies were IgG. Shown is OD450 at 1:100 dilution, using anti-monkey IgG conjugate. **c)** JO-4 concentrations in tissues. **d)** anti-JO-4 antibodies (OD450 per 100mg/tissue)

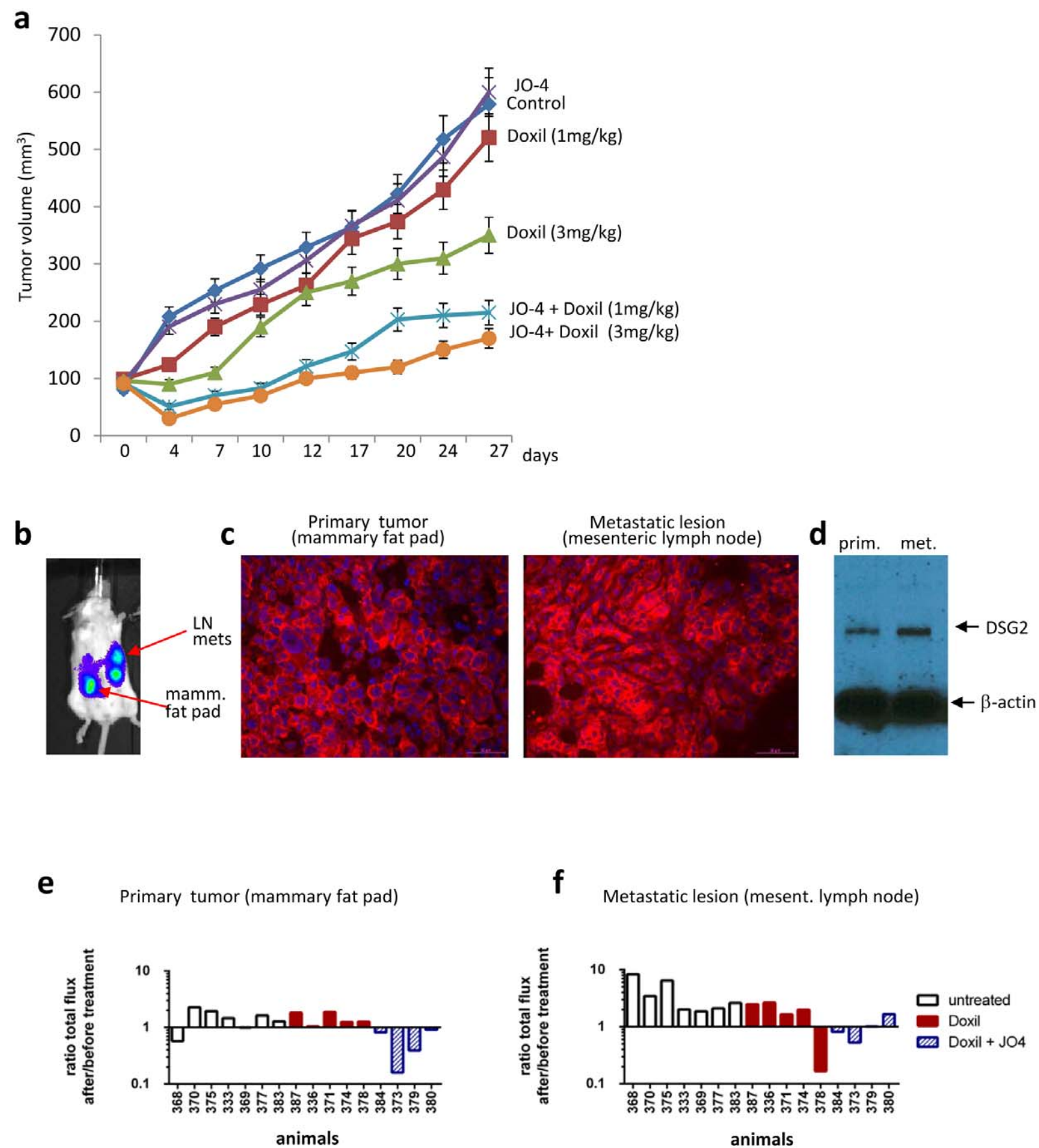
**Fig.6. NHP study #2 (JO-4+Doxil): Immunofluorescence analysis of tissue sections.** **a)** Presence of JO-4 in tissues. Staining for JO-4 appears in green, nuclei are blue. **b)** Staining of adrenals sections with anti JO4 antibodies (green) and anti-DSG2 antibodies (red). **c)** Staining of adrenals section with anti JO-4 antibodies (red) and anti-monkey IgG-FITC from NIH Nonhuman Primate Reagent Resource (green). **d)** Staining for JO-4 (red) and the Kupffer cell marker F4/80 (green). **e)** Staining of adrenal and kidney sections for Doxil using antibodies against PEG (red).

**Fig. 7. NHP study #2 (JO-4+Doxil): Analysis of Doxil concentrations measured by ELISA. a)** serum Doxil levels. **b)** Doxil concentration in tissues. Shown are average values from two independent samples of each organ.

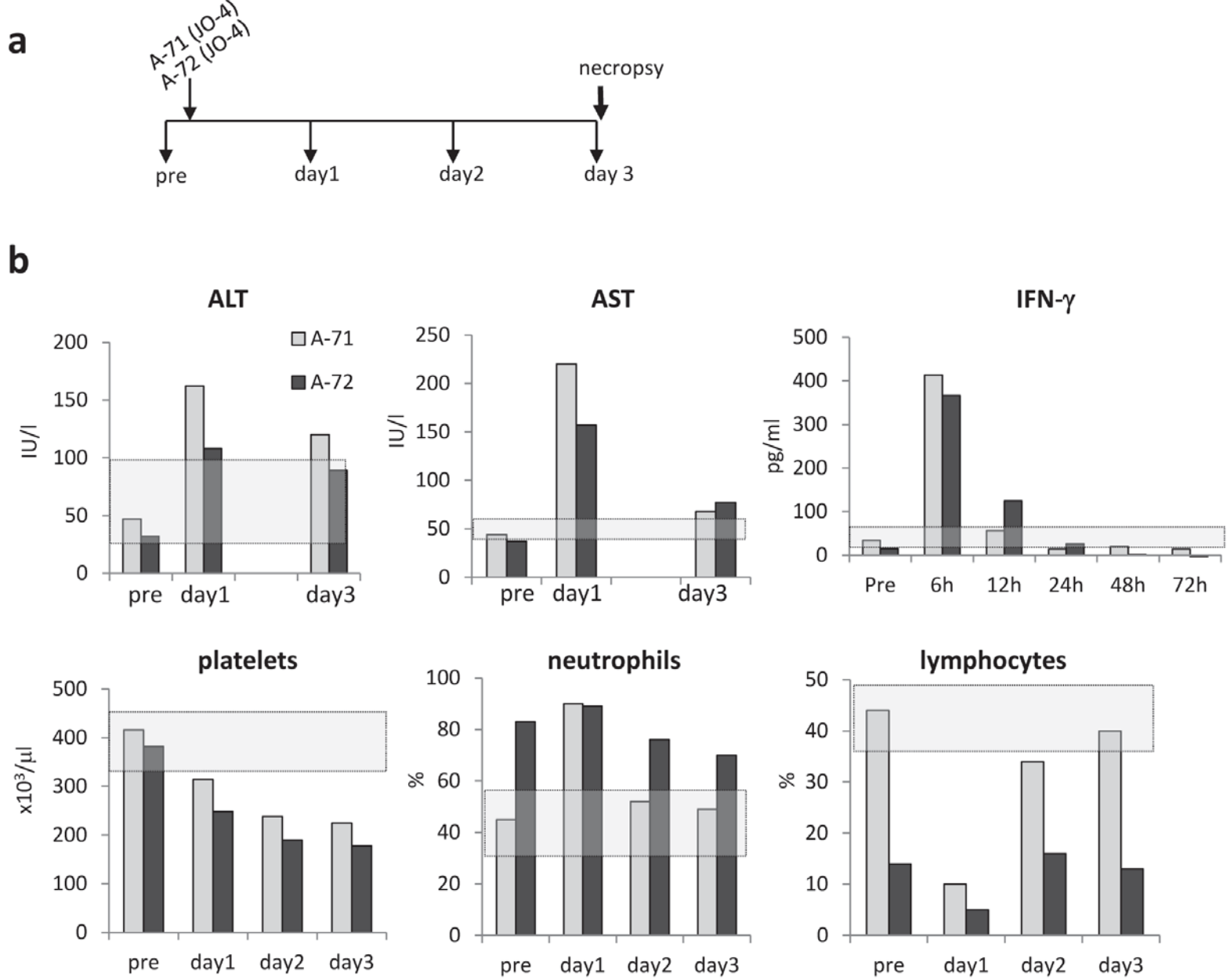


**Figure 1**

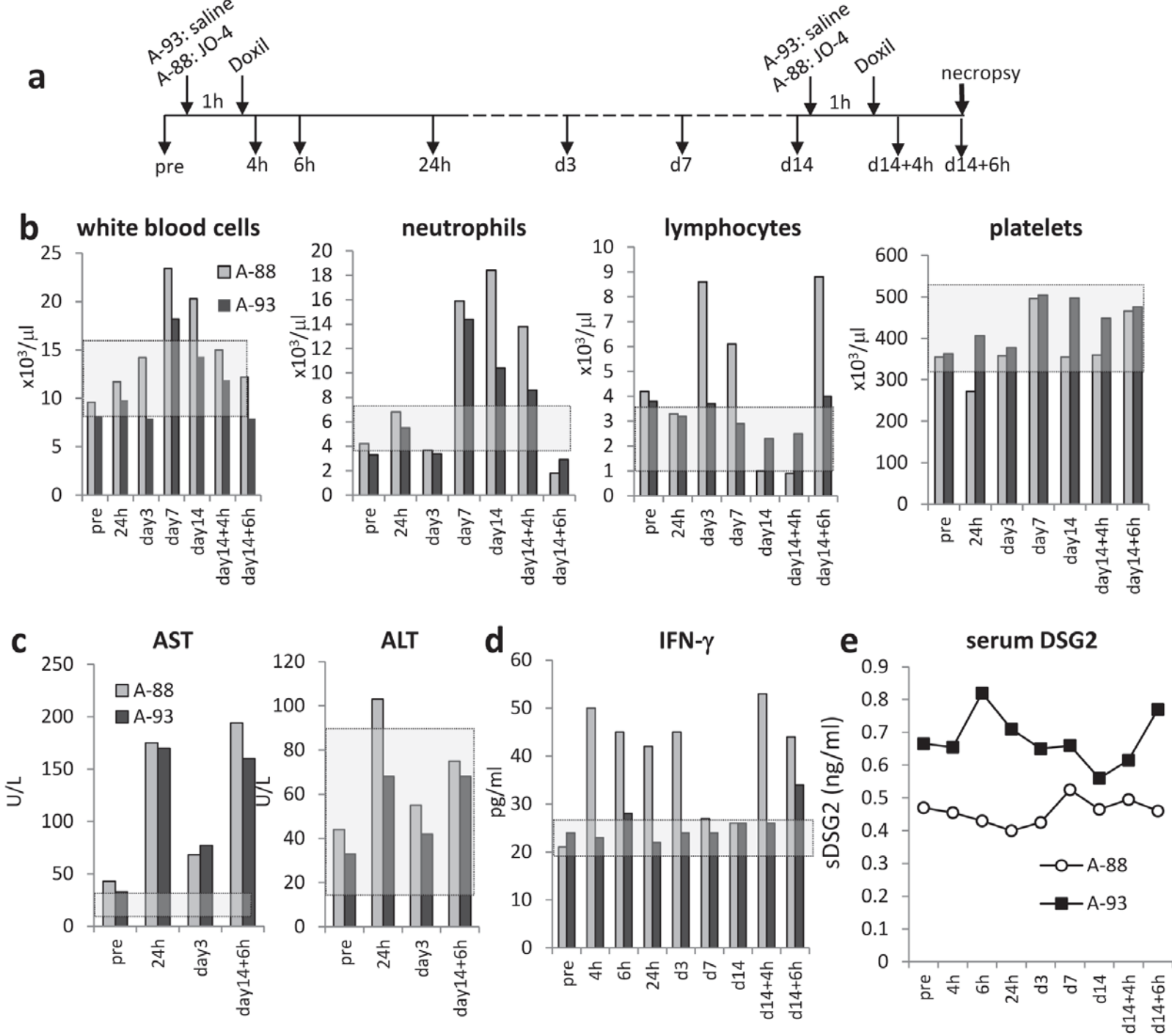




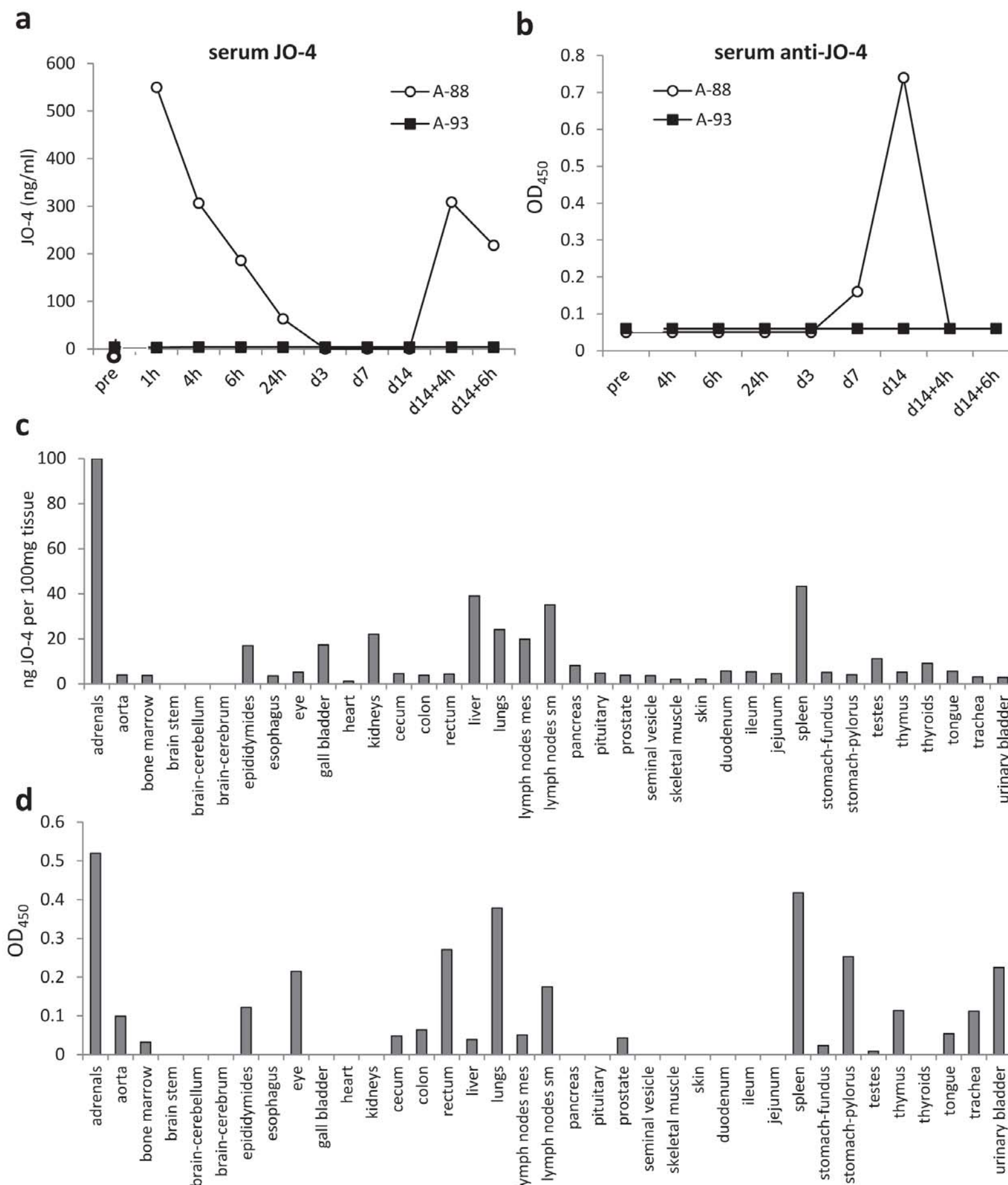
**Figure 2**



**Figure 3**

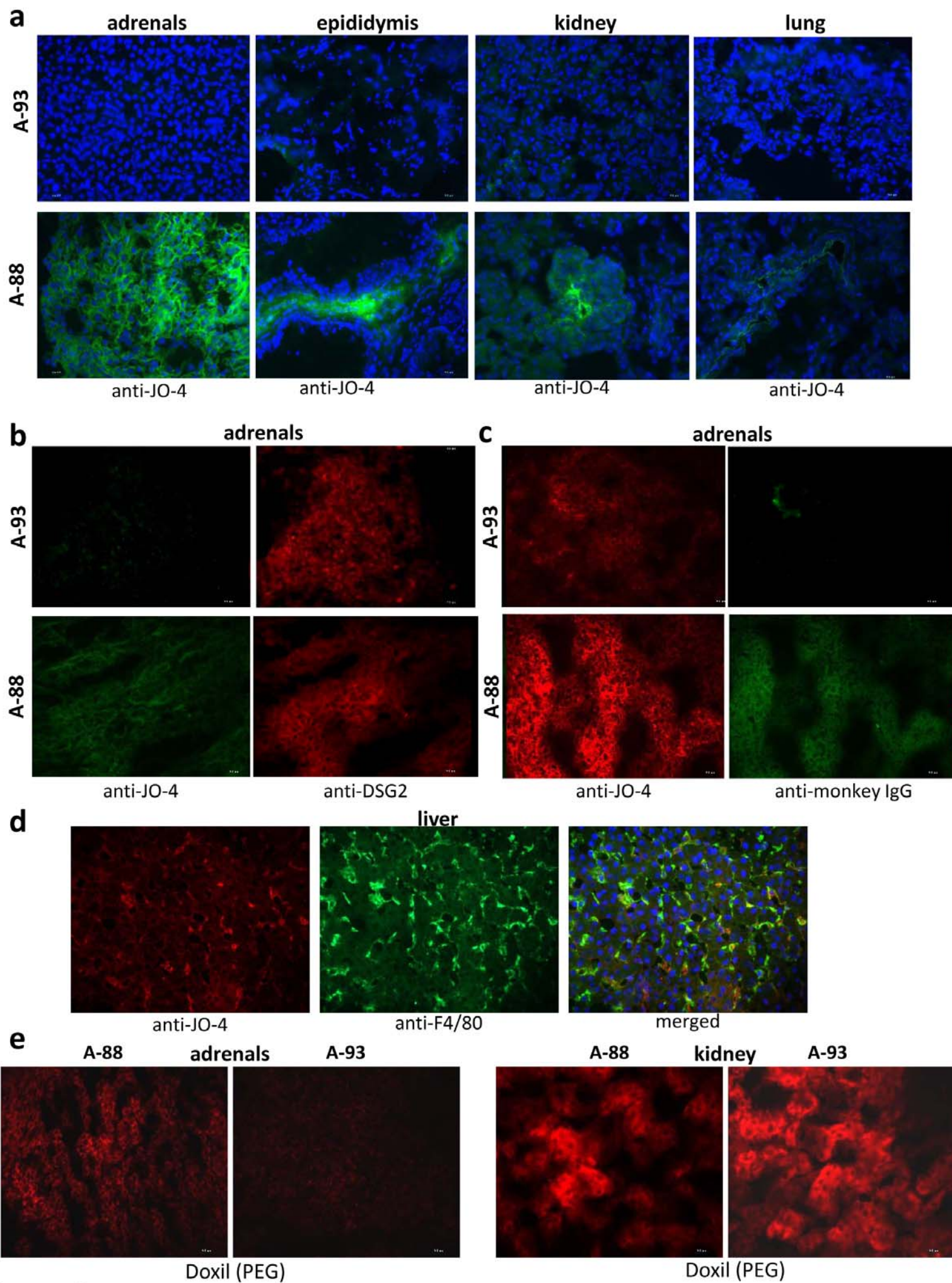


**Figure 4**



**Figure 5**





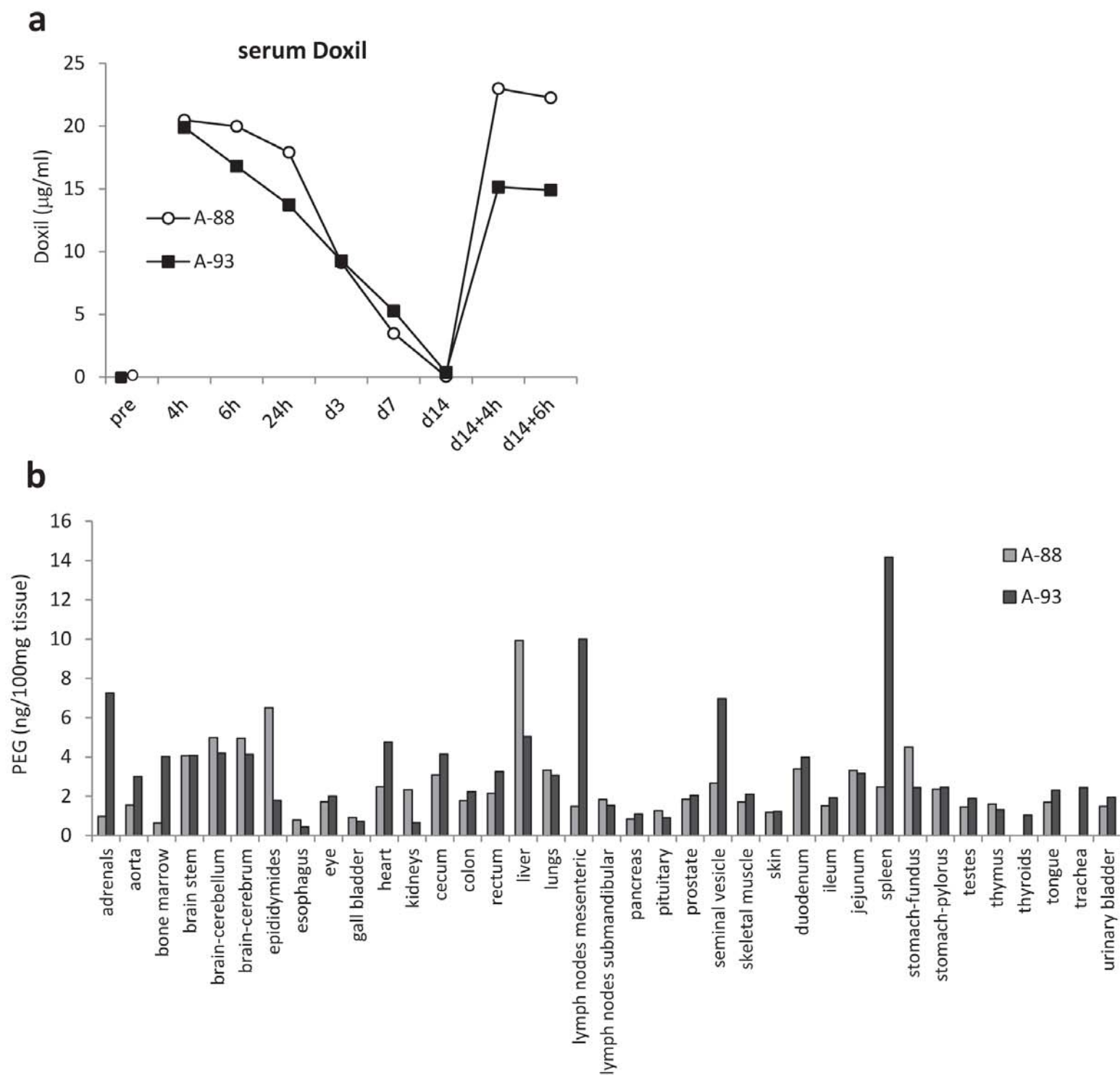
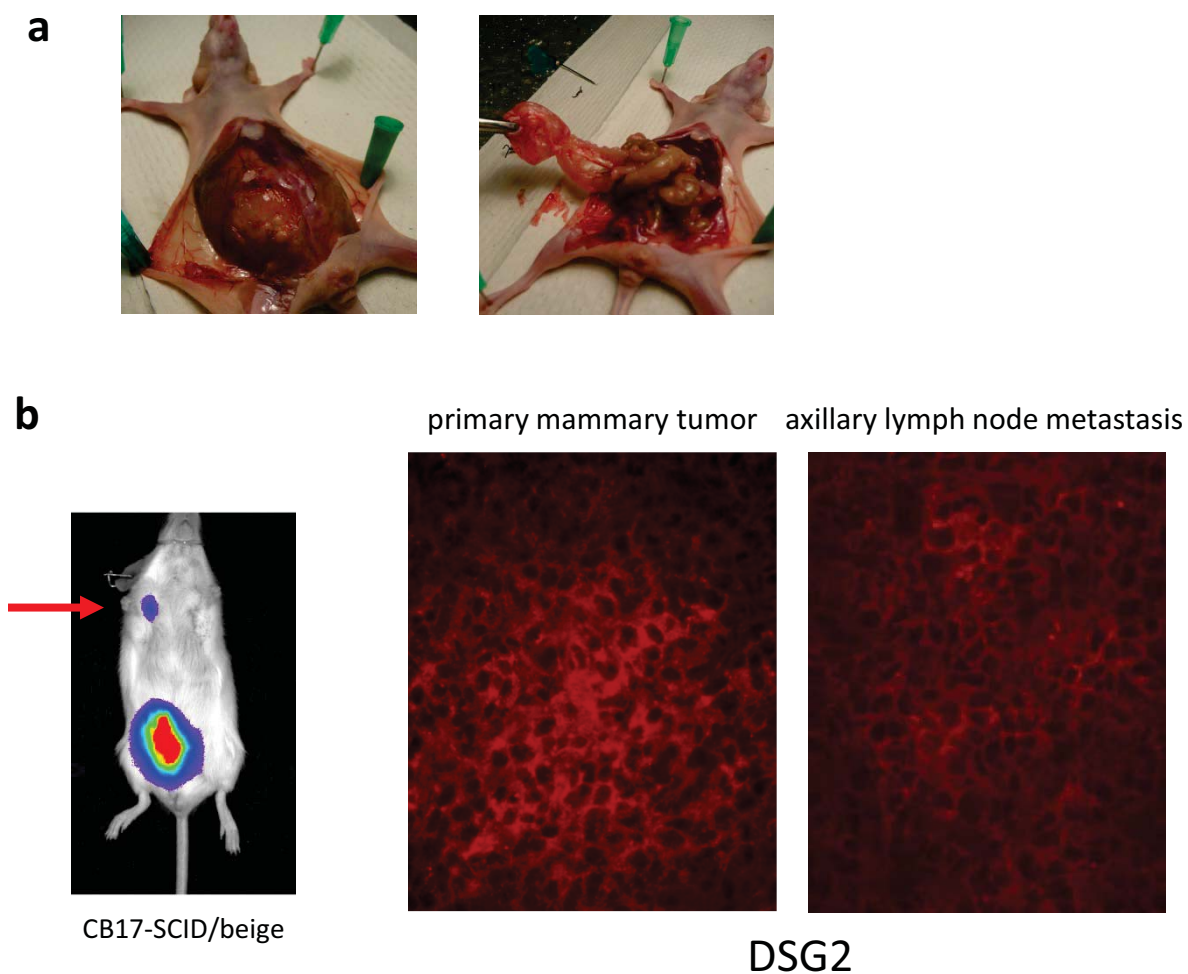
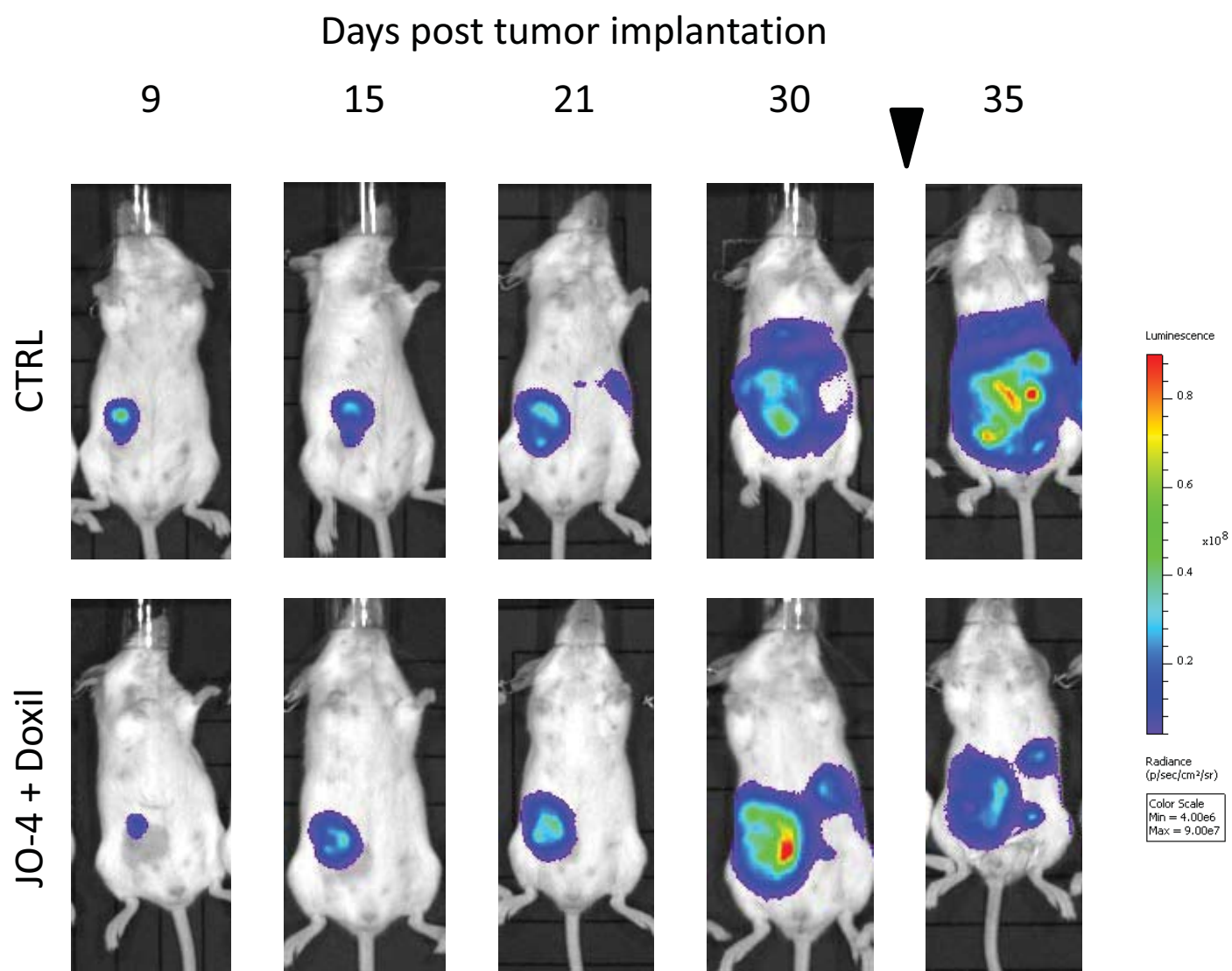


**Figure 7**



**Suppl. Fig.1 Mouse model with invasive cancer and spontaneous metastases.** Mammary fat pad tumor derived from MDA-MB-231-luc-D3H2LN were established. **a)** The primary tumor invades and penetrates the peritoneum. **b)** primary tumors were removed when they reached a volume of ~200mm and before they became attached to the peritoneum. 5 weeks later axillary metastases were observed by *in vivo* luciferase imaging. The image also shows residual primary tumor that re-grew. Right panel: DSG2 immunofluorescence analysis of sections from the primary tumor and axillary lymph node metastases. DSG2 appears in red in cell membranes. The images are representative for the other animals.





**Suppl. Fig.2 Monitoring of therapeutic effect of JO-4+Doxil by *in vivo* imaging.** Shown are a representative control untreated (CTRL, top) and treated animal (bottom). Treatment was started at day 31.



University of Washington  
National Primate Research Center

Accession # 12-165  
Submission Date 26 July 2012

## DIAGNOSTIC LABORATORY NECROPSY REPORT

Requester DR Investigator Lieber Animal ID # A10271  
Species Mfl Requester's Phone \_\_\_\_\_

Date of Death July 26, 2012 Date of Necropsy July 26, 2012 Time 8:30am Pathologist AB

Nutritional Condition: ☒ Adequate ☐ Marginal ☐ Poor ☐ Obese

Other Tests Required: ☐ Sero ☐ Micro ☐ Parasit ☐ Other \_\_\_\_\_

Other Diagnostic Samples \_\_\_\_\_

Type of report: ☒ Final 31 Aug 2012 ☒ Preliminary 27 July 2012 ☐ Amended \_\_\_\_\_

Clinical History: this animal was assigned to the "Safety studies with a companion therapeutic for chemotherapy drugs and monoclonal antibodies to treat cancer" protocol. There was a transient mild leukocytosis and neutrophilia on July 24<sup>th</sup> and mild elevation in ALT and AST on July 25-26.

Gross Description: a 4.81 year old, 5.54 kg, male *M. fascicularis* is submitted in good nutritional and post mortem condition. No external lesions or gross lesions are seen.

Gross Diagnosis(es): None

### Histological Findings:

Gastro-intestinal tract: there is moderate to occasionally severe, lymphocytic plasmacytic and mildly eosinophilic inflammation, extending from the stomach into the large intestine. Plasma cells often predominate. There are multifocal hyperplastic lymphoid aggregates in the deep mucosa and submucosa, coalescing in the ileum. There are mixed bacteria in the lumen, and rare ciliates. Villi are blunted in the duodenum and appear more robust in the jejunum. Low numbers of small lymphocytes extend into the mucosal epithelium within villi to mid mucosa.

Sections from the brain, cerebellum, brain stem, eye, lymph nodes (mesenteric (slide 4) and submandibular (slide 5), diffuse mild to moderate reactive hyperplasia), left and right adrenal glands, left and right kidneys (few sloughed renal tubular epithelial cells), urinary bladder, lung (normal peribronchial and perivascular lymphoid tissue, occasional mild respiratory epithelial hyperplasia), left and right testes, seminal vesicle, prostate gland, thymus, bone marrow core and cytology / impression smear (mild myeloid hyperplasia with orderly maturation and adequate erythroid and megakaryocytic cells and iron stores), trachea (mild, multifocal submucosal lymphoid hyperplasia), liver and gall bladder (minimal lymphocytic, plasmacytic, neutrophilic and eosinophilic cholangiohepatitis), spleen (mild lymphoid follicular hyperplasia, mild to moderate mixed extramedullary hematopoiesis), heart (moderate myofiber anisokaryosis), aorta, skeletal muscle, skin, esophagus and pancreas are examined and no histologic changes seen with the exception of those stated.

---

Final Principal Diagnosis(es):

---

1. Gastroenterocolitis, diffuse, moderate to severe, lymphocytic, plasmacytic and mildly eosinophilic.
- 
- 

Cause of Death: Experimental euthanasia.

Histology Comments: histologic examination is consistent with gastroenterocolitis, changes which are commonly seen within the colony. The etiology of these changes are likely multifactorial. Interpret with antemortem physical exam findings to evaluate clinical significance. The transient leukocytosis / neutrophilia may have been due to stress, as it was mild and resolved quickly. Other minor histologic changes as stated are unlikely to have been clinically significant.

Pathologist\_\_\_\_\_AB\_\_\_\_\_

University of Washington  
National Primate Research Center

Accession # 12-166  
Submission Date July 26, 2012

### DIAGNOSTIC LABORATORY NECROPSY REPORT

Requester DR Investigator Lieber Animal ID # A10272  
Species Mfl Requester's Phone \_\_\_\_\_

Date of Death July 26, 2012 Date of Necropsy July 26, 2012 Time 9:30am Pathologist AB

Nutritional Condition: ☒ Adequate ☐ Marginal ☐ Poor ☐ Obese

Other Tests Required: ☐ Sero ☐ Micro ☐ Parasit ☐ Other \_\_\_\_\_

Other Diagnostic Samples \_\_\_\_\_

Type of report: ☒ Final 31 Aug 2012 ☒ Preliminary July 27, 2012 ☐ Amended \_\_\_\_\_

Clinical History: this animal was assigned to the "Safety studies with a companion therapeutic for chemotherapy drugs and monoclonal antibodies to treat cancer" protocol. The hematology data shows leukocytosis and neutrophilia July 23-26, with monocytosis in the 26<sup>th</sup>, and mild elevation in AST on July 24 and 26.

Gross Description: a 5 year old, 6.96 kg, male *M. fascicularis* is submitted in good nutritional and post mortem condition. No external lesions are seen. Internal organs are grossly normal.

Gross Diagnosis(es): None

Gross comments: No gross lesions are seen. Microscopic examination is pending.

#### Histological Findings:

Brain stem: there is multifocal, mild perivascular acute hemorrhage within the brain stem, unassociated with inflammation or gliosis, interpreted to be most consistent with an agonal change.

Lung: there is multifocal, minimal to mild interstitial, mixed and neutrophilic pneumonia with scattered syncytial cells, mild alveolar edema and mild type II pneumocyte hyperplasia. Alveoli in these areas contain small amounts of foamy macrophages or are obscured by collapsed interstitium. Peribronchial and perivascular lymphoid aggregates appear to be normal.

Left and right testes: there are low numbers of multinucleated cells within the seminiferous tubules, along with sloughed tubular cells. Spermatogenesis appear to be progressing in some tubules and is arrested or sparse in others. The epididymis contains dense clusters of spermatids in some tubules and other are sparse.

Seminal vesicles: tubules contain lakes of eosinophilic proteinaceous material and oval basophilic structures (spermatid heads). There are overall low numbers of spermatids.

Prostate gland: There are rare small aggregates of lymphocytes and plasma cells with fewer neutrophils within the interstitial connective tissue. Small lymphocytes occasionally extend into the tubular

epithelium. The tubular lumens are predominantly empty or contain small amounts of protein material, cell debris and sloughed epithelial cells.

Spleen: lymphoid follicles appear to be of normal size, with occasional mild hyperplasia. The splenic stroma is congested with abundant extramedullary hematopoiesis, especially of myeloid cells progressing to numerous mature neutrophils.

Bone marrow: there is moderate to occasionally marked myeloid hyperplasia, progressing to mature neutrophils and eosinophils. Erythroid cells appear adequate and are maturing, and adequate megakaryocytes are present. Iron is sparse.

Gastro-intestinal tract: there is diffuse, moderate to occasionally marked lymphocytic, plasmacytic inflammation within the stomach, small and large intestines. Fewer eosinophils and neutrophils are seen. Villi are blunted. There are multifocal hyperplastic lymphoid aggregates and follicles in the deep mucosa to submucosa. Mixed bacteria and ingesta are present in the lumen.

Sections from the cerebrum, cerebellum, pituitary gland, eye, inguinal (slide 5), mesenteric (slide 6) and submandibular (slide 7) lymph nodes (mild to moderate lymphoid follicular hyperplasia with focal tattoo ink (inguinal node)), left and right adrenal glands, left and right kidneys (rare, mild interstitial lymphocytic, plasmacytic nephritis and rare tubular epithelial cell degeneration and luminal proteinaceous material), liver (mild lymphocytic, plasmacytic periportal cholangiohepatitis, mild centrilobular hepatocellular vacuolization), urinary bladder, heart (mild anisokaryosis), thymus, pancreas, trachea, esophagus, aorta, thyroid and parathyroid gland, aorta, skin, skeletal muscle and examined and no abnormalities found with the exception of those minor stated changes described above.

---

Final Principal Diagnosis(es):

---

1. Multifocal, minimal to mild interstitial pneumonia, with mild alveolar histiocytosis; lung.
  2. Multifocal reduced spermatogenesis; testes.
  3. Splenic extramedullary hematopoiesis with myeloid predominance.
  4. Myeloid hyperplasia, moderate to marked: bone marrow.
  5. Gastroenterocolitis, diffuse, moderate to marked, chronic to mixed, with villous blunting.
- 

Cause of Death: Experimental euthanasia.

Histology Comments: There is evidence of myeloid hyperplasia with the bone marrow (cytology and fixed tissue) and spleen. This may be associated with an inflammatory stimulus and is consistent with the leukocytosis / neutrophilia seen in the hematology data, with WBC count of 25,440 on July 24th. Stress may be playing a role in the leukocytosis (but is not typically associated with myeloid hyperplasia). No infectious agents are seen within the examined tissue sections. There is diffuse gastro-enterocolitis, which may be contributing to an inflammatory response. Testicular maturation may vary in animals of the age range of 3 to 5 years of age, and the variability in spermatogenesis may be at least partially due to age / immaturity.

Pathologist \_\_\_\_\_ AB \_\_\_\_\_

University of Washington  
National Primate Research Center

Accession # 14-139  
Submission Date 14 July 2014

### DIAGNOSTIC LABORATORY NECROPSY REPORT

Requester DM Investigator AL Animal ID # A11293  
Species Mf Requester's Phone \_\_\_\_\_

Date of Death 14 Jul 2014 Date of Necropsy 14 Jul 2014 Time 4:50 pm Pathologist AB

Nutritional Condition: ☒ Adequate ☐ Marginal ☐ Poor ☐ Obese

Other Tests Required: ☐ Sero ☐ Micro ☐ Parasit ☐ Other \_\_\_\_\_

Other Diagnostic Samples \_\_\_\_\_

Type of report: ☒ Final 30 Jul 2014 ☒ Preliminary 14 July 2014 ☐ Amended \_\_\_\_\_

Clinical History: this animal was assigned to the "toxicology studies with adenovirus proteins in NHPs" protocol. No clinical abnormalities are noted. Current CBC and chemistry panel appear unremarkable.

Gross Description: this 5 year, 11 month old, 6.2 kg intact male cynomolgous macaque is presented in good nutritional and post mortem condition. The right cheek pouch is distended by spongy bedding material; the pouch appears normal after removal of the material. No other significant external lesions are observed, and all body systems, including the musculoskeletal, nervous, cardiovascular, respiratory, digestive, urogenital, endocrine, lymphatic and integumentary systems appear grossly unremarkable.

#### Gross Diagnosis(es):

1. Unremarkable gross exam

#### Gross Comments:

There were no significant gross lesions. Histology is pending. Touch imprints of bone marrow were prepared in necropsy and are stained with Wrights giemsa.

#### Histological Findings:

Lungs: sections from two lobes contain multifocal bronchiolar and alveolar aggregates of macrophages, multinucleated cells, and neutrophils, sometimes filling smaller air spaces. There is occasional amphophilic to fibrous foreign material surrounded by or within the multinucleated cells. Minimal fibroplasia is present in the surrounding connective tissue. Sections from three lobes display multifocal, mild to moderate perivascular and peribronchiolar lymphohistiocytic aggregates and pneumoconiosis with occasional alveolar histiocytic cells.

Gastrointestinal tract: there is multifocal to diffuse, moderate to severe lymphocytic, plasmacytic and eosinophilic mucosal inflammation, with multifocal, scattered moderately hyperplastic lymphoid follicles, especially in the stomach, ileum, cecum and colon. Plasma cells display multifocal Mott cell

differentiation. Villi are diffusely blunted within the duodenum and more mildly blunted in the jejunum. The colonic mucosa is diffusely edematous.

Sections of brain, cerebellum, brainstem, pituitary gland, eye and lacrimal glands, spleen (normal lymphoid activity, moderate, mixed myeloid and erythroid hematopoiesis), lymph nodes (axillary, inguinal, hilar (mild lymphoid hyperplasia, sinus histiocytosis with occasional pigmented macrophages), liver (mild centrilobular hepatocellular atrophy and minimal periportal lymphohistiocytic inflammation), gall bladder, heart (few/minimal random perivascular lymphohistiocytic cells (normal background)), aorta, kidneys (minimal parietal epithelial hyperplasia), urinary bladder, trachea, esophagus, pancreas, salivary gland, thyroid glands, adrenal glands, tongue, skeletal muscle, testicle (occasional mildly reduced spermatogenesis), epididymis (normal amounts of spermatids), seminal vesicle, prostate gland, skin (thigh and ventral abdomen with mammary gland – few dermal individual pigmented macrophages) and bone marrow histology and cytology (normal megakaryocytic, myeloid and erythroid numbers and maturation, approximately 2:1 M:E, adequate iron stores) are unremarkable besides stated minor changes.

---

Final Principal Diagnosis(es):

---

1. Pneumonia, multifocal / patchy (two lobes), mild to moderate, macrophagic and neutrophilic, with intra- and extra-cellular foreign material.
  2. Gastroenterocolitis, multifocal to diffuse, moderate to severe, mixed with villous blunting and fusion and multifocal lymphoid hyperplasia.
- 
- 

Cause of Death:                      Experimental euthanasia.

Histology Comments:    the inflammatory foci in the lungs are seen in two lobes and were unlikely to have been detectable clinically. The foreign material is seen in macrophages in bronchioles and adjacent alveoli and most likely represents aspirated ingesta or other material, unrelated to the experimental protocol. Gastroenterocolitis is commonly observed in the colony, and development of this lesion is most likely multifactorial, with potential factors including nutritional, stress or possibly food intolerances or allergies. Other minor changes are interpreted to be nonspecific background or incidental findings.

Pathologist\_\_\_\_\_AB\_\_\_\_\_

University of Washington  
National Primate Research Center

Accession # 14-138  
Submission Date 14 July 2014

### DIAGNOSTIC LABORATORY NECROPSY REPORT

Requester DM Investigator AL Animal ID # A11288  
Species Mfl Requester's Phone \_\_\_\_\_

Date of Death 14 Jul 2014 Date of Necropsy 14 Jul 2014 Time 3:40pm Pathologist AB

Nutritional Condition: ☒ Adequate ☐ Marginal ☐ Poor ☐ Obese

Other Tests Required: ☐ Sero ☐ Micro ☐ Parasit ☐ Other \_\_\_\_\_

Other Diagnostic Samples \_\_\_\_\_

Type of report: ☒ Final 29 Jul 2014 ☒ Preliminary 14 July 2014 ☐ Amended \_\_\_\_\_

Clinical History: this animal was assigned to the "toxicology studies with adenovirus proteins in NHPs" protocol. Daily clinical observations indicate normal activity, appetite and normal stools. CBC shows mild lymphocytosis (nonspecific reactivity to a number of possible antigens), and chemistry panel is unremarkable.

Gross Description: this 5 year old, 5.6 kg intact male cynomolgous macaque is presented euthanized in good post mortem and nutritional (adequate muscling and adipose stores) condition. No significant external lesions are observed, and all body systems, including the musculoskeletal, nervous, cardiovascular, respiratory, digestive, urogenital, endocrine, lymphatic and integumentary systems appear grossly unremarkable.

Gross Diagnosis(es):

1. Unremarkable gross exam

Gross Comments:

There were no significant gross lesions. Histology is pending. Touch imprints of bone marrow were prepared in necropsy and are stained with Wrights giemsa.

Histological Findings:

Gastrointestinal tract: there is multifocal to diffuse, moderate lymphocytic, plasmacytic inflammation within the mucosa with scattered hyperplastic lymphoid follicles, especially in the stomach, ileum and cecum. Plasma cells predominate in the stomach and small intestine, with scattered Mott cell differentiation. Fewer eosinophils are observed proximally and are present in approximately equal amounts to the mononuclear cells in the colon. Villi are robust (jejunum) to occasionally mildly blunted (duodenum).

Sections of brain, cerebellum, brainstem, pituitary gland, proximal cervical spinal cord, eye and lacrimal glands (few periductal lymphocytes), spleen (robust follicular activity, moderate mixed myeloid and erythroid hematopoiesis), lymph nodes (axillary (mild lymphoid hyperplasia with sinus histiocytes and few pigmented macrophages (skin tattoo ink)), inguinal, hilar), liver (mild centrilobular hepatocellular atrophy

and mild periportal lymphohistiocytic inflammation), gall bladder, heart (few/minimal random perivascular and focal subvalvular small lymphocytes (normal background)), aorta, kidneys (mild, multifocal glomerular endothelial and parietal epithelial hyperplasia, focal/single glomerular fibrin thrombus, and focal corticomedullary lymphohistiocytic infiltrates), urinary bladder, lungs (mild perivascular, peribronchial and peribronchiolar lymphohistiocytic aggregates and minimal pneumoconiosis), trachea, esophagus, pancreas, salivary gland (mild, multifocal lymphohistiocytic aggregates), thyroid glands, parathyroid glands, tongue, skeletal muscle, testicle (occasional mildly reduced spermatogenesis), epididymis (normal amounts of spermatids), seminal vesicle, prostate gland, skin (thigh and ventral abdomen with mammary gland) and bone marrow histology and cytology (normal megakaryocytic, myeloid and erythroid numbers and maturation, approximately 2-3:1 M:E, adequate iron stores) are unremarkable besides stated minor changes.

---

Final Principal Diagnosis(es):

---

1. Gastroenterocolitis, multifocal to diffuse, moderate, mixed with mild villous blunting (duodenum) and lymphoid hyperplasia.
- 
- 

Cause of Death: Experimental euthanasia.

Histology Comments: gastroenterocolitis is commonly seen in the colony and etiologies are likely multifactorial, and stress, nutritional/food intolerances, or allergies are possibly playing a role. A few seminiferous tubules in each testis display reduced spermatogenesis, which may be due to normal variation in hormonal levels (FSH, LH, testosterone) or response to such hormones. Normal amounts of mature spermatids are present in the epididymis.

Pathologist \_\_\_\_\_ AB \_\_\_\_\_



## **Appendix #2**

Resubmitted Project 3 of FHCRC Ovarian Cancer SPORE proposal

## **A. Specific Aims**

Our goal is to overcome treatment resistance in patients with epithelial ovarian cancer (EOC). Although a majority of patients respond initially to chemotherapy subsequent disease recurrence and treatment resistance occurs in almost all patients. A central resistance mechanism is the maintenance of tight junctions between malignant cells that prevent drug penetration into the tumor. We have generated JO, a small recombinant protein that binds to desmoglein 2 (DSG2), a junction protein that is overexpressed in ovarian cancer. Binding of JO to DSG2 triggers signaling pathways that are reminiscent of an epithelial-to-mesenchymal transition (EMT) and results in transient opening of tight junctions in epithelial tumors, including ovarian cancer xenografts. We have shown that the intravenous injection of JO increases the intratumoral penetration and efficacy of monoclonal antibodies and chemotherapeutic drugs in a broad range of human xenograft models as well as in human DSG2 (hDSG2) transgenic mice with syngeneic epithelial cancers. Further studies have shown that the effective doses of chemotherapy can be reduced when the chemotherapy drugs are combined with JO. The application of JO has not been associated with toxicities in hDSG2 transgenic mice and monkeys, mostly due to the fact that in normal epithelium DSG2 is not readily accessible to intravenously injected JO. The central goal of this proposal is the clinical translation of JO in combination with PEGylated liposomal doxorubicin (PLD) for ovarian cancer therapy. In this context, we have performed pre-clinical efficacy and safety studies in mouse models of ovarian cancer with JO and PLD. In a pilot study, we demonstrated that the co-administration of JO and PLD (40mg/m<sup>2</sup>) was well tolerated in monkeys. We have submitted a pre-IND application (see Appendix) which has been reviewed by the FDA. The FDA did not raise concerns that would delay the clinical development of the JO/PLD approach. Based on the FDA's recommendations, we now have clear guidelines for the next steps in completing the IND package. The FDA's suggestions for JO manufacturing, preclinical toxicity studies, and the clinical trial have been addressed in the research plan of this proposal. Our goal is to submit a full IND application by Year 2 and to initiate a Phase I trial of JO/PLD combination therapy in EOC patients by Year 3. As detailed in Background and Significance, PLD is an ideal agent for use in combination with JO; however, it is highly likely that JO co-treatment will improve tumor penetration and effectiveness of a number of therapeutics important in EOC as well as other cancers. Successful completion of these studies could have a profound impact on cancer therapy across numerous solid tumors with a number of different drugs.

### **Specific Aim 1. Evaluate the safety of JO / PLD administration in two preclinical models to support an IND filing.**

**1.1. cGMP manufacturing of JO.** A manufacturing protocol for JO at a large scale has already been established. cGMP manufacturing and quality control of a clinical lot of JO will be performed by the FHCRC Biologics Manufacturing Core. The final product will meet cGMP standards and will be used for GLP toxicology studies and the clinical trial. **1.2. Perform toxicity studies in hDSG2 transgenic mice.** A dose-escalation toxicology study in hDSG2 transgenic mice will be conducted with the clinical JO lot (alone and in combination with PLD) by a GLP certified testing facility. **1.3. Perform GLP toxicity studies in *Macaca fascicularis*.** As a second species for toxicology studies, we have selected *Macaca fascicularis*. We demonstrated that DSG2 biodistribution in *Macaca fascicularis* is similar to that in humans and that JO binds to monkey DSG2. Hematological parameters, JO/PLD pharmacokinetics, and anti-JO/PLD immune responses will be monitored followed by a full necropsy.

### **Specific Aim 2. Evaluate the safety and efficacy of JO administration in combination with PLD in ovarian cancer patients.**

**2.1. Evaluate safety.** The primary goal of this trial is to confirm the safety of JO when administered in combination with a fixed 40mg/m<sup>2</sup> dose of PLD in patients with progressive, persistent or recurrent ovarian/fallopian tube cancer, who have previously received standard therapies. Up to three different doses of JO will be utilized depending on toxicity, with the initial cohort of patients treated at a starting dose determined by the non-human primate (NHP) toxicology studies. Dose modification will be done following the modified continual reassessment method (CRM) with patients treated in cohorts of 2. We will treat patients for four cycles (treatment given every 4 weeks). The trial will be coordinated through the POCRC Clinical Core and performed at the Swedish Cancer Institute at Swedish Medical Center in Seattle. We expect that up to 15 patients will be required. **2.2. Evaluate therapeutic efficacy.** Tumor response will be assessed using clinical examinations, serum CA125 values and study directed imaging (CT or MRI) performed prior to every other cycle of therapy as well as at the end of the treatment period. **2.3. Gain additional knowledge about the biological effects of JO in patients.** We will use the blood samples and analyze i) JO pharmacokinetics, ii) serum DSG2 concentration, iii) anti-JO immune responses (antibodies, T-cells), iv) anti-tumor T-cell responses, v) metabolic serum markers, and vi) circulating tumor cells. If available, ascites/biopsy samples will be included in these analyses.

## B. Research Strategy

### B.1. Background and Significance

**Epithelial phenotype of cancer:** Greater than 80% of all cancer cases are carcinomas, formed by the malignant transformation of epithelial cells. One of the key features of epithelial tumors is the presence of intercellular junctions, which link cells to one another and act as barriers to the penetration of molecules with a molecular weight of >400 daltons (Da) (18, 27, 29). One of these junction proteins, DSG2, is upregulated in malignant cells (5, 20). For example, in more than 60 ovarian cancer biopsies with different histological types analyzed, we consistently found higher expression levels of DSG2 in ovarian cancer cells than in the surrounding normal tissue or tumor stroma cells (3). As an example, Figure 1A shows epithelial junctions marked by DSG2 on a biopsy from a patient with serous ovarian cancer. For most carcinomas, progression to malignancy is accompanied by a loss of epithelial differentiation and a shift towards a mesenchymal phenotype, *i.e.* EMT (47). EMT increases migration and invasiveness of many cell types and is often one of the conditions for tumor infiltration and metastasis. However, following invasion or metastasis, cells that have undergone the process of EMT can also revert to a well-differentiated epithelial phenotype (10). In support, there exist numerous examples of advanced carcinomas showing that mesenchymal cells can regain characteristics of epithelial cells or undergo mesenchymal to epithelial transition (MET) (10). As an example, Fig.1B shows DSG2 immunohistochemical analysis of a breast cancer metastasis in the liver.

**Intratumoral drug penetration and resistance:** Potential causes of drug resistance in solid tumors include genetically and epigenetically determined factors expressed in individual cells and those related to the solid tumor environment. The latter include tumor stroma cells and proteins that form a dense matrix as well as stated above, junctions that seal the space between tumor cells (9). To be effective drugs have to diffuse throughout the tumor to achieve a lethal concentration in all of the tumor cells. However, most drugs, and in particular nanoparticle- or liposome based drugs (diameters  $\sim$ >100nm), do not diffuse more than a few cell layers from blood vessels implying that more distant tumor cells receive only sub-therapeutic drug exposure (9, 32, 45). Furthermore, several studies have shown that the up regulation of epithelial junction proteins correlated with increased resistance to therapy, including therapy with the two major classes of cancer drugs - monoclonal antibodies and chemotherapeutics (14, 28, 35).

In summary, the epithelial phenotype of ovarian cancer cells and their ability to form physical barriers protect the tumor cells from attacks by the host-immune system or from elimination by cancer therapeutics (10).

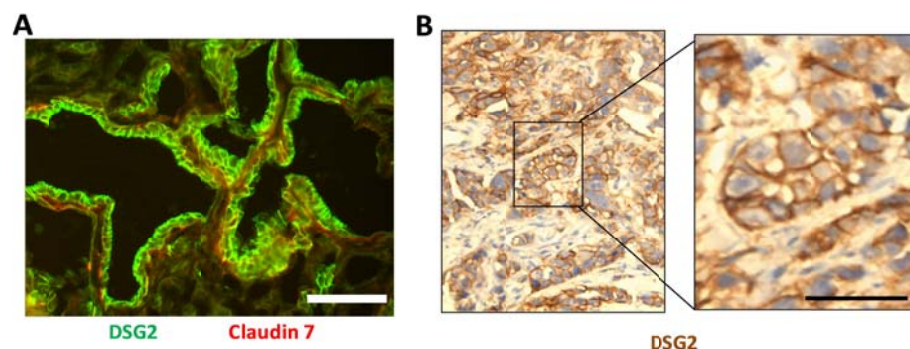


**Figure 1. DSG2 is present in epithelial junctions of ovarian and breast cancer.**

**A)** Immunofluorescence analysis of an ovarian cancer biopsy. The section was stained with antibodies against the junction proteins DSG2 (green) and claudin 7 (red). **B)** DSG2 immunohistochemistry on a section of a metastatic breast cancer lesion. DSG2 staining appears in brown. The scale bars are 20  $\mu$ m.

**Adenovirus serotype 3 derived junction opener:** We have recently reported that a group of human adenoviruses uses DSG2 as a receptor for infection (52). Among DSG2-targeting viruses is serotype 3 (Ad3). Ad3 is able to efficiently breach the epithelial barrier in the airway tract and infect airway epithelial cells. This is achieved by the binding of Ad3 to DSG2, and subsequent intracellular signaling that results in transient opening of tight junctions between epithelial cells. We have capitalized on this mechanism and created a recombinant protein that contains the minimal structural domains from Ad3 that are required to open the intercellular junctions in epithelial tumors. This protein is called "junction opener" ("JO"). The term used in previous publications was "JO-1" (3, 4, 50, 51). JO is a self-dimerizing recombinant protein derived from the Ad3 fiber (51) (Fig.2A). JO has a molecular weight of approximately 60 kDa. It can be easily produced in *E. coli* and purified by affinity chromatography. JO binds with picomolar affinity to DSG2 and causes clustering of several DSG2 molecules on the cell membrane. Binding of JO to DSG2 triggers shedding of the DSG2 extracellular domain and activation of pathways that are reminiscent of an epithelial-to-mesenchymal transition (EMT), including the phosphorylation of MAP kinases and the downregulation of junction proteins (4, 50, 52). Both mechanisms result in transient opening of epithelial junctions (Fig.2C). We have recently shown that during adenovirus replication, viral protein complexes (PtDd) similar to JO are released from infected cells, open the junctions between neighboring cells and thus allow *de novo* produced virus to spread in epithelial

tumors (30). A similar positive feed-forward mechanism should work for JO penetration in tumors considering that junction opening can be detected within 1 hour after intravenous JO injection and that JO serum half-life is ~6 hours.

We have shown in over 25 xenograft models that the intravenous injection of JO increased the efficacy of cancer therapies, including many different monoclonal antibodies and chemotherapy drugs, in a broad range of epithelial tumors (3, 4). Further studies have shown that the effective doses of chemotherapy can be reduced when the chemotherapy drugs are combined with JO. Furthermore, our studies have demonstrated that combining JO with chemotherapy drugs markedly reduced the toxic side effects of chemotherapy in mouse tumor models (3). The application of JO was safe and well-tolerated in toxicology studies carried out in human DSG2-transgenic mice and a limited number of macaques (4, 52).

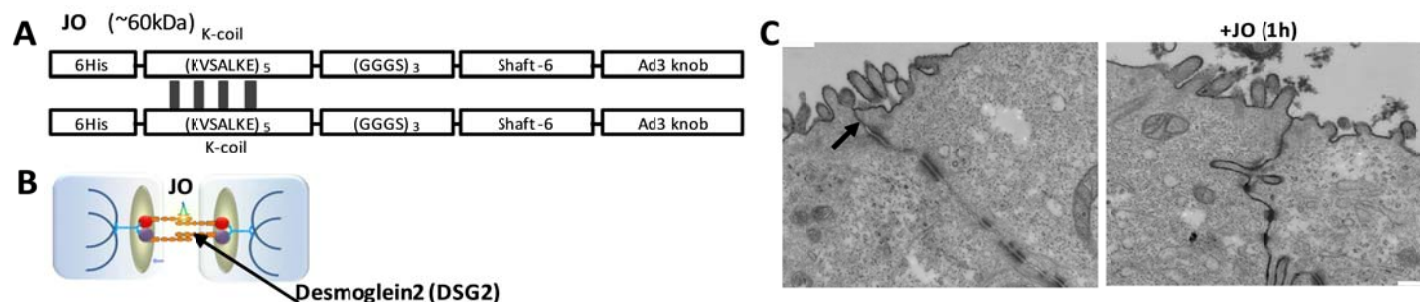


**Figure 2. Transient opening of epithelial junctions by JO in vitro.** **A)** Schematic structure of JO containing an N-terminal His-tag, a dimerization domain [K-coil (55)], a flexible linker, one fiber shaft motif, and the Ad3 fiber knob domain. The Ad3 fiber knob/shaft domain forms trimers which are then dimerized through the K-coil motif. JO is produced in *E-coli* (at a yield of ~10mg/l) and purified with Ni-NTA columns. **B)** Simplified diagram showing the structure of epithelial junctions with desmosomes and DSG2, the receptor for JO. **C)** Transmission electron microscopy of junctional areas in polarized colon cancer T84 cells. Cells were either treated with PBS (left panel) or JO (right panel) for 1h on ice, washed, and then incubated for 1h at 37°C. The electron-dense dye ruthenium red (2) was then added together with the fixative. If tight junctions (above the desmosomes, marked by an arrow) are closed, the dye only stains the apical membrane (black line). If tight junctions are open, the dye penetrates between the cells and stains the baso-lateral membrane. The scale bar is 1µm. Magnification is 40,000x.

**Previous experience in humans:** There is no previous human experience with JO. JO contains the fiber knob domain of adenovirus serotype 3 and binds to DSG2 in a way similar to Ad3. This implies that studies performed with Ad3 or Ad3 fiber knob containing Ads are relevant for predicting potential side effects of JO in a clinical trial. For more than a decade, Ad5 vectors that possess Ad3 fibers (Ad5/3), which also infect cells through DSG2 (51), have been used for cancer therapy in animal models and humans with a very good safety profile after intravenous injection (26, 40). A recent phase I trial demonstrated safety of an intraperitoneally applied Ad5/3-based oncolytic vector in recurrent ovarian cancer patients (24). Last year, we performed a study with an oncolytic vector based on Ad3 (21). In this study, twenty-five patients with chemotherapy refractory cancer were treated intravenously with a fully serotype 3-based oncolytic adenovirus Ad3-hTERT-E1A. The only grade 3 adverse reactions observed were self-limiting cytopenias. Signs of possible efficacy were seen in 11/15 (73%) patients evaluable for tumor markers. Particularly promising results were seen in breast cancer patients and especially those receiving concomitant trastuzumab (21). The latter might suggest that Ad3 acts in a similar way to JO on tumor junctions and increases drug penetration.

**PLD treatment in ovarian cancer:** PLD is a PEGylated, liposome-encapsulated form of doxorubicin. The effective size of the liposome is ~100nm. PLD has a central role in the treatment of ovarian cancer. PLD is FDA approved for treatment of advanced ovarian cancer patients failing first line platinum therapy and is a preferred agent in this setting. When used as a monotherapy objective response rates from 10%-26% have been reported (17, 31, 33). In a randomized phase III trial, PLD therapy demonstrated improved Progression-Free Survival (PFS) and Overall Survival (OS) compared with therapy using topotecan in patients with platinum sensitive disease (16). PLD has also been investigated in combination therapy with carboplatin. Results from the Phase III CALYPSO trial confirmed that carboplatin-PLD (CD) is non-inferior to carboplatin-paclitaxel (CP) in patients with platinum sensitive recurrent ovarian cancer. In the first line setting CD therapy achieves similar response rates, PFS and OS to CP (6, 41). At the FDA recommended dose of 50mg/m<sup>2</sup> monotherapy with PLD is associated with grade 3 or worse toxicity in 30% of patients with hand-foot syndrome and stomatitis/mucositis being the most common side effects. Doses have to be reduced to as low as 30mg/m<sup>2</sup> in combination regimens which may be limiting efficacy.

**Rationale for combination of JO with PLD.** Several lines of evidence suggest that PLD is an ideal agent for use in combination with JO. The large size of the PLD complex limits penetration of the drug into tumors. Studies using radio- or immune-labeled liposomes in mouse xenograft tumor models demonstrate following extravasation from leaky tumor vessels that doxorubicin liposomes localize to the perivascular space and extra-cellular matrix (22, 54) with minimal tumor cell uptake (25). Unlike other chemotherapy drugs, e.g. camptothecins, doxorubicin does not form small metabolites that are capable of tumor penetration. Our own studies (detailed below) have confirmed poor intratumoral penetration of PLD in xenograft tumor models (3) and that when combined with JO, PLD tumor penetration is enhanced, toxicity is reduced and efficacy is maintained at lower systemic doses of PLD. This raises the possibility that in addition to improving the anti-tumor effects of PLD monotherapy, JO co-therapy may also salvage the effectiveness of PLD in combination chemotherapy regimens for ovarian cancer where the PLD dose has to be reduced below the generally accepted effective dose of 40mg/m<sup>2</sup>. Ovarian cancer cells surviving PLD therapy undergo a unique phenotypic transformation that includes upregulation of MHC-1 and Fas expression which increases the susceptibility of surviving tumor cells to immune mediated cell death (1). As demonstrated in our preliminary work in ovarian cancer mouse models, JO reduces intratumoral regulatory T-cells and enhances anti-tumor CD8 T-cell response, properties which are likely to complement the phenotypic changes and enhance immune mediated death mechanisms for tumor cells surviving PLD therapy.

**The central hypothesis of the proposal is that the relatively large size of PLD (~100nm) impedes efficient intratumoral penetration in epithelial ovarian tumors and that the combination of JO and PLD can overcome this problem allowing for increased anti-tumor efficacy. Furthermore, based on our preclinical studies as well as the experience with Ad3 fiber-containing viruses, we anticipate that intravenous injection of JO will be well tolerated in humans.**

**Significance:** PLD is used to treat patients with ovarian cancer that has progressed or recurred after platinum-based chemotherapy. Response rates to PLD are low, the response duration is short, and the toxicity is significant. There is a great need for improvement of both the efficacy and the safety of PLD therapy in ovarian cancer patients.

**B.2. Innovation:** There are no epithelial junction openers used clinically for cancer therapy. A number of chemical detergents, surfactants, calcium-chelating agents and phospholipids have been used to increase drug absorption through the GI tract epithelium. Recently, Kytogenics Pharmaceuticals, Inc. has developed a tight junction opener based on chitosan derivatives. It is thought to act by electronegative forces applied to tight junction proteins (<http://www.kytogenics.com>). However, all of these agents act indiscriminately to mechanically disrupt junctions and are therefore unable to be used systemically. Our therapeutic, JO, is a small protein that can be produced in *E.coli* and easily purified. It binds to DSG2, which is accessible in epithelial cancer cells and triggers an epithelial-to-mesenchymal-transition that results in transient opening of epithelial junctions.

### **B.3. Approach**

#### **B.3a. Preliminary data with JO and PLD supporting the clinical trial**

The studies that yielded the data shown below have been supported by the NCI (Supplement for R01-CA144057, DRP-FHCR Ovarian Cancer SPORE), the DoD (Translation Pilot Award/Ovarian Cancer Research), and Samyang Biotech (Gift).

**B.3a-1. JO enhances PLD chemotherapy in xenograft models of ovarian cancer.** To support this proposal, we evaluated PLD in xenograft models with ovarian cancer cells (ovc316). Ovc316 cells are derived from a patient biopsy and closely model the heterogeneity and plasticity seen in tumors *in situ* (44). Mice with pre-established ovc316 tumors were intravenously injected with JO, followed one hour later by an intravenous injection of PLD (Doxil<sup>TM</sup>). The ability of JO to open up intercellular junctions increased the penetration and amount of PLD in tumors. Immunofluorescence analysis of tumor sections from JO/PLD treated animals showed PLD distributed over a greater distance from blood vessels (Fig.3A). More than 10-fold higher amounts of PLD per gram tumor tissues were measured by ELISA when PLD was combined with JO. The enhancing effect of JO on PLD therapy was shown in a model with ovc316-derived mammary fat pad tumors (Fig.3B). This study also shows higher anti-tumor efficacy of JO plus "low"-dose Doxil (1mg/kg), compared to "high" dose Doxil alone (3mg/kg), indicating that it is possible to lower the effective dose of Doxil when combined with JO. The second model was an orthotopic model with intraperitoneal ovc316 tumors (Fig.3C). While all mice



treated with PLD alone died by day 80 after tumor inoculation, the combination of JO and PLD resulted in long-term survival (>160 days) of ~80% of animals. Additionally, we have shown JO efficacy in xenograft models of breast, lung, prostate, gastric, colon, and skin cancer models (3, 4) (also see pre-IND application/Appendix).

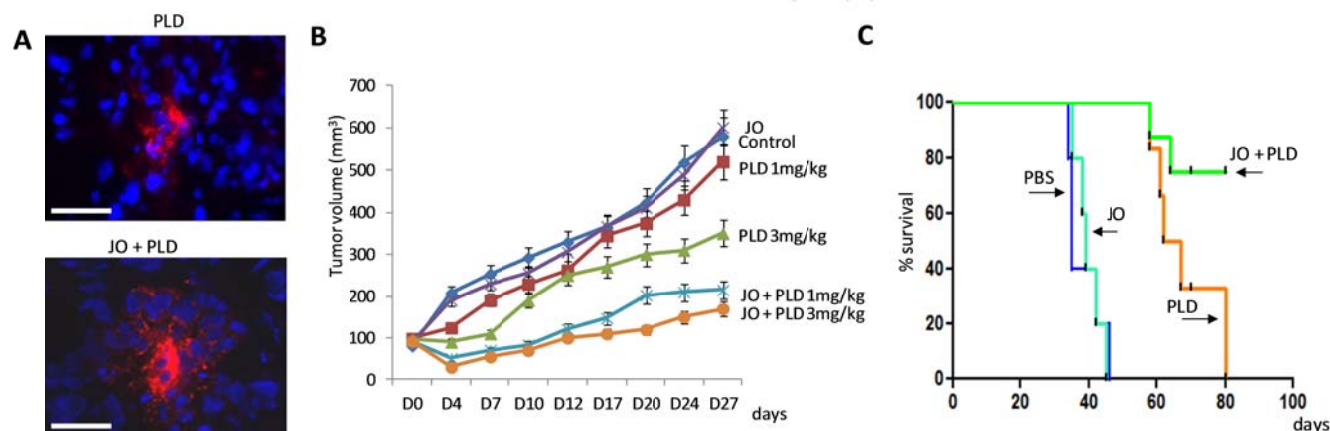


**Figure 3. JO enhances PLD therapy in an ovarian cancer model.** **A)** Better penetration and accumulation of PLD in tumors. Immunofluorescence analysis of tumor sections 2 hours after intravenous PLD or JO/PLD injection. PLD is stained red using antibodies that specifically bind to PEG in nanoparticles. The scale bars are 20  $\mu$ m. **B)** Efficacy study in mammary fat pad tumor model using primary ovarian cancer (ovc316) cells. Treatment was started when tumors reached a volume of 100 mm<sup>3</sup>. Mice were injected intravenously PLD (1mg/kg or 3mg/kg) alone or in combination with 2mg/kg JO. Treatment was repeated weekly. N=10. **C)** Survival study/intraperitoneal model. CB17-SCID/beige mice with intraperitoneal tumors derived from ovc316 cells. Treatment was started at day 25 after tumor cell implantation and repeated weekly. Mice were injected intravenously with 2mg/kg JO or PBS, followed by an intravenous injection of PLD/Doxil (1mg/kg) or PBS one hour later. Onset of ascites was taken as the endpoint in therapy studies. Shown is the survival of animals in a Kaplan Meier graph. n=10.  $p < 0.001$  for PLD vs JO + PLD.

### B.3a-2. JO enhances PLD chemotherapy in immunocompetent models.

**Tumor-specificity of JO action:** Because JO does not bind to mouse cells (50), we generated human DSG2 (hDSG2) transgenic mice that expressed human DSG2 at a level and in a pattern seen in humans (50). Furthermore, we established syngeneic tumor cell lines (TC1 and MMC (39)) with ectopic hDSG2 expression at levels seen in human tumors (3). In epithelial tissues of hDSG2 transgenic mice, hDSG2 is specifically localized to junctions (50). Furthermore, JO triggers junction opening in hDSG2-expressing epithelial mouse tumor cells indicating that hDSG2 interacts with mouse signaling and cytoskeletal proteins thus overriding a potential function of mouse DSG2 in the maintenance of junctions in transgenic mice. (Notably, there are no mouse DSG2-specific antibodies available). Using hDSG2 transgenic mice, we demonstrated that JO predominantly accumulates in tumors (3). A number of factors could account for this finding, including: *i)* overexpression of hDSG2 by tumor cells, *ii)* better accessibility of hDSG2 on tumor cells, due to a lack of strict cell polarization compared to hDSG2-expressing normal epithelial cells, and *iii)* a high degree of vascularization and vascular permeability in tumors. Because of its preferential binding to and action on epithelial junctions of tumors, JO appears to create a “sink” for therapeutic drugs in tumors, which decreases the levels and exposure of these drugs in normal tissues, at least in mouse tumor models (with a tumor weight to body weight ratio of 1:20 (50). This “sink” effect will most likely be less pronounced in cancer patients.

**Repeated JO/PLD treatment:** JO is an adenovirus-derived protein and therefore potentially immunogenic. This might not be a critical issue if JO is used in combination with chemotherapy, which suppresses immune responses to foreign proteins. This expectation is supported by studies with oncolytic adenovirus vectors in which immunosuppression allowed for repeated vector application (7, 11, 46). Furthermore, we have demonstrated that JO remains active *in vitro* and *in vivo* even in the presence of anti-JO antibodies generated by JO vaccination of mice (3). This may be due to the fact that JO binds to DSG2 with a very high avidity thus disrupting potential complexes between JO and anti-JO antibodies. (Notably, JO is a dimer of a trimeric fiber knob, which contributes to the picomolar avidity to DSG2 (51).) To test the potential for anti-JO antibody responses to adversely affect the therapeutic effects of JO, we performed repeated injections of JO in an immunocompetent hDSG2 mouse tumor model (Fig.4). After two treatment cycles of JO and PLD, treatment was stopped and tumors were allowed to re-grow. The third and fourth treatment cycles were started on days 28 and 32, respectively. At the time of the third cycle, serum anti-JO antibodies were detectable by ELISA in the JO/PLD treated group of animals. However, the antibody levels were ~10-fold lower than in the group which received JO without PLD. In both the third and fourth treatment cycles JO had an enhancing effect on

PLD therapy, demonstrating that JO continues to be effective after multiple treatment cycles even in the presence of detectable antibodies.

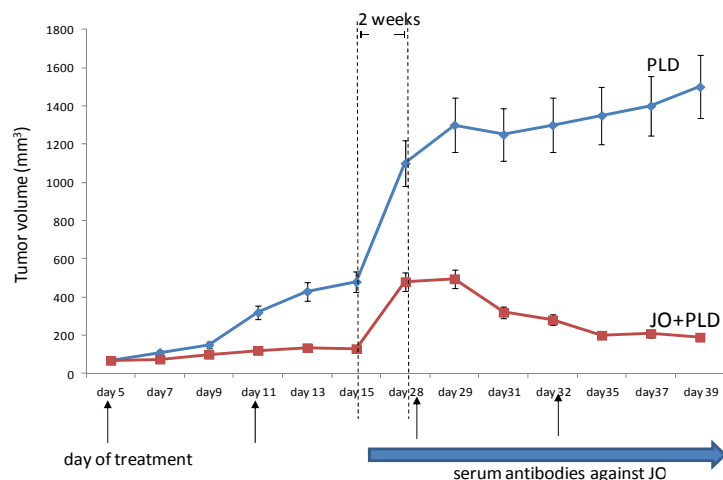


**Figure 4. JO/PLD therapy in immunocompetent hDSG2 transgenic mice.** A total of  $4 \times 10^6$  MMC-hDSG2 cells were injected into the mammary fat pad of hDSG2 transgenic mice. When tumors reached a volume of  $\sim 80 \text{ mm}^3$ , JO (2 mg/kg) or PBS was injected intravenously followed one hour later by PLD (i.v. 1.5 mg/kg). Treatment was repeated as indicated at day 5 and 11. Tumors were then allowed to regrow for about 2 weeks. At this time, serum was analyzed for anti-JO antibodies. Two more treatment cycles were performed at day 28 and day 32.  $N=5$ .

### B.3a-3. JO safety studies.

**Safety in hDSG2 transgenic mice:** Intravenous injection of JO (2, 5, and 10 mg/kg) into hDSG2 transgenic mice (with or without pre-existing anti-JO antibodies) was well tolerated. There were no critical abnormalities found in hematologic and serum chemistry parameter and histopathology with 2 and 5 mg/kg. At a dose of 10 mg/kg, we observed a mild lymphocytopenia and intestinal inflammation that subsided by day 3 after injection. We speculate that the favorable safety profile of JO is due to the fact that hDSG2 in tissues other than the tumor is not readily accessible to intravenously injected JO. The hDSG2 transgenic mouse model was also used to obtain biodistribution and pharmacokinetic data for JO. These studies showed a serum half-life of 6 hours and hDSG2-dependent accumulation of JO in epithelial cells of the small intestine and colon (3). We also found hDSG2-independent uptake by liver, spleen, and lymph node macrophages.

**Safety in non-human primates (NHP):** We demonstrated that DSG2 biodistribution in *Macaca fascicularis* is similar to that in humans and that JO binds to monkey DSG2 (50). In a first study, two animals were injected with JO (0.6 mg/kg) and monitored for 72 hours, followed by a full necropsy. No laboratory (hematologic or chemistry) or histological abnormalities were observed. JO serum clearance and JO biodistribution were similar to that observed in hDSG2 transgenic mice. JO half-life in serum was 8 hours. A full pathology report was included in the pre-IND package (see pre-IND application, section 4.6.2. in Appendix). A second study in male\* *M. fascicularis* was performed to address the question whether JO increases PLD toxicity. (\*Female animals were not available to complete the study in time for the submission of the SPORE grant). One animal was injected intravenously with JO at a dose of 2 mg/kg, i.e. at a dose that was effective in mouse models. Another animal was injected with saline. One hour later both animals received an intravenous injection of PLD (Doxil<sup>TM</sup>) at a dose of  $40 \text{ mg/m}^2$  (1.1 mg/kg), i.e. at a dose that will be used in the clinical trial. Animals were monitored daily and blood samples were collected at 4, 6, and 24 hours and then at day 3, 7 and 14 after Doxil injection. At day 14, animals received a second cycle of treatment. At six hours after the second Doxil injection, animals were euthanized and a gross necropsy was performed by a certified veterinary pathologist. The rationales for the second injection cycle followed by the necropsy were to *i*) assess potential anaphylactic reactions in a treated animal with serum antibodies against JO and *ii*) study the effect of JO on Doxil serum clearance and tissue uptake. Analysis of vital symptoms, blood parameters, and organ histology did not show remarkable signs of toxicity (see preIND application, section 4.6.3. in Appendix). Upon necropsy, no significant treatment related abnormalities in gross examination of organs and histological analysis of tissue sections were observed. Therefore, the combination of JO and Doxil was well tolerated in an adequate animal model. Serum and tissue samples were used to measure JO and Doxil concentrations as well as antibodies against JO. Considering the limitations of the study ( $N=1$ ), a series of cautious conclusions can be made: *i*) The concentration of shed DSG2 in the serum did not increase after JO injection, indicating minimal interaction with DSG2 on normal tissues. (In contrast, in mouse tumor models, JO triggered the cleavage and shedding of DSG2 in xenograft tumors, because in tumors, not all DSG2 is trapped in junctions (4)). *ii*) As expected, serum IgG antibodies against JO developed after one week. However the concentration of anti-JO antibodies was at a level that was completely saturated after the second JO injection (no detectable anti-JO antibodies at 4 hours after the second injection). Serum antibodies had no effect on the pharmacokinetics of JO after the second injection. Corresponding JO/anti-JO IgG immune complexes were found by ELISA and immunofluorescence

analysis of tissue sections in a series of lymphoid (spleen, lymph nodes) and non-lymphoid organs (adrenals, epididymis, lung, kidney, gall bladder, and pancreas. *iii*) Non-opsonized JO was detected (at concentrations less than 50ng per 100mg of tissue) in adrenals, epididymis, lung, liver, and kidneys. *iv*) JO pretreatment resulted in a longer Doxil retention in the blood. Depositions of Doxil were found in the liver, adrenals, epididymis, brain, kidney, lymph nodes, and spleen. JO slightly increased the Doxil concentration in adrenals (2.1-fold) and epididymis (1.3-fold); it decreased Doxil concentrations in the liver (1.4-fold), spleen (1.7-fold), lymph nodes (1.4-fold), and brain (1.5-fold). There was no JO-related increase of Doxil in the heart or cardiac damage-supporting abnormalities in the ECG and blood chemistry analyses. In summary, our studies in DSG2 transgenic mice and NHPs did not show JO-related toxicity. JO accumulation in a number of epithelial tissues was detectable however did not appear to have a detrimental effect. This is in agreement with our hypothesis that in normal epithelial tissue, DSG2 is trapped in desmosomal junctions and not readily accessible to ligands.

**Risk of inducing metastasis:** JO binding to DSG2 on tumor cells triggers pathways involved in EMT, a process which has been associated with tumor metastasis. However, none of our *in vivo* studies have shown any evidence of increased tumor growth or metastasis after treatment with JO. Furthermore, at day 3 after JO injection into mice bearing Her2/neu-positive HCC1954 tumors, there was no significant increase in the percentage of circulating Her2/neu-positive cells in the blood (3). This is likely due to the fact that tumor metastasis requires more than transient activation of EMT pathways. Detachment from epithelial cancers and migration of tumor cells is only possible after long-term crosstalk between malignant cells and the tumor microenvironment, resulting in changes in the tumor stroma and phenotypic reprogramming of epithelial cells into mesenchymal cells (19). In the context of the clinical trial, we will attempt to measure circulating tumor cells before and after JO injection.

**Risk of anaphylactic responses:** We screened serum samples of 58 ovarian cancer patients for pre-existing antibodies against JO. We found (by ELISA) detectable binding IgG antibodies in less than 10% of these samples. No anti-JO IgA, E, and M antibodies were detected. Based on this, one of the inclusion criteria for the clinical trial will be the absence of anti-JO antibodies.

#### **B.3a-4. Preliminary data supporting studies outlined in Specific Aim 2.3.**

**JO facilitates anti-tumor T-cell responses:** Using an immunocompetent hDSG2-transgenic mouse tumor model, we showed that JO injection reduced the number of intratumoral Tregs, which in turn allowed pre-existing anti-tumor CD8 T-cells to control tumor growth (Fig.5). We used hDSG2 transgenic mice and syngeneic TC1 cells that expressed human DSG2. TC1 cells express HPV E6 and E7 and trigger E7-specific T-cells in C57Bl/6 mice. However, these tumor-specific T-cells are unable to control tumor growth and 100% of tumor-bearing animals reached the study endpoint by day 20. Two injections of JO into tumor-bearing mice at days 6 and 14 resulted in complete tumor regression in 60% of mice (Fig.5A). This effect was due to an increased number of E7-specific T-cells (Fig.5B) and could be blocked by systemic depletion of CD8 cells. Importantly, we also found in flow cytometry analyses of tumor-infiltrating leukocytes that the number of Tregs (CD25+/FoxP3+) was about 6-fold less in JO treated animal tumors compared to PBS injected animals (Fig.5C). Notably, JO alone had no significant therapeutic effect in the neu/hDSG2 breast cancer model (Fig.4), most likely due to tolerance towards tumor antigens in this model (39).

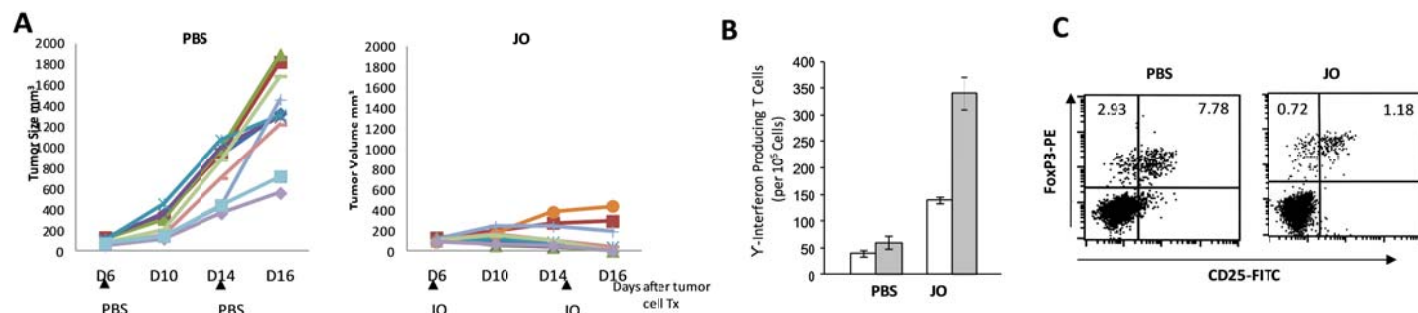


**Figure 5. JO facilitates anti-tumor T-cell responses.** **A)** hDSG2 transgenic mice with established subcutaneous syngeneic TC1-hDSG2 tumors were intravenously injected with PBS or JO (2mg/kg) at days 6 and 14 after tumor cell transplantation and tumor volumes were measured. Each line represents an individual animal. N=10. **B)** Analysis of frequencies of IFN $\gamma$ -producing E7 specific T-cells in the spleen 4 days after PBS or JO injection. Shown are the frequencies of IFN $\gamma$  producing T-cells specific to the HPV16 E749-57 carrying the H-2Db restricted peptide (RAHYNIVTF) (grey bars) or an unrelated control peptide (white bars). N=3 animals per group. The differences in the JO group are



significant ( $p < 0.05$ ). **C) Analysis of intratumoral (CD25+/FoxP3+) Tregs four days after PBS or JO injection.** Shown are representative flow cytometry data.

We will submit a separate grant application to study the mechanisms behind JO facilitated anti-tumor immune responses. In the context of the clinical trial (Specific Aim 2.3.2), we propose to use PBMCs to study anti-tumor immune responses.

### **B.3b Experimental approach:**

#### **Specific Aim 1. Evaluate the safety of JO / PLD administration in two preclinical models to support an IND filing**

**Hypothesis:** Because DSG2 is trapped in junctions of normal epithelial cells, no critical toxicity after intravenous JO injection is expected.

**Aim 1.1: cGMP manufacturing of JO.** We will produce a single clinical grade cGMP lot of JO. The singular lot would be sufficient to first do the GLP toxicology studies while the remaining vialled material is held for subsequent clinical use. JO is produced in *E.coli* and purified by immobilized metal chelate affinity chromatography. cGMP production will be performed by the FHCRC Biologics Manufacturing Core (<http://sharedresources.fhcrc.org/core-facilities/biologics-production>) under the direction of Dr. Ron Manger, who has significant experience in the production of cGMP grade therapeutic proteins. The facility is primarily designed to produce clinical grade proteins intended for intravenous administration in humans. Manufacturing and purification of products are performed in dedicated clinical areas of the facility in compliance with regulatory standards. The facility will also perform the quality control of the produced protein. The protein bulk will be defined and released as bulk Drug Substance. Drug quality control testing will be done as suggested by the FDA's response to our pre-IND application. Details are described in the pre-IND package (Appendix). A cGMP-compliant manufacturing protocol for JO at large scale has already been established. The generation and characterization of a master *E.coli* cell bank has been completed. Furthermore, we demonstrated that after 9 months of storage at  $-80^{\circ}\text{C}$ , JO did not lose activity (test ongoing). Therefore, production, quality control, and release of the cGMP lot can be completed within 6 months after the start of funding. The following (already established) potency assays of the cGMP product will be performed: DSG2 binding assay: The clinical function of the product is to bind to DSG2 triggering intracellular signaling. Binding of JO to DSG2 will be measured by ELISA. Rabbit polyclonal antibodies against DSG2 will be used for capture followed by recombinant DSG2, the cGMP JO lot/reference sample, mouse mAb against the Ad3 fiber knob, and anti-mouse IgG-HRP. PEG permeability assay: A total of  $5 \times 10^5$  T84 cells will be seeded on 12mm transwell inserts and cultured for 20 days until the transepithelial electrical resistance (TEER) remains constant, i.e. tight junctions have formed. The cells will be exposed to JO for 15 min at room temperature.  $1 \mu\text{Ci}$  of [ $^{14}\text{C}$ ] polyethylene glycol-4000 (MW: 4,000Da) will be added to the inner chamber. Medium aliquots will be harvested from the inner and outer chambers and measured by a scintillation counter. Permeability will be calculated as described elsewhere (53). JO preparations are considered to be functionally potent if they increase PEG permeability >3-fold within 30 min.

#### **Aim: 1.2: Perform toxicity studies in hDSG2 transgenic mice.**

Justification for using hDSG2 transgenic mice for GLP toxicology studies. The homology between the human and mouse DSG2 gene is 77.1% and neither Ad3 nor JO bind to mouse cells (50). We therefore generated transgenic mice that contain the 90kb human DSG2 locus, including all regulatory regions. These mice express human DSG2 in a pattern and at a level similar to humans (50). Furthermore, we have shown that JO triggers hDSG2-mediated signaling and opening of epithelial junctions in epithelial mouse tumor cells that ectopically express hDSG2 (50) as well as in primary lung epithelial cells from hDSG2 transgenic mice. This indicates that human DSG2 can interact with mouse cytoskeletal proteins and kinases and implies that hDSG2 transgenic mice are an adequate model to study downstream effects of JO binding to DSG2 after intravenous injection. We will use a model for spontaneous ovarian cancer that is transgenic for human DSG2. Our collaborator Ronny Drapkin (Dana Farber/Harvard Cancer Center) has developed a spontaneous fallopian tube/ovarian cancer model with high-grade serous carcinomas appearing within 2-4 months after birth (38). It involves a Pax8 promoter driven Cre recombinase to delete tumor suppressor genes Tp53, pTen, and Brca1. For our studies, we will cross-breed the Pax8-Cre mice with hDSG2 transgenic mice. Double transgenic mice will be identified by genotyping. Tumor growth in the spontaneous cancer model can be monitored based on serum CA125 (38).

Design of GLP toxicology study in hDSG2-transgenic mice. While we accumulated a substantial amount of efficacy and safety data in hDSG2 transgenic mice in the PI's lab (see IND package, section 4.5; Figs. 23-31), the FDA requested an additional study at a certified GLP testing facility using JO produced under cGMP

compliant conditions. These studies will be performed by Bioanalytical Systems, Inc. (BASi) (<http://www.basinc.com/about/index.html>). Groups #1 to 7 (Table 1) will receive 4 injections of JO and/or PLD one week apart, based on the clinical protocol. Studies will be performed in naïve hDSG2 transgenic mice and hDSG2 transgenic mice that have been vaccinated with JO and have mounted T- and B-cell responses against the protein. Studies in pre-immune animals will address potential allergic side effects of JO injection. The vast majority of preclinical studies performed in the PI's lab were done with a JO dose of 2mg/kg. This will be the NOAEL ("no observed adverse effect level") starting dose for the toxicology studies. In addition, we plan to exceed the maximum dose that we estimate to use in the clinical trial. This dose is usually 10-fold higher than the NOAEL (15). In our case, this would be 20mg/kg. If dose-limiting toxicity (DLT) occurs in Group #3, we will lower the "high dose". The standard PLD dose in humans is (40mg/m<sup>2</sup>), which corresponds to a dose of 1.1mg/kg in mice. Notably, PLD is a large molecule, predominantly sequestered in vascular space, in which case allometric dose scaling is not appropriate. For combination treatment, PLD will be injected one hour after JO. Groups #8 and 9 will be hDSG2 transgenic mice with spontaneous, hDSG2-expressing ovarian/fallopian tube tumors. Mice will be injected when serum CA125 becomes detectable and followed for 4 weeks. Tumor bearing mice better reflect the target patient group in the clinical trial. After each treatment cycle, blood samples will be collected from all animals on day 1 of injection at 3 time points – pre-dose, 6, and 24 hours post-dose, and then twice per week. The samples will be analyzed for: *i*) full blood CBC and chemistry, and *ii*) serum cytokines, *iii*) JO concentrations, *iv*) PLD concentration and *v*) IgG, IgM, IgA, and IgE antibodies against JO, PEG and His tag. After 4 weeks, six animals will be euthanized and complete necropsy and histological examination will be performed. Specific attention will be given to GI-tract and cardiac toxicities. Four animals will be followed post-treatment for 2 weeks with weekly blood analysis. JO and PLD concentrations will be measured in all collected tissues by ELISA. Tissue sections will be analyzed by immunohistochemistry for the presence of JO and PLD. Splenocytes will be used for ELISPOT assays to quantitate JO-specific  $\gamma$ -interferon-producing CD4 and CD8 T-cells. All assays for safety assessments will be performed under GLPs at BASi. The exploratory assays for T-cell responses are established in the PI's lab.

**Animal numbers:** For the toxicology studies, we selected a group size of 10 animals. We arrived at this number by setting a large effect size, which was based on our previous studies, and a desired power of 0.8 at a significance level of 0.05.

**Table 1: Design of GLP toxicology studies in hDSG2-transgenic mice.**

Group	Dosing	Route	Regiment	Duration	N	
1	JO (2mg/kg) naïve mice, no tumor	IV	Every week	4 weeks	10	6 animals→necropsy 4 animals→follow up
2	JO (2mg/kg) pre-immune mice, no tumor	IV	Every week	4 weeks	10	6 animals→necropsy 4 animals→follow up
3	JO "high-dose") naïve mice, no tumor	IV	Every week	4 weeks	10	6 animals→necropsy 4 animals→follow up
4	JO ("high-dose") pre-immune mice, no tumor	IV	Every week	4 weeks	10	6 animals→necropsy 4 animals→follow up
5	PLD (40mg/m <sup>2</sup> ) naïve mice, no tumor	IV	Every week	4 weeks	10	6 animals→necropsy 4 animals→follow up
6	JO ("high dose") + PLD (40mg/m <sup>2</sup> ) naïve mice, no tumor	IV	Every week	4 weeks	10	6 animals→necropsy 4 animals→follow up
7	JO ("high dose") + PLD (40mg/m <sup>2</sup> ) preimmune mice, no tumor	IV	Every week	4 weeks	10	6 animals→necropsy 4 animals→follow up
8	JO ("high dose") spontaneous tumors	IV	Every week	4 weeks	10	6 animals→necropsy 4 animals→follow up
9	JO ("high dose") + PLD (40mg/m <sup>2</sup> ) spontaneous tumors	IV	Every week	4 weeks	10	6 animals→necropsy 4 animals→follow up

### ***Aim 1.3: Perform GLP toxicity studies in *Macaca fascicularis****

**Justification for using *Macaca fascicularis* for GLP toxicology studies.** JO does not efficiently bind to mouse (50), rat, hamster, and dog PBMC or transformed cell lines (data not shown) and the DSG2 gene homology for these species compared to human DSG2 is less than 80%. Although hDSG2 transgenic mice allow us to study a number of variables in a large number of animals, it is unclear whether the hDSG2-mouse system accurately models a homologous system with human DSG2 in human cells. A better model is NHPs. The DSG2 gene

homology between humans and macaques is 96.6%. Biodistribution in *Macaca fascicularis* is similar to humans (50). JO binds to monkey DSG2 and triggers junction opening at a level that is comparable to human cells (50). This justifies the use of *Macaca fascicularis* for GLP toxicology studies after intravenous JO injection. The studies will be conducted in accordance with the US FDA Good Laboratory Practice Regulations. The GLP-certified test site will be BASi.

**JO dose finding study.** In our previous studies, intravenous injection of 0.6mg/kg and 2mg/kg (in combination with PLD/Doxil<sup>TM</sup>) was well tolerated. To determine the highest non-severely toxic dose (HNSTD) and correlative pharmacokinetics attributes for JO, animals will be injected with JO at a dose of 4mg/kg and 10mg/kg (N=2 per dose level) and monitored as described in B.3a-3. A necropsy will be performed at day 7 and pathology and histology reports will be compiled.

**GLP toxicology study for combination therapy.** Three JO dose cohorts will be analyzed (Table 2). The maximum JO dose will be the HNSTD found in the dose-finding study. With this dose, we expected to reach JO dose-limiting toxicity (DLT) in combination with PLD. This will allow us to estimate the maximum tolerated dose (MTD) of JO when combined with PLD in humans. The lower doses will be in the range of 20 to 50% of the HNSTD. The PLD dose will be 1.1mg/kg which corresponds to 40mg/m<sup>2</sup> in humans. For the combination treatment, PLD will be injected 1 hour after JO. The design of the clinical trial involves 4 treatment cycles 4 weeks apart (i.e. the standard treatment regimen for PLD). Common PLD toxicities in patients (hand-food symptoms, stomatitis) develop late. Furthermore, accumulative PLD cardiotoxicity is a potential side effect after multiple treatment cycles. To assess late and accumulative toxicities, we will treat animals in 4 cycles with an interval of 4 weeks. To decrease the formation of JO-antibody immune complexes, animals will also receive dexamethasone treatment for 48 hours during JO injection (13).

**Table 2: Design of cGMP toxicology studies in non-human primates.**

Group	Dosing	Route	Regiment	Interval	
1	PLD (40mg/m <sup>2</sup> )	IV	Every 4 week	4 weeks	2 animals→necropsy
2	JO (20% HNSTD) PLD (40mg/m <sup>2</sup> )	IV	Every 4 week	4 weeks	4 animals→necropsy 2 animals→follow up
3	JO (50% HNSTD) PLD (40mg/m <sup>2</sup> )	IV	Every 4 week	4 weeks	4 animals→necropsy 2 animals→follow up
4	JO (HNSTD) PLD (40mg/m <sup>2</sup> )	IV	Every 4 week	4 weeks	4 animals→necropsy 2 animals→follow up

Physical examinations will be performed daily by a qualified veterinarian on all study animals prior to initiation and on all animals prior to their respective necropsy. Body weights will be recorded once prior to treatment and weekly thereafter. Blood samples will be collected and analyzed as described for hDSG2 transgenic mice and in B.3a-3. Animals will be euthanized six hours after the last injection and a gross necropsy will be performed by a certified veterinary pathologist at BASi. A standard set of tissues (~66/animal) will be collected and preserved in 10% formalin. All collected tissues will be examined by a veterinary pathologist. An audited draft of the final report will be available 6 weeks following the final necropsy. The report will assess functional effects on the major physiological systems (e.g., cardiovascular, respiratory, renal, and central nervous systems considering hematology, histopathology, urinalysis).

**Animal numbers:** For non-rodent species, the FDA recommended 4 animals/group for the main study groups, and 2 animals/group for recovery groups.

## **Specific Aim 2. Evaluate the safety and efficacy of JO administration in combination with PLD in patients with epithelial ovarian cancer.**

In project Year 2, we will submit a full IND application and in Year 3 initiate a Phase I trial of intravenous JO in combination with PLD in patients with recurrent ovarian cancer. Eligibility criteria for the trial include patients with progressive, persistent, or recurrent state ovarian/fallopian tube cancer who have received standard therapies. Patients with only a single prior platinum regimen must have a progression-free interval (PFI) of less than 6 months. Patients who have failed second or greater line therapy will also be eligible. Exclusion criteria include a) prior therapy with an anthracycline compound including PLD, b) severe cardiovascular disease and c) pre-existing anti-JO antibodies. Up to 15 patients will be enrolled. Recruitment and enrollment of study participants will be done in collaboration with the SPORE Clinical Core. The Clinical Core unites UW/SCCA and Swedish Medical Center, the two major ovarian cancer treatment centers in the Pacific Northwest. Combined these 2 centers treat roughly 180 incident ovarian cancer cases annually.

The primary objective of this trial is to estimate the MTD of JO when used in combination with PLD. For these purposes, we plan to give a fixed dose of PLD of 40 mg/m<sup>2</sup>. We plan to conduct the trial with Doxil<sup>TM</sup>. We will attempt to secure an adequate supply of the Doxil preparation for our study and consider Lipodox<sup>TM</sup>, another PLD, in the event of shortage of Doxil. JO will be infused 1 hour prior to administration PLD. Patients will receive dexamethasone 20mg p.o. 12 and 6 hours prior to JO injection to suppress anti-JO antibodies formation. Patients will receive a total of 4 cycles of therapy with cycles being delivered at 4 week intervals. Up to three doses of JO will be tested depending on toxicity. The HNSTD from the combination treatment study in NHPs will be used to set the safe starting dose for JO in the clinical trial using a 1/5th safety factor of the HNSTD (i.e. 0.2 HNSTD) for the first patient cohort. Subsequent cohorts will be treated at JO doses of 0.5 and 1.0 the HNSTD. Dose modification will be done following the modified continual reassessment method (CRM), a modern Bayesian adaptive method for dose finding (15, 34). The number of patients per cohort will be 2. The CRM starts with a prior distribution for the dose-toxicity relationship, and after each cohort of two patients is treated the dose-toxicity curve is updated based on the observed data. The subsequent group of 2 patients is then treated at the dose that is closest to the targeted dose-limiting toxicity (DLT) rate of 30% with the caveat that an increment of one dose level is the maximum allowed. The target DLT rate of 30% is consistent with prior reports of toxicities associated with single agent PLD at a dose of 40mg/m<sup>2</sup> in patients with recurrent ovarian cancer (23, 43). This procedure will be followed until a total of 15 patients have been treated, and the MTD will be estimated as the dose that is closest to the targeted DLT rate after the last patient is treated and observed for DLT. A DLT is defined as any toxicity  $\geq$  grade 3. DLT's will be assessed through the first 3 rounds of treatment. While it is not expected, if we see cumulative toxicities after the fourth round of treatment, consideration will be given to fitting a dose-toxicity curve at the end of the trial based on these "later" toxicities for purposes of estimating the MTD. Based on our preliminary data we anticipate that JO/PLD therapy will not be associated with rates of significant toxicity exceeding the toxicities of PLD alone. Consequently we will use a "flat" dose-toxicity curve as a starting point for the CRM.

**Aim 2.1: Documentation of safety:** The primary goal of this trial is to confirm the feasibility and safety of JO when administered in combination with PLD. Patients will be treated in a dedicated Phase I trial unit. Patients in the first dose cohort will be observed overnight and discharged no sooner than 23 hours post JO infusion provided no toxicities are observed. The t<sub>1/2</sub> of JO is 6 hours in macaques after a 2 mg/kg dose. Provided no late toxicities are observed in the first cohort, the observation period for subsequent cohorts may be reduced to 12 hours following JO infusion. All patients will be seen in outpatient follow-up on day +1, +2, +3 and then weekly. Standard protocols for monitoring of patients treated with Phase I agents will be followed (Table 3) and toxicities will be managed consistent with standard medical care. Patients with signs of significant toxicities will be admitted as appropriate. Blood will be drawn before injection, 1, 2, 3, 4, 6, 12, 24, 48 and 72 hours post-injection, and then weekly. Standard safety monitoring will be performed, i.e. clinical status, physical examination including vital signs, weight, hematologic parameters, serum chemistry studies, coagulation studies and electrocardiograms. In addition to potential JO-related toxicity, patients will also need to be monitored for toxicities related to PLD, including infusion reactions, hand-foot syndrome, mucocitis, myelosuppression, cardiotoxicity and hepatic damage. We expect to see less PLD-associated toxicity, which can be easily evaluated by monitoring the hand-and-foot syndrome, in which patients develop painful blistering. Considering our preliminary findings in macaques, we will also specifically evaluate for adrenal gland toxicity including laboratory testing. All toxicities will be graded using NCI Common Terminology Criteria for Adverse Events (CTCAE) Version 4.0 and standard protocols followed for reporting adverse events.

**Post-treatment monitoring:** In addition to their clinical status, patients will be followed post-treatment for antibodies against JO, PEG and His-tag (every 2 months), until antibody levels return to pre-treatment levels. Clinical trial protocols including inclusion/exclusion criteria, procedures, clinical and laboratory evaluations, criteria for interrupting the trial, rules for discontinuing injections in an individual subject, rules for suspension of the entire study, and statistical considerations are outlined in the pre-IND application, section 2 (Appendix) and included as examples. These protocols were developed based on data available at the time of the pre-IND application (2/14/13). Since then, protocols for the NHP toxicity studies and the clinical trial have been revised in the current proposal based on new data and to achieve a more efficient trial design. We anticipate additional revisions pending results from the proposed pre-clinical studies and additional feedback from the FDA.

**Aim 2.2: Evaluation of therapeutic effects:** Although not a primary endpoint of the study, tumor response will be assessed using clinical examinations, serum CA125 and imaging (CT or MRI) prior to every other cycle of therapy as well as at the end of the treatment period. Standard Response Evaluation Criteria In Solid Tumors (RECIST) criteria will be applied to assess a therapeutic response for patients evaluable by measurable or non-measurable disease and Gynecological Cancer Intergroup criteria for treatment response in relapsed cancer for patients who are evaluable by CA125 level only. Tissue samples will be collected from all patients who require clinically indicated biopsy to document disease persistence or progression.

**Table 3. Monitoring scheme**

	Pre-Enrollment	Each Cycle	Day 1 <sup>#</sup> -3 post	Week 1, 2, 3, 4 post
<b>Treatment (JO/PLD)</b>		Day 0		
<b>Clinical Analysis</b>				
Clinical status/adverse events	X	X	X	X
Physical examination	X	X	X	X
EKG	X	X	X	
CT or MRI of Abdomen/Pelvis <sup>1</sup>	X			
Cardiac EF by Echogram or MUGA <sup>1</sup>	X			
Chest X-ray (CXR) <sup>2</sup>	X			
Blood collection (CBC, diff, PLTS; Chem 23)	X		X	X
CA125	X	X		
Urine analysis	X	X	X	X
Adrenal function (urine: free cortisol, aldosterone, 17-Ketosteroids) (serum: DHEAS, testosterone)	X	X		
Pregnancy Test	X			
Ascites/Tumor biopsy (if possible) <sup>3</sup>	X			
Serum cytokines <sup>4</sup>	X	X	X	X
JO and DSG2 in serum <sup>4</sup>	X	X	X	X
PLD concentrations in serum <sup>4</sup>	X	X	X	X
Anti-JO, -PEG, -His tag antibodies in serum <sup>4</sup>	X	X	X	X
Anti-JO T-cells in PBMCs <sup>4</sup>	X			X
Circulating tumor cells <sup>4</sup>	X			X

<sup>#</sup> Day 1 follow-up evaluation and testing will be performed in hospital prior to discharge.

<sup>1</sup>Repeated every other cycle. Multi Gated Acquisition Scans will be done before the start of cycle 1 and after 4 cycles of PLD to exclude significant cardiac toxicity.

<sup>2</sup>Repeated every other cycle if initially abnormal

<sup>3</sup>Obtain tissue block from a diagnostic surgery or procedure. If patient undergoes biopsy (including para or thoracentesis for clinical indication during treatment we will attempt to collect tissue samples to be used to perform immunohistochemistry for DSG2, and other junction proteins.

<sup>4</sup>to be done in PI's lab.

**Aim 2.3: Gain additional knowledge about the biological effects of JO in patients.**

**Aim 2.3.1: JO and Doxil pharmacokinetics:** Serum samples will be stored at -80°C. JO concentrations will be measured by ELISA, using rabbit polyclonal anti-Ad3 fiber antibodies for antigen capture and mouse monoclonal anti-Ad3 knob/anti-mouse IgG-HRP for detection (3). The detection limit of this ELISA is 50 pg/ml. Doxil will be measured using an ELISA based on anti-PEG antibodies that we have used earlier (3).

**Aim 2.3.2. Immune responses:** Binding anti-JO antibodies (IgG, IgM, IgA, IgE) will be measured by ELISA (3). Plates will be coated with rabbit polyclonal anti-Ad3 fiber antibodies, followed by recombinant JO, human serum samples (1:2 to 1:1000 dilution), and either anti-human IgG-HRP, anti-human IgM-HRP, anti-human IgG-HRP, or anti-human IgE-HRP. For patients who become seropositive for JO, binding antibodies will be monitored until they return to baseline.

**Neutralizing anti-JO1 antibodies (IgG, IgM, IgA, IgE):** The assay will be performed as described previously (4). Human colon epithelial T84 cells will be cultured in transwell plates until transepithelial resistance is constant. JO or PBS mixed with heat-inactivated human serum samples (at a final concentration of 20%) will be added to the inner chamber, followed by  $^{14}\text{C}$ -PEG-4,000 1 hour later. Radioactive counts will be measured 1 hour later in the outer chamber. High affinity mouse monoclonal antibodies against Ad3 fiber will be used as a negative control.

**Anti-PLD/PEG antibodies:** PLD consists of doxorubicin HCL encapsulated in STEALTH liposomes coated with an outer layer of methoxypolyethylene glycol (MPEG). An anti-PEG antibody assay will be performed using the commercial kit from ANP Tech:

[http://anptinc.com/index.php?option=com\\_content&view=article&id=124&Itemid=92](http://anptinc.com/index.php?option=com_content&view=article&id=124&Itemid=92)

**JO specific T-cells by ELISpot:** PBMCs will be used to evaluate the induction of JO- and tumor-specific T-cell responses (8, 26). PBMCs will be isolated by Percoll gradient. Cells will be frozen in CTL-CryoABCTM serum-free media (Cellular Technology Ltd.). For quantification of JO-specific T-cells, PBMC will be incubated with JO and control peptides (5 $\mu\text{g}/\text{ml}$ ) and then subjected to ELISpot assays (h-INF-gammaELIPOST PRO 10 plate kit) as described elsewhere (8, 12).

**Tumor-specific T-cell immunity by ELISPOT:** Preliminary studies in immunocompetent mice indicate that JO increases the frequency of tumor-specific T-cells in the tumor. This observation warrants the analysis of anti-tumor T-cells in the peripheral blood of patients. PBMCs will be used to evaluate the induction of tumor specific T-cell responses (8, 26). ELISPOT will be performed according to MABtech manufacturer instructions (h-INF-gammaELIPOST PRO 10 plate kit). For the anti-tumor response *i*) survivin (BIRC5 PONAB) peptide, *ii*) a pool of CEA+Ny-ESO-1 peptides, *iii*) a pool of c-Myc+SSX2, MAGE-3 and WT-1 peptides (ProImmune), as well as IGFBP peptides (36) will be used. Of note, no pre-stimulation of PBMCs will be done in order to avoid artificial or incorrect signals and also to ensure adequate viability of cells which might be compromised during prolonged culture. In addition to these T-cell studies, we will analyze circulating Tregs (FoxP3+, CD4/CD25+) by flow cytometry of PBMCs as described earlier (48, 49). All immunological assays are established in the Pls lab (12, 48, 49).

**Expected outcome:** Our data shown in Fig.4 indicate that multiple cycles of JO/ PLD treatment are effective in immunocompetent animals despite anti-JO serum antibodies. Should we find that anti-JO T-cell responses affect the safety or efficacy of the approach, we will focus on creating JO variants in which immunodominant epitopes were mutated. Should the studies indicate that JO improves anti-tumor immune response, we will attract additional funding for more detailed mechanistic studies in animal models.

### ***Aim 2.3.3: JO's action on the tumor***

**DSG2 shedding:** JO triggers autocatalytic cleavage of DSG2 in tumors (4), thus increasing the levels of serum hDSG2 in hDSG2 transgenic mice with syngeneic tumors (50). We will therefore measure DSG2 serum concentrations in patient samples by ELISA as described earlier (50). We will also perform immunoprecipitation of serum protein with anti-DSG2 mAbs and analyze the material by Western blot and MS-MS to better understand the mechanisms for JO-triggered DSG2 shedding in humans.

**Circulating tumor cells (CTCs):** Although our studies with xenograft tumor models did not indicate that JO treatment increases CTCs (3), we will address this potent risk factor by measuring CTCs in peripheral blood using the CellSearch system and reagents (Veridex) (42). In this assay, a CTC is defined as EpCAM+, cytokeratin+, CD45-, and is positive for the nuclear stain DAPI. The normal reference range for CellSearch is <2 CTC/7.5 mL of blood. Furthermore, because it is believed that ovarian cancer CTC have undergone an EMT and lost EpCAM expression, we will use a CTC detection system based on a broader antibody cocktail that covers epithelial (EpCAM, HER2, MUC1, EGFR) as well as mesenchymal markers (cMET, N-cadherin, CD318) (37).

**Studies on biopsy and ascites samples:** If tumor biopsies are available, we will perform immunohistochemistry analyses for DSG2 and apoptosis markers, as well as staining for infiltrating immune cells (CD4, CD8, CD68, FoxP3). Selected findings will be validated by Western blot of tumor lysates or by flow cytometry of tumor cell suspensions obtained by collagenase/dispase digest (44). If pre- and post-treatment ascites samples are available, we will include them in T-cell and CTC assays.

**Expected outcome:** The additional data will help to better understand the JO action on the tumor and will, potentially, create the basis for new treatment approaches that involve JO.

## HUMAN SUBJECTS

### 1. PROTECTION OF HUMAN SUBJECTS

This Human Subjects Research meets the definitions of a clinical trial.

#### 1.1. Risks to Human Subjects

**1.1.a. Human Subjects Involvement, Characteristics, and Design.** This proposal will conduct a Phase I clinical trial of JO when administered in combination with a fixed 40mg/m<sup>2</sup> dose of PLD in patients with progressive, persistent or recurrent ovarian/fallopian tube cancer who have previously received standard therapies. The primary objectives of this trial are to evaluate the safety and determine the MTD of JO administration in combination with a fixed dose of PLD in patients with recurrent ovarian cancer. Secondary objectives are to a) evaluate the biologic effects of JO/PLD combination therapy, b) assess JO and PLD pharmacokinetics and c) evaluate anti-tumor effects of the combination therapy.

Patients 18 years of age or older with epithelial ovarian or fallopian tube cancer that is progressive, persistent or recurrent following standard therapies are eligible to participate. Patients who have failed second or greater line therapy will also be eligible. Patients who have received only one prior platinum-based regimen must have a progression-free interval of less than 6 months. Standard exclusion criteria including performance and end-organ function assessed by clinical examination and laboratory testing will be employed. Additionally, patients cannot have received prior therapy with PLD or an anthracycline. Patients with clinically significant cardiovascular disease (uncontrolled hypertension, Myocardial infarction or unstable angina within 6 months of study enrollment, history of serious ventricular arrhythmia, New York Heart Association (NYHA) Class II or higher congestive heart failure) or patients with baseline ejection fraction < or = 50% as assessed by echocardiogram or MUGA will also be excluded. Additional exclusion criteria include pre-existing anti-JO antibodies.

This trial will enroll 15 subjects unless there is excessive toxicity. We will test up to three dose levels of JO in combination with a fixed dose of Doxil™ (40mg/m<sup>2</sup>). In the event of a shortage of Doxil we will consider using the PLD Lipodox™. Enrolled eligible patients will be treated for four cycles on a standard schedule of treatment given once every 4 weeks, or until toxicity or tumor progression. JO dose escalation will be done following the modified continual reassessment method (CRM). The number of patients per cohort will be 2. The CRM starts with a prior distribution for the dose-toxicity relationship, and after each cohort of two patients is treated the dose-toxicity curve is updated based on the observed data. The subsequent group of 2 patients is then treated at the dose closest to the targeted dose-limiting toxicity (DLT) rate of 30% with the caveat that an increment of one dose level is the maximum allowed. This procedure will be followed until a total of 15 patients have been treated. A DLT is defined as any toxicity greater than or equal to grade 3.

Twelve and six hours prior to JO injection patients will receive dexamethasone 20mg p.o. to suppress anti-JO antibody formation. Intravenous infusion of Doxil will start 1 hour after the completion of intravenous infusion of JO. The highest non-severely toxic dose (HNSTD) from the combination treatment study in non-human primates will be used to set the safe starting dose for JO in the trial using a 1/5<sup>th</sup> safety factor of the HNSTD for the first patient cohort.

Standard protocols for monitoring patients treated with Phase I agents will be followed as described in Table 3 in 2.1.

**Documentation of Safety.** Patients will be treated in a dedicated Phase I trial unit. Patients in the first dose cohort will be observed overnight and discharged 23 hours post JO infusion provided no toxicities are observed. The t<sub>1/2</sub> of JO is 8 hours and concentration of JO is < 100 ng/ml 12 hours after a 2 mg/kg dose in non-human primates. Provided no late toxicities are observed in the first cohort, the observation period for subsequent cohorts may be reduced to 12 hours following JO infusion. All patients will be seen in outpatient follow-up on day +1, +2, +3 and then weekly. Standard protocols for monitoring of patients treated with Phase I agents will be followed (Table 3) and toxicities will be managed consistent with standard medical care. Patient with signs of significant toxicities will be admitted as appropriate. Toxicity will be evaluated using NCI Common Terminology Criteria for Adverse Events (CTCAE) Version 4.0. Standard protocols will be followed for reporting unexpected and serious adverse events (as detailed in Sec D1.5 below). Rules for pausing and/or stopping the study will be put in place in the event excessive toxicity is observed.

Subjects will also have approximately 50 cc blood drawn at various time points: prior to injection, 1, 2, 3, 4, 6, 12, 24, 48 and 72 hours post-injection, and then weekly. Safety parameters that will be measured include

clinical status, physical examination, weight, hematologic parameters, serum chemistry studies, coagulation studies, adrenal function, blood cell counts and electrocardiograms. We will assess Doxil-specific toxicity by monitoring for infusion reactions, hand-foot syndrome, mucocitis, myelosuppression, cardiotoxicity, and hepatic damage.

Patients will be followed post-treatment for antibodies against JO, PEG and His-tag (every 2 months), until antibody levels return to pre-treatment levels.

Tumor response will be assessed using clinical examinations, serum levels of CA125 prior to each cycle of therapy, and imaging (CT or MRI) prior to every other cycle of therapy as well as at the end of the treatment period.

**1.1.b. Sources of Material.** Research materials obtained from participating subjects include, but are not limited to: (1) medical records to assess eligibility, (2) blood specimens used for clinical evaluation, and (3) research bloods to evaluate JO and PLD kinetics, immunology and biologic effects.

During the course of the study we will record vital signs, results from clinical laboratory and physical evaluations, results of laboratory assays and adverse events self-reported or observed during the study and during follow-up. We will collect basic demographics including race and ethnicity.

Accessing the link between personal identifying information and the research samples are restrictive. The principal investigators are responsible for designating which research staff can access the link. Electronic data will be maintained in a password-protected computer database. This data is backed-up on a regular basis and stored off-site. All hard copy records will be stored in locked file cabinets at all times unless being reviewed.

In addition to the secured files and database, only the coded unique study number and DOB will be provided to those processing the blood samples.

In order to evaluate the results of this study, the following people and government agencies may get access to subject identities: (1) Doctors and research staff taking part in the study, (2) FDA, (3) NIH, (4) Fred Hutchinson Cancer Research Center – Cancer Consortium IRB and (5) SPORE Clinical and Path Cores.

**1.1.c. Potential Risks.** The potential risks may include: (1) PLD toxicities (2) adverse reactions such as anaphylaxis, (3) venous access for blood tests and treatment infusion, (3) minimally invasive clinical procedures including EKG, CT imaging, Cardiac EF and Chest X-ray, (4) infusion of JO and PLD. The likelihood of these risks is discussed together with procedures for minimizing risk in section D.1.2.b. below.

The alternatives to this study include standard chemotherapy or other approved and experimental therapies available at many medical centers specifically for patients with progressive or recurrent ovarian cancer. These may include: FDA approved EOC chemotherapies other than PLD, novel chemotherapeutic agents, and immune based treatments.

## **1.2. Adequacy of Protection Against Risks**

**1.2.a. Recruitment and Informed Consent.** Subjects will be self-referred or referred by their primary oncologist. This study will be posted on the Fred Hutchinson Cancer Research Center Recruitment Website, the Swedish Cancer Institute Clinical Trials website, and ClinicalTrials.gov. The SPORE Clinical Core will assist in patient recruitment.

Once a patient has been evaluated for eligibility, has been deemed eligible and agrees to pursue participation, they will be sent or given for initial review: (1) the study consent form, and (2) medical records release (HIPAA) form. An appointment will be made for them to meet with a Study Physician, Research Nurse or qualified Research Assistant for an informed consent appointment.

The consenting procedure usually takes 1 to 2 hours with time spent reviewing procedures, the specifics of the research study, risks, benefits and alternative and the specifics of our research group. It is emphasized that this is a phase I study and may be of no clinical benefit to the patient. There is no coercion to enroll and the subjects are assured that a decision to not enroll in no way influences their relationship with their primary oncologist or their ongoing medical care. After all questions are answered and if agreeable, the subjects will sign the consent documents and be provided a copy for their records.

### **D.1.2.b. Protections Against Risk.**

#### ***Pregnancy***



This study may be harmful to an unborn child. The risks to an unborn child are unknown. Pregnant women are not eligible to participate and a pregnancy test will be performed at the start of the trial, prior to beginning treatment. Women of child bearing potential must agree to use an adequate form of birth control during the entire study period.

#### *JO infusion*

Subjects may experience infusion reactions. There is no previous human experience with JO however based on our animal studies we do not expect serious adverse reactions. Except for a mild, transient diarrhea and mild lymphopenia, intravenous injection of JO had no critical side effects on other tissues or hematologic parameters in hDSG2 mice. We will therefore pay specific attention to blood cell counts in patients. Non-human primate studies showed no laboratory or histological abnormalities, however JO slightly increased Doxil concentrations in adrenals so we will monitor adrenals for potential toxicity during the trial.

Pre-clinical studies suggest that JO treatment may induce formation of anti-JO antibodies. We have seen no evidence of increased toxicity or a reduction in JO efficacy with JO retreatment in animals with pre-existing JO antibodies. However to reduce the risk of developing anti-JO antibodies in clinical trial participants Dexamethasone 20mg will be administered p.o. 12 and 6 hours prior to each JO infusion. Patient vital signs will be closely monitored in the first 23 hours after injection and they will also be followed post-treatment for antibodies against JO, PEG and His-tag every 2 months until antibody levels return to pre-treatment levels.

JO binding to DSG2 on tumor cells triggers pathways involved in EMT, a process which has been associated with tumor metastasis, however none of our *in vivo* studies have shown evidence of increased tumor growth or metastasis after injection with JO. We will monitor for potential signs of metastasis by measuring circulating tumor cells before and after JO injection.

In preclinical studies in mouse tumor models, we found that the optimal therapeutic effect of JO is achieved when given 1 hour before the chemotherapeutic drug. We will maintain this treatment regiment in the clinical trial. It will also allow us to adjust for potential anaphylactic reactions related the JO infusion.

#### *PLD infusion*

Subjects may experience the following common side effects: hand-foot syndrome, mucocitis, myelosuppression, myelosuppression and nausea. More serious effects may include cardiotoxicity and infusion reactions consisting of shortness of breath, chest pain or anaphylactoid reaction. Doxil toxicity will be evaluated post-injection by careful monitoring of patients using physical examination and diagnostic tests such as lab values. Toxicities will be graded according to NCI CTC version 4 and promptly reported. Management of toxicities consists of following the protocol for dose reductions or holding treatment.

#### *Venous Access*

Venous access and treatment administration will be provided using central venous access device accessed by a trained professional to minimize the risk of drug extravasation. Although rare, if an extravasation occurs approved hospital procedures will be followed. During blood draws, subjects may experience pain, bruising, lightheadedness, fatigue, or on rare occasions infection. Subjects are encouraged to hydrate prior to blood draws. If they experience any side effects related to an intravenous treatment or blood draw site, they are instructed to contact one of the participating research study staff to describe their symptoms/reactions.

#### *EKG*

Subjects may develop a mild rash where the electrodes (soft patches) were attached. This rash often disappears without treatment.

#### *CT of Abdomen/Pelvis*

Risks of CT scans are allergies to the contrast dye and exposure to radiation, however the risk from one scan is small. The most common contrast given in a vein contains iodine. Patients who are allergic to iodine may experience nausea or vomiting, sneezing, itching or hives. Patients will be asked about iodine allergies prior to the scan and if an allergy is suspected will be given steroids and/or anti-histamines prior to the test or non-iodinated contrast dyes may be used. Risk of anaphylaxis is rare. Subjects will be closely monitored during the procedure and if there are any serious problems the procedure will be stopped.

#### *Chest X-ray*

Chest x rays have few risks and the amount of radiation is small. A lead apron will be used to protect certain parts of the patient's body from radiation.

#### *Confidentiality*

The link between the subject and their personal health information and the unique study ID number are restricted to research staff designated by the Project Directors who will ensure confidentiality and managed according to the requirements of the Health Insurance Portability and Accountability Act of 1996 (HIPAA).

### **1.3. Potential Benefits of the Proposed Research to Human Subjects and Others.**

Risks associated with this study are reasonable as there are limited options for patients with progressive or recurrent ovarian cancer following primary treatment. The benefits to this study are unknown. The treatment may help the subject's condition or it may not. It will, however, benefit patients with cancer in the future as we will gain substantial knowledge from this first-in-human trial.

### **1.4. Importance of Knowledge to be Gained.**

PLD is currently used to treat patients with ovarian cancer that has progressed or recurred after platinum-based chemotherapy, however response rates are low, response duration is short, and the toxicity is significant. A central resistance mechanism is the maintenance of tight junctions between malignant cells that prevent drug penetration to the tumor. Adding JO to PLD treatment may cause transient opening of these tight junctions, allowing more of the drug to reach the tumor and potentially reducing the amount of drug needed for effective therapy thereby reducing toxic side effects.

### **1.5. Data Safety and Monitoring Plan**

The Project Directors are responsible for every aspect of the design, conduct and final analysis of the protocol. Regulations defining the responsibilities for assessment and report of all adverse events (AE), serious AE and unexpected AE are defined by the Code of Federal Regulations: 21 CFR 312.32 and Common Terminology Criteria for Adverse Events (CTCAE) Version 3.0 published by the Cancer Therapy Evaluation Program (CTEP), a division of the NCI/NIH.

This clinical study will rely upon the monitoring of the trial by the Project Directors in conjunction with a Research Nurse, Project Manager, SPORE Statistician, an independent Medical Monitor and an Independent Study Monitor assigned by the Clinical Trials Support Office of the Fred Hutchinson Cancer Research Center. A Medical Monitor will meet with the PDs prior to subjects being recruited in order to review the conduct and monitoring mechanisms for the study. The Medical Monitor will then meet bi-annually throughout the data collection period with the PDs, Study Physician(s), P.A.-C, Research Nurse(s), Research Assistant(s) and other applicable clinical research staff members as determined by the PDs. The Medical Monitor will review subject recruitment and retention, adherence to protocol, follow-up, data quality, and participant risk versus benefit. If a serious adverse event occurs the P.I.s will be notified immediately and Medical Monitor will be notified along with the IRB and appropriate federal agencies (i.e. FDA).

Adverse events will be monitored as: Patients are monitored for the development of end organ damage by assessing adverse events with EKG, serum chemistries, liver function studies, complete blood counts and physical exams performed every visit with evaluation beginning after the first treatment. All adverse events for all systems are graded on a scale of 1-5 and attribution is assigned, using the Common Terminology Criteria for Adverse Events. If an adverse event occurs during more than one cycle of treatment, then only the most severe adverse event is reported. All information pertaining to toxicity is recorded on the source document.

Procedure for reporting adverse events:

- a. Identify the classification/attribution of the adverse event as defined above using the NCI Common Terminology Criteria for Adverse Events.
- b. After appropriate medical intervention has been instituted, the Principal Investigator or his/her designee will be notified within 24 hours.
- c. File appropriate reports immediately by phone/fax with appropriate agencies, as described above.
- d. Notify the patient's primary physician or referring physician within a medically appropriate timeframe, depending on the classification of the adverse event.
- e. Submit written reports to appropriate agencies.
- f. Document the adverse event in the patient's study chart, using a progress note to describe the event and treatment, if appropriate.
- g. Copies of all forms/correspondence relating to the adverse event would be filed in the patient's study chart.

**Agency Reporting Requirements:**

**Fred Hutchinson Cancer Research Center: Cancer Consortium IRB** – Expedited adverse event reporting should be reported to the IRB as soon as possible but within 10 calendar days.

Expedited adverse events must meet all three reporting requirements:

1. Unexpected
2. Related or possibly related to the research procedures
3. Serious, meaning it resulted in any of the following outcomes: death, life-threatening event, inpatient hospitalization or prolongation of existing hospitalization, persistent or significant disability/incapacity/or change in psychosocial status, a congenital anomaly, or requires intervention to prevent permanent impairment or damage.

The most current consent document(s) should be attached. The PI or designee must sign the Expedited Reporting Form for Unanticipated Problems or Noncompliance. The Expedited Reporting Form for Unanticipated Problems or Noncompliance and Adverse Event Reporting Form should be submitted directly to the Institutional Review Office. Submit only the original documents. If documents are being modified, submit a Research Modification Form and modified documents, if applicable.

**FDA (for trials using an Investigational New Drug (IND))** – As the sponsor of the IND for this study we will follow 21 CFR Part 312 for safety reports to the FDA. In summary written reports are submitted to the FDA for an event that is Related to the product and Serious and Unexpected using the FDA Form 3500A MedWatch form. The safety report may be called or faxed to the appropriate contact for this IND as soon as possible but in no event later than 7 calendar days.

**NCI** - As the Sponsor of the IND for this study we will follow the controlling regulations of the Food and Drug Administration as required by the NCI. Thus, all adverse events observed during the study will be reported to the NCI in the form of a progress report. Temporary or permanent suspension of an NCI funded clinical trial is to be reported to the NCI grant program director responsible for the grant.

**1.6. ClinicalTrials.gov.** If this project is funded we will register the trial with ClinicalTrials.gov.

**Key Personnel Training in the Use of Human Subjects in Research**

The leaders of the project and all key personnel involved with human subjects research within this project have completed approved institutional training in the Use of Human Subjects in Research that covers the following content:

1. Introduction and Historical Perspective
2. Ethical Principles
3. Regulations and Process
4. Informed Consent
5. Research with Investigational Biologics, Drugs and Devices
6. Behavioral Research
7. Research with Protected Populations: Prisoners
8. Research with Protected Populations: Minors
9. Research with Protected Populations: Pregnant Women and Fetuses in Utero
10. Research with Protected Populations: Vulnerable Subjects: A Definition
11. Records-Based Research
12. Genetic Research
13. Research Integrity

## **INCLUSION OF WOMEN AND MINORITIES**

All participants in this ovarian cancer research study will be women. Members of any race will be included if they present with eligibility based on the criteria listed elsewhere. The FHCRC and affiliated institutes continue to be challenged to meet accrual goals for under-represented groups. In general, the population pool from which we will be drawing our study group is 94.4% Caucasian, 2.3% Asian American, 1.8% American Indian/Alaskan Native, and 1% African American. The Targeted/Planned Enrollment Table shows the gender and ethnic breakdown.

## Planned Enrollment Report

**Study Title:** Project 3: Combination Therapy of JO and PEGylated Liposomal Doxorubicin in Patients with Epithelial Ovarian Cancer

**Domestic/Foreign:** Domestic

**Comments:**

Racial Categories	Ethnic Categories				Total
	Not Hispanic or Latino		Hispanic or Latino		
	Female	Male	Female	Male	
American Indian/Alaska Native	0	0	0	0	0
Asian	2	0	0	0	2
Native Hawaiian or Other Pacific Islander	0	0	0	0	0
Black or African American	1	0	0	0	1
White	11	0	0	0	11
More than One Race	0	1	0	0	1
Total	14	1	0	0	15

Study 1 of 1

## **INCLUSION OF CHILDREN**

Children aged 18-21 who meet eligibility requirements are eligible for this trial.

## VERTEBRATE ANIMALS

### **Mice at the University of Washington**

All animal procedures at the UW will be performed under the supervision of the University of Washington Institutional Animal Care and Use Committee. The studies are covered by our IACUC protocol #3108-1 (PI: Lieber). Animals will be housed in the UW Animal Facility, located in the K-wing (-2 level) of the Magnuson Health Sciences Building.

We will provide to BASi:

-40 naïve hDSG2 transgenic mice (6-12 weeks old)

-40 preimmune hDSG2 transgenic mice

-20 hDSG2 transgenic mice with spontaneous ovarian/fallopian tube tumors (detectable CA125 serum levels)

#### **1. Experimental procedures**

##### Human DSG2 transgenic mice:

We will use a model for spontaneous ovarian cancer that is transgenic for human DSG2. Our collaborator Ronny Drapkin (Dana Farber/Harvard Cancer Center) has developed a spontaneous fallopian tube/ovarian cancer model with high-grade serous carcinomas appearing within 2-4 months after birth<sup>1</sup>. It involves a Pax8 promoter driven Cre recombinase to delete tumor suppressor genes Tp53, pTen, and Brca1. For our studies, we will cross-breed the Pax8-Cre mice with human DSG2 transgenic mice. Double transgenic mice will be identified by genotyping. Tumor growth in the spontaneous cancer model can be monitored based on serum CA125<sup>1</sup>.

##### Procedures:

intravenous injection of JO-1 to establish pre-immunity. A total of 2mg/kg of JO-1 in 200ul of PBS will be injected into the tail vein.

**Table 1: Design of GLP toxicology studies in hDSG2-transgenic mice (based on FDA recommendations).**

Group	Dosing	Route	Regiment	Duration	N	
1	JO (2 mg/kg) naïve mice, no tumor	IV	Every week	4 weeks	10	6 animals→necropsy 4 animals→follow up
2	JO (2 mg/kg) pre-immune mice, no tumor	IV	Every week	4 weeks	10	6 animals→necropsy 4 animals→follow up
3	JO ("high-dose") naïve mice, no tumor	IV	Every week	4 weeks	10	6 animals→necropsy 4 animals→follow up
4	JO ("high-dose") pre-immune mice, no tumor	IV	Every week	4 weeks	10	6 animals→necropsy 4 animals→follow up
5	PLD (40 mg/m <sup>2</sup> ) naïve mice, no tumor	IV	Every week	4 weeks	10	6 animals→necropsy 4 animals→follow up
6	JO ("high dose") + PLD (40 mg/m <sup>2</sup> ) naïve mice, no tumor	IV	Every week	4 weeks	10	6 animals→necropsy 4 animals→follow up
7	JO ("high dose") + PLD (40 mg/m <sup>2</sup> ) preimmune mice, no tumor	IV	Every week	4 weeks	10	6 animals→necropsy 4 animals→follow up
8	JO ("high dose") spontaneous tumors	IV	Every week	4 weeks	10	6 animals→necropsy 4 animals→follow up
9	JO ("high dose") + PLD (40 mg/m <sup>2</sup> ) spontaneous tumors	IV	Every week	4 weeks	10	6 animals→necropsy 4 animals→follow up

#### **2. Justify the use of animals**

New approaches for cancer treatment with PLD can only be studied *in vivo*. Tumor cell cultures *in vitro* do not reflect the complex interaction between tumor cells and the host. Mice are an adequate model for tumor xenografts to demonstrate bridged activity between two compounds as used in this application.

### **3. Provide information on the veterinary care of the animals involved.**

Animals will be monitored for behavior every day and weighed twice a week. The university will weigh mice daily if there is a question about their health or weight loss. If they encounter weight loss of 20% or other signs of morbidity (absence of grooming, eating or drinking, watery eyes, wet fur, inflammation of sutures), the affected animals will be euthanized. Routine veterinary care is provided by the Department of Comparative Medicine, which oversees the operation of the animal facility. The facilities for animal maintenance and procedure rooms are certified and periodically inspected by the Institutional Animal Care and Use Committee.

### **4. Describe the procedures for ensuring that discomfort, distress, pain and injury will be limited to that which is unavoidable in the conduct of scientifically sound research.**

There are no experimental contradictions to withhold analgesics from animals at any time, although the procedures will be limited to injection of the therapeutic and blood draws. Animals are routinely monitored by the center and if they show signs of distress will be treated or euthanized as deemed appropriate by the attending veterinarian.

### **5. Describe any method of euthanasia to be used and the reasons for its selection.**

Mice will be sacrificed through an Avertin overdose. This method is consistent with recommendations of the Panel on Euthanasia of the American Veterinary Medical Association.

### **6. Animal number selection using statistical power calculations**

For the toxicology studies, we selected a group size of 8 animals. We arrived at this number by setting a large effect size, which was based on our previous studies, and a desired power of 0.8 at a significance level of 0.05.

### **Mice at BASi**

BASi is fully accredited by the Association for Assessment and Accreditation of Laboratory Animal Care International (AAALAC International) and registered with and inspected by the U.S. Department of Agriculture (USDA-APHIS).

JO-1 injection, blood sampling and necropsy will be performed under BASi IACUC protocol #XXX

#### **Procedures:**

- a) intravenous injection of JO-1 to establish pre-immunity. A total of 2mg/kg of JO-1 in 200ul of PBS will be injected into the tail vein.
- b) blood sampling: retroorbital, saphenous vein.

Experimental groups are described in Table 1.

Groups #1 to 7 (Table 1) will receive 4 injections of JO and/or PLD one week apart, based on the clinical protocol. Studies will be performed in naïve hDSG2 transgenic mice and hDSG2 transgenic mice that have been vaccinated with JO and have mounted T- and B-cell responses against the protein. Studies in pre-immune animals will address potential allergic side effects of JO injection. The vast majority of preclinical studies performed in the PI's lab were done with a JO dose of 2mg/kg. This will be the NOAEL ("no observed adverse effect level") starting dose for the toxicology studies. In addition, we plan to exceed the maximum dose that we estimate to use in the clinical trial. This dose is usually 10-fold higher than the NOAEL<sup>2</sup>. In our case, this would be 20mg/kg. If dose-limiting toxicity (DLT) occurs in Group #3, we will lower the "high dose". The standard PLD dose in humans is (40mg/m<sup>2</sup>), which corresponds to a dose of 1.1mg/kg in mice. Notably, PLD is a large molecule, predominantly sequestered in vascular space, in which case allometric dose scaling is not appropriate. For combination treatment, PLD will be injected one hour after JO. Groups #8 and 9 will be hDSG2 transgenic mice with spontaneous hDSG2 expressing ovarian/fallopian tube tumors. Mice will be injected when serum CA125 becomes detectable and followed for 4 weeks. Tumor bearing mice better reflect the target patient group in the clinical trial. After each treatment cycle, blood samples will be collected from all animals on day 1 of injection at 3 time points – pre-dose, 6, and 24 hours post-dose, and then twice per week. The samples will be analyzed for: *i*) full blood CBC and chemistry, and *ii*) serum cytokines, *iii*) JO concentrations, *iv*) PLD concentration and *v*) IgG, IgM, IgA, and IgE antibodies against JO, PEG and His tag. After 4 weeks, six animals will be euthanized and complete necropsy and histological examination will be performed. Specific attention will be given to GI-tract and cardiac toxicities. Four animals will be followed post-



treatment for 2 weeks with weekly blood analysis. JO and PLD concentrations will be measured in all collected tissues by ELISA. Tissue sections will be analyzed by immunohistochemistry for the presence of JO and PLD. Splenocytes will be used for ELISPOT assays to quantitate JO-specific  $\gamma$ -interferon-producing CD4 and CD8 T-cells. All assays for safety assessments will be performed under GLPs at BASi. The exploratory assays for cellular responses are established in the PI's lab.

**Animal numbers:** For the toxicology studies, we selected a group size of 10 animals. We arrived at this number by setting a large effect size, which was based on our previous studies, and a desired power of 0.8 at a significance level of 0.05.

## **Macaques at BASi**

### **1. Experimental procedures**

The studies will be conducted in accordance with the US FDA Good Laboratory Practice Regulations. The GLP-certified test site will be BASi.

**JO dose finding study.** In our previous studies, intravenous injection of 0.6mg/kg and 2mg/kg (in combination with PLD/Doxil) was well tolerated. To determine the highest non-severely toxic dose (HNSTD) and correlative pharmacokinetics attributes for JO, animals will be injected with JO at a dose of 4mg/kg and 10mg/kg (N=2) and monitored as described in B.3a-3. A necropsy will be performed at day 7 and pathology and histology reports will be compiled.

**GLP toxicology study for combination therapy.** Three JO dose cohorts will be analyzed (Table 2). The maximum JO dose will be the HNSTD found in the dose-finding study. With this dose, we expected to reach JO dose-limiting toxicity (DLT) in combination with PLD. This will allow us to estimate the maximum tolerated dose (MTD) of JO when combined with PLD in humans. The lower doses will be in the range of 20 to 50% of the HNSTD. The PLD dose will be 1.1mg/kg which corresponds to 40 mg/m<sup>2</sup> in humans. For the combination treatment, PLD will be injected 1 hour after JO. The design of the clinical trial involves 4 treatment cycles 4 weeks apart (i.e. the standard treatment regiment for PLD). Common PLD toxicities in patients (hand-food symptoms, stomatitis) develop late. Furthermore, accumulative PLD cardiotoxicity is a potential side effect after multiple treatment cycles. To assess late and accumulative toxicities, we will treat animals in 4 cycles with an interval of 4 weeks. To decrease the formation of JO-antibody immune complexes, animals will also receive prednisolone treatment for 48 hours during JO injection <sup>3</sup>.

**Table 2: Design of cGMP toxicology studies in non-human primates.**

Group	Dosing	Route	Regiment	Interval	
1	PLD (40 mg/m <sup>2</sup> )	IV	Every 4 week	4 weeks	2 animals→necropsy
2	JO (20% HNSTD) PLD (40 mg/m <sup>2</sup> )	IV	Every 4 week	4 weeks	4 animals→necropsy 2 animals→follow up
3	JO (50% HNSTD) PLD (40 mg/m <sup>2</sup> )	IV	Every 4 week	4 weeks	4 animals→necropsy 2 animals→follow up
4	JO (HNSTD) PLD (40 mg/m <sup>2</sup> )	IV	Every 4 week	4 weeks	4 animals→necropsy 2 animals→follow up

Physical examinations will be performed daily by a qualified veterinarian on all study animals prior to initiation and on all animals prior to their respective necropsy. Body weights will be recorded once prior to treatment and weekly thereafter. Blood samples will be collected and analyzed as described for hDSG2 transgenic mice and in B.3a-3. Animals will be euthanized six hours after the last injection and a gross necropsy will be performed by a certified veterinary pathologist at BASi. A standard set of tissues (~66/animal) will be collected and preserved in 10% formalin. All collected tissues will be examined by a veterinary pathologist. An audited draft of the final report will be available 6 weeks following the final necropsy. The report will assess functional effects on the major physiological systems (e.g., cardiovascular, respiratory, renal, and central nervous systems considering hematology, histopathology, urinalysis, and EKG/MCGs).

**Animal numbers:** For non-rodent species, the FDA recommended 4 animals/group for the main study groups, and 2 animals/group for recovery groups.

## 2. Justify the use of animals

Justification for using *Macaca fascicularis* for GLP toxicology studies. JO-1 does not efficiently bind to mouse<sup>4</sup>, rat, hamster, and dog PBMC (Table 3) or transformed cell lines (data not shown) and the DSG2 gene homology for these species compared to human DSG2 is less than 80%. Although hDSG2 transgenic mice allow us to study a number of variables in a large number of animals, it is unclear whether the hDSG2-mouse system accurately models a homologous system with human DSG2 in human cells. A better model is non-human primates. The DSG2 gene homology between humans and macaques is 96.6%. Biodistribution in *Macaca fascicularis* is similar to humans<sup>4</sup>. JO-1 binds to monkey DSG2 and triggers junction opening at a level that is comparable to human cells<sup>4</sup>. This justifies the use of *Macaca fascicularis* for GLP toxicology studies after intravenous JO-1 injection.

Species	DSG2 homology	gene	Rel. binding of <sup>3</sup> H-Ad3-GFP on PBMC
Human	100%		100%
Chimpanzee	99.0%		N/A
Macaque	96.6%		98%
Mouse	77.1%		5%
DSG2-tg mouse	100%		96%
Rat	76.5%		6%
Hamster	N/A		11%
Dog	78.7%		19%
Cow	76.6%		N/A

**Table 3: DSG2 gene homology and binding of the parental virus Ad3 to PBMC from different species.** Ad3 is labeled with <sup>3</sup>H thymidine and bound particles can be measured with a scintillation counter. Binding to human PBMCs was taken at 100%.

## 3. Provide information on the veterinary care of the animals involved.

A full-time attending veterinarian is on site and maintains the facilities in accordance with AAALAC accreditation standards. In addition, a part-time consultant veterinarian is available when needed. The attending veterinarian is also available for after-hours calls. Animals are observed at least two times each day by facility personnel. Anytime an animal is observed in a condition indicating severe pain or distress, or that may indicate an animal is in a life-threatening condition, it is to be brought to the attention of the attending veterinarian and study director immediately, and appropriate action is taken and recorded in the study record. The proposed studies do not involve surgery.

## 4. Describe the procedures for ensuring that discomfort, distress, pain and injury will be limited to that which is unavoidable in the conduct of scientifically sound research.

There are no experimental contradictions to withhold analgesics from animals at any time. In the event that any aspect of this study causes more than normally expected brief pain or distress to the animals, the Study Director shall determine, in consultation with the Attending Veterinarian, if administration of appropriate sedatives, analgesics, or anesthetics, or other therapies would be contraindicated by the objectives of the study and document the resultant course of action. Animals that experience severe or chronic pain or distress that cannot be relieved will be euthanized.

The BASi Evansville IACUC reviews the care and use of animals in proposed and ongoing protocols/procedures with respect to compliance with USDA regulations as governed by the Animal Welfare Act (9CFR) and all applicable amendments, AAALAC guidelines as provided in the Guide for the Care and Use of Laboratory Animals (NCR, 1996), and Public Health Service Policy on Humane Care and Use of Laboratory Animals. Protocols/procedures raising concerns from IACUC members and/or study personnel will be reviewed with the study director to discuss the necessity of the protocol/procedure and/or possible alternatives. If the IACUC determines that a protocol/procedure is unacceptable, i.e. causing unnecessary pain and distress, the IACUC will act to prevent the initiation/continuation of the project.

The proposed studies do anticipate the use of restraining devices for intravenous dosing and blood collection purposes.

## 5. Describe any method of euthanasia to be used and the reasons for its selection.

In the proposed studies, the monkeys will be euthanized by intravenous sodium pentobarbital followed by exsanguination in accordance with the AVMA Guidelines on Euthanasia (June 2007).

## 6. Animal number selection

For non-rodent species, the FDA recommended 4 animals/group for the main study groups, and 2 animals/group for recovery groups.

1. Perets R, Wyant GA, Muto KW, et al. Transformation of the fallopian tube secretory epithelium leads to high-grade serous ovarian cancer in Brca;Tp53;Pten models. *Cancer Cell*. 2013;24(6):751-765. Prepublished on 2013/12/18 as DOI S1535-6108(13)00459-5 [pii] 10.1016/j.ccr.2013.10.013.
2. Garrett-Mayer E. The continual reassessment method for dose-finding studies: a tutorial. *Clin Trials*. 2006;3(1):57-71. Prepublished on 2006/03/17 as DOI.
3. Dykes AC, Walker ID, Lowe GD, Tait RC. Combined prednisolone and intravenous immunoglobulin treatment for acquired factor VIII inhibitors: a 2-year review. *Haemophilia*. 2001;7(2):160-163. Prepublished on 2001/03/22 as DOI hae489 [pii].
4. Wang H, Beyer I, Persson J, et al. A new human DSG2-transgenic mouse model for studying the tropism and pathology of human adenoviruses. *J Virol*. 2012;86(11):6286-6302. Prepublished on 2012/03/30 as DOI JVI.00205-12 [pii] 10.1128/JVI.00205-12.

## REFERENCES

1. **Alagkiozidis, I., A. Facciabene, C. Carpenito, F. Benencia, Z. Jonak, S. Adams, R. G. Carroll, P. A. Gimotty, R. Hammond, G. A. Danet-Desnoyers, C. H. June, D. J. Powell, Jr., and G. Coukos.** 2009. Increased immunogenicity of surviving tumor cells enables cooperation between liposomal doxorubicin and IL-18. *J Transl Med* **7**:104.
2. **Amieva, M. R., R. Vogelmann, A. Covacci, L. S. Tompkins, W. J. Nelson, and S. Falkow.** 2003. Disruption of the epithelial apical-junctional complex by *Helicobacter pylori* CagA. *Science* **300**:1430-1434.
3. **Beyer, I., H. Cao, J. Persson, H. Song, M. Richter, Q. Feng, R. Yumul, R. van Rensburg, Z. Li, R. Berenson, D. Carter, S. Roffler, C. Drescher, and A. Lieber.** 2012. Coadministration of epithelial junction opener JO-1 improves the efficacy and safety of chemotherapeutic drugs. *Clin Cancer Res* **18**:3340-3351.
4. **Beyer, I., R. van Rensburg, R. Strauss, Z. Li, H. Wang, J. Persson, R. Yumul, Q. Feng, H. Song, J. Bartek, P. Fender, and A. Lieber.** 2011. Epithelial junction opener JO-1 improves monoclonal antibody therapy of cancer. *Cancer Res* **71**:7080-7090.
5. **Biedermann, K., H. Vogelsang, I. Becker, S. Plaschke, J. R. Siewert, H. Hofler, and G. Keller.** 2005. Desmoglein 2 is expressed abnormally rather than mutated in familial and sporadic gastric cancer. *J Pathol* **207**:199-206.
6. **Bookman, M. A., B. E. Greer, and R. F. Ozols.** 2003. Optimal therapy of advanced ovarian cancer: carboplatin and paclitaxel vs. cisplatin and paclitaxel (GOG 158) and an update on GOG0 182-ICON5. *Int J Gynecol Cancer* **13**:735-740.
7. **Bouvet, M., B. Fang, S. Ekmekcioglu, L. Ji, C. D. Bucana, K. Hamada, E. A. Grimm, and J. A. Roth.** 1998. Suppression of the immune response to an adenovirus vector and enhancement of intratumoral transgene expression by low-dose etoposide. *Gene Ther* **5**:189-195.
8. **Cerullo, V., S. Pesonen, I. Diaconu, S. Escutenaire, P. T. Arstila, M. Ugolini, P. Nokisalmi, M. Raki, L. Laasonen, M. Sarkioja, M. Rajacki, L. Kangasniemi, K. Guse, A. Helminen, L. Ahtiainen, A. Ristimaki, A. Raisanen-Sokolowski, E. Haavisto, M. Oksanen, E. Karli, A. Karioja-Kallio, S. L. Holm, M. Kouri, T. Joensuu, A. Kanerva, and A. Hemminki.** 2010. Oncolytic adenovirus coding for granulocyte macrophage colony-stimulating factor induces antitumoral immunity in cancer patients. *Cancer Res* **70**:4297-4309.
9. **Choi, I. K., R. Strauss, M. Richter, C. O. Yun, and A. Lieber.** 2013. Strategies to increase drug penetration in solid tumors. *Front Oncol* **3**:193.
10. **Christiansen, J. J., and A. K. Rajasekaran.** 2006. Reassessing epithelial to mesenchymal transition as a prerequisite for carcinoma invasion and metastasis. *Cancer Res* **66**:8319-8326.
11. **Dhar, D., J. F. Spencer, K. Toth, and W. S. Wold.** 2009. Pre-existing immunity and passive immunity to adenovirus 5 prevents toxicity caused by an oncolytic adenovirus vector in the Syrian hamster model. *Mol Ther* **17**:1724-1732.
12. **DiPaolo, N., S. Ni, A. Gaggar, R. Strauss, S. Tuve, Z. Y. Li, D. Stone, D. Shayakhmetov, N. Kiviat, P. Toure, S. Sow, B. Horvat, and A. Lieber.** 2006. Evaluation of adenovirus vectors containing serotype 35 fibers for vaccination. *Mol Ther* **13**:756-765.
13. **Dykes, A. C., I. D. Walker, G. D. Lowe, and R. C. Tait.** 2001. Combined prednisolone and intravenous immunoglobulin treatment for acquired factor VIII inhibitors: a 2-year review. *Haemophilia* **7**:160-163.
14. **Fessler, S. P., M. T. Wotkowicz, S. K. Mahanta, and C. Bamdad.** 2009. MUC1\* is a determinant of trastuzumab (Herceptin) resistance in breast cancer cells. *Breast Cancer Res Treat* **118**:113-124.
15. **Garrett-Mayer, E.** 2006. The continual reassessment method for dose-finding studies: a tutorial. *Clin Trials* **3**:57-71.
16. **Gordon, A. N., J. T. Fleagle, D. Guthrie, D. E. Parkin, M. E. Gore, and A. J. Lacave.** 2001. Recurrent epithelial ovarian carcinoma: a randomized phase III study of pegylated liposomal doxorubicin versus topotecan. *J Clin Oncol* **19**:3312-3322.
17. **Gordon, A. N., C. O. Granai, P. G. Rose, J. Hainsworth, A. Lopez, C. Weissman, R. Rosales, and T. Sharpington.** 2000. Phase II study of liposomal doxorubicin in platinum- and paclitaxel-refractory epithelial ovarian cancer. *J Clin Oncol* **18**:3093-3100.

18. **Green, S. K., M. C. Karlsson, J. V. Ravetch, and R. S. Kerbel.** 2002. Disruption of cell-cell adhesion enhances antibody-dependent cellular cytotoxicity: implications for antibody-based therapeutics of cancer. *Cancer Res* **62**:6891-6900.
19. **Guarino, M.** 2007. Epithelial-mesenchymal transition and tumour invasion. *Int J Biochem Cell Biol* **39**:2153-2160.
20. **Harada, H., K. Iwatsuki, M. Ohtsuka, G. W. Han, and F. Kaneko.** 1996. Abnormal desmoglein expression by squamous cell carcinoma cells. *Acta Derm Venereol* **76**:417-420.
21. **Hemminki, O., I. Diaconu, V. Cerullo, S. K. Pesonen, A. Kanerva, T. Joensuu, K. Kairemo, L. Laasonen, K. Partanen, L. Kangasniemi, A. Lieber, S. Pesonen, and A. Hemminki.** 2012. Ad3-hTERT-E1A, a Fully Serotype 3 Oncolytic Adenovirus, in Patients With Chemotherapy Refractory Cancer. *Mol Ther* **20**:1821-1830.
22. **Huang, S. K., P. R. Stauffer, K. Hong, J. W. Guo, T. L. Phillips, A. Huang, and D. Papahadjopoulos.** 1994. Liposomes and hyperthermia in mice: increased tumor uptake and therapeutic efficacy of doxorubicin in sterically stabilized liposomes. *Cancer Res* **54**:2186-2191.
23. **Johnston, S. R., and M. E. Gore.** 2001. Caelyx: phase II studies in ovarian cancer. *Eur J Cancer* **37 Suppl** 9:S8-14.
24. **Kim, K. H., I. Dmitriev, J. P. O'Malley, M. Wang, S. Saddekni, Z. You, M. A. Preuss, R. D. Harris, R. Aurigemma, G. P. Siegal, K. R. Zinn, D. T. Curiel, and R. D. Alvarez.** 2012. A phase I clinical trial of Ad5.SSTR/TK.RGD, a novel infectivity-enhanced bicistronic adenovirus, in patients with recurrent gynecologic cancer. *Clin Cancer Res* **18**:3440-3451.
25. **Kirpotin, D. B., D. C. Drummond, Y. Shao, M. R. Shalaby, K. Hong, U. B. Nielsen, J. D. Marks, C. C. Benz, and J. W. Park.** 2006. Antibody targeting of long-circulating lipidic nanoparticles does not increase tumor localization but does increase internalization in animal models. *Cancer Res* **66**:6732-6740.
26. **Koski, A., L. Kangasniemi, S. Escutenaire, S. Pesonen, V. Cerullo, I. Diaconu, P. Nokisalmi, M. Raki, M. Rajecki, K. Guse, T. Ranki, M. Oksanen, S. L. Holm, E. Haavisto, A. Karioja-Kallio, L. Laasonen, K. Partanen, M. Ugolini, A. Helminen, E. Karli, P. Hannuksela, T. Joensuu, A. Kanerva, and A. Hemminki.** 2010. Treatment of cancer patients with a serotype 5/3 chimeric oncolytic adenovirus expressing GMCSF. *Mol Ther* **18**:1874-1884.
27. **Lavin, S. R., T. J. McWhorter, and W. H. Karasov.** 2007. Mechanistic bases for differences in passive absorption. *J Exp Biol* **210**:2754-2764.
28. **Lee, C. M., and I. F. Tannock.** 2010. The distribution of the therapeutic monoclonal antibodies cetuximab and trastuzumab within solid tumors. *BMC Cancer* **10**:255.
29. **Lipinski, C. A., F. Lombardo, B. W. Dominy, and P. J. Feeney.** 2001. Experimental and computational approaches to estimate solubility and permeability in drug discovery and development settings. *Adv Drug Deliv Rev* **46**:3-26.
30. **Lu, Z. Z., H. Wang, Y. Zhang, H. Cao, Z. Li, P. Fender, and A. Lieber.** 2013. Penton-Dodecahedral Particles Trigger Opening of Intercellular Junctions and Facilitate Viral Spread during Adenovirus Serotype 3 Infection of Epithelial Cells. *PLoS Pathog* **9**:e1003718.
31. **Markman, M., A. Kennedy, K. Webster, G. Peterson, B. Kulp, and J. Belinson.** 2000. Phase 2 trial of liposomal doxorubicin (40 mg/m<sup>2</sup>) in platinum/paclitaxel-refractory ovarian and fallopian tube cancers and primary carcinoma of the peritoneum. *Gynecol Oncol* **78**:369-372.
32. **Minchinton, A. I., and I. F. Tannock.** 2006. Drug penetration in solid tumours. *Nat Rev Cancer* **6**:583-592.
33. **Muggia, F. M., J. D. Hainsworth, S. Jeffers, P. Miller, S. Groshen, M. Tan, L. Roman, B. Uziely, L. Muderspach, A. Garcia, A. Burnett, F. A. Greco, C. P. Morrow, L. J. Paradiso, and L. J. Liang.** 1997. Phase II study of liposomal doxorubicin in refractory ovarian cancer: antitumor activity and toxicity modification by liposomal encapsulation. *J Clin Oncol* **15**:987-993.
34. **O'Quigley, J., M. Pepe, and L. Fisher.** 1990. Continual reassessment method: a practical design for phase 1 clinical trials in cancer. *Biometrics* **46**:33-48.
35. **Oliveras-Ferraros, C., A. Vazquez-Martin, S. Cufi, B. Queralt, L. Baez, R. Guardeno, X. Hernandez-Yague, B. Martin-Castillo, J. Brunet, and J. A. Menendez.** 2011. Stem cell property epithelial-to-mesenchymal transition is a core transcriptional network for predicting cetuximab (Erbix) efficacy in KRAS wild-type tumor cells. *J Cell Biochem* **112**:10-29.

36. **Park, K. H., E. Gad, V. Goodell, Y. Dang, T. Wild, D. Higgins, P. Fintak, J. Childs, C. Dela Rosa, and M. L. Disis.** 2008. Insulin-like growth factor-binding protein-2 is a target for the immunomodulation of breast cancer. *Cancer Res* **68**:8400-8409.
37. **Pecot, C. V., F. Z. Bischoff, J. A. Mayer, K. L. Wong, T. Pham, J. Bottsford-Miller, R. L. Stone, Y. G. Lin, P. Jaladurgam, J. W. Roh, B. W. Goodman, W. M. Merritt, T. J. Pircher, S. D. Mikolajczyk, A. M. Nick, J. Celestino, C. Eng, L. M. Ellis, M. T. Deavers, and A. K. Sood.** 2011. A novel platform for detection of CK+ and CK- CTCs. *Cancer Discov* **1**:580-586.
38. **Perets, R., G. A. Wyant, K. W. Muto, J. G. Bijron, B. B. Poole, K. T. Chin, J. Y. Chen, A. W. Ohman, C. D. Stepule, S. Kwak, A. M. Karst, M. S. Hirsch, S. R. Setlur, C. P. Crum, D. M. Dinulescu, and R. Drapkin.** 2013. Transformation of the fallopian tube secretory epithelium leads to high-grade serous ovarian cancer in Brca;Tp53;Pten models. *Cancer Cell* **24**:751-765.
39. **Persson, J., I. Beyer, R. Yumul, Z. Li, H. P. Kiem, S. Roffler, and A. Lieber.** 2011. Immuno-therapy with anti-CTLA4 antibodies in tolerized and non-tolerized mouse tumor models. *PLoS One* **6**:e22303.
40. **Pesonen, S., P. Nokisalmi, S. Escutenaire, M. Sarkioja, M. Raki, V. Cerullo, L. Kangasniemi, L. Laasonen, C. Ribacka, K. Guse, E. Haavisto, M. Oksanen, M. Rajecki, A. Helminen, A. Ristimaki, A. Karioja-Kallio, E. Karli, T. Kantola, G. Bauerschmitz, A. Kanerva, T. Joensuu, and A. Hemminki.** 2010. Prolonged systemic circulation of chimeric oncolytic adenovirus Ad5/3-Cox2L-D24 in patients with metastatic and refractory solid tumors. *Gene Ther* **17**:892-904.
41. **Pignata, S., G. Scambia, G. Ferrandina, A. Savarese, R. Sorio, E. Breda, V. Gebbia, P. Musso, L. Frigerio, P. Del Medico, A. V. Lombardi, A. Febbraro, P. Scollo, A. Ferro, S. Tamberi, A. Brandes, A. Ravaoli, M. R. Valerio, E. Aitini, D. Natale, L. Scaltriti, S. Greggi, C. Pisano, D. Lorusso, V. Salutati, F. Legge, M. Di Maio, A. Morabito, C. Gallo, and F. Perrone.** 2011. Carboplatin plus paclitaxel versus carboplatin plus pegylated liposomal doxorubicin as first-line treatment for patients with ovarian cancer: the MITO-2 randomized phase III trial. *J Clin Oncol* **29**:3628-3635.
42. **Poveda, A., S. B. Kaye, R. McCormack, S. Wang, T. Parekh, D. Ricci, C. A. Lebedinsky, J. C. Tercero, P. Zintl, and B. J. Monk.** 2011. Circulating tumor cells predict progression free survival and overall survival in patients with relapsed/recurrent advanced ovarian cancer. *Gynecol Oncol* **122**:567-572.
43. **Rose, P. G., J. H. Maxson, N. Fusco, K. Mossbrugger, and M. Rodriguez.** 2001. Liposomal doxorubicin in ovarian, peritoneal, and tubal carcinoma: a retrospective comparative study of single-agent dosages. *Gynecol Oncol* **82**:323-328.
44. **Strauss, R., Z. Y. Li, Y. Liu, I. Beyer, J. Persson, P. Sova, T. Moller, S. Pesonen, A. Hemminki, P. Hamerlik, C. Drescher, N. Urban, J. Bartek, and A. Lieber.** 2011. Analysis of epithelial and mesenchymal markers in ovarian cancer reveals phenotypic heterogeneity and plasticity. *PLoS One* **6**:e16186.
45. **Tannock, I. F., C. M. Lee, J. K. Tunggal, D. S. Cowan, and M. J. Egorin.** 2002. Limited penetration of anticancer drugs through tumor tissue: a potential cause of resistance of solid tumors to chemotherapy. *Clin Cancer Res* **8**:878-884.
46. **Thomas, M. A., J. F. Spencer, K. Toth, J. E. Sagartz, N. J. Phillips, and W. S. Wold.** 2008. Immunosuppression enhances oncolytic adenovirus replication and antitumor efficacy in the Syrian hamster model. *Mol Ther* **16**:1665-1673.
47. **Turley, E. A., M. Veiseh, D. C. Radisky, and M. J. Bissell.** 2008. Mechanisms of Disease: epithelial-mesenchymal transition-does cellular plasticity fuel neoplastic progression? *Nature clinical practice*.
48. **Tuve, S., B. M. Chen, Y. Liu, T. L. Cheng, P. Toure, P. S. Sow, Q. Feng, N. Kiviat, R. Strauss, S. Ni, Z. Y. Li, S. R. Roffler, and A. Lieber.** 2007. Combination of tumor site-located CTL-associated antigen-4 blockade and systemic regulatory T-cell depletion induces tumor-destructive immune responses. *Cancer Res* **67**:5929-5939.
49. **Tuve, S., Y. Liu, K. Tragoolpua, J. D. Jacobs, R. C. Yumul, Z. Y. Li, R. Strauss, K. E. Hellstrom, M. L. Disis, S. Roffler, and A. Lieber.** 2009. In situ adenovirus vaccination engages T effector cells against cancer. *Vaccine* **27**:4225-4239.
50. **Wang, H., I. Beyer, J. Persson, H. Song, Z. Li, M. Richter, H. Cao, R. van Rensburg, X. Yao, K. Hudkins, R. Yumul, X. B. Zhang, M. Yu, P. Fender, A. Hemminki, and A. Lieber.** 2012. A new human DSG2-transgenic mouse model for studying the tropism and pathology of human adenoviruses. *J Virol* **86**:6286-6302.

51. **Wang, H., Z. Li, R. Yumul, S. Lara, A. Hemminki, P. Fender, and A. Lieber.** 2011. Multimerization of adenovirus serotype 3 fiber knob domains is required for efficient binding of virus to desmoglein 2 and subsequent opening of epithelial junctions. *J Virol* **85**:6390-6402.
52. **Wang, H., Z. Y. Li, Y. Liu, J. Persson, I. Beyer, T. Moller, D. Koyuncu, M. R. Drescher, R. Strauss, X. B. Zhang, J. K. Wahl, 3rd, N. Urban, C. Drescher, A. Hemminki, P. Fender, and A. Lieber.** 2011. Desmoglein 2 is a receptor for adenovirus serotypes 3, 7, 11 and 14. *Nat Med* **17**:96-104.
53. **Yang, Z., M. Horn, J. Wang, D. D. Shen, and R. J. Ho.** 2004. Development and characterization of a recombinant madin-darby canine kidney cell line that expresses rat multidrug resistance-associated protein 1 (rMRP1). *AAPS J* **6**:77-85.
54. **Yuan, F., M. Leunig, S. K. Huang, D. A. Berk, D. Papahadjopoulos, and R. K. Jain.** 1994. Microvascular permeability and interstitial penetration of sterically stabilized (stealth) liposomes in a human tumor xenograft. *Cancer Res* **54**:3352-3356.
55. **Zeng, Y., M. Pinard, J. Jaime, L. Bourget, P. Uyen Le, M. D. O'Connor-McCourt, R. Gilbert, and B. Massie.** 2008. A ligand-pseudoreceptor system based on de novo designed peptides for the generation of adenoviral vectors with altered tropism. *J Gene Med* **10**:355-367.



André M. Lieber, M.D., Ph.D  
Professor of Medicine, Adjunct Professor of Pathology  
University of Washington  
Box 357720  
Seattle, WA 98195

August 26, 2014

Dear Dr. Lieber,

This letter is in support of your SPORC grant titled "A Combination Therapy of JO and PEGylated Liposomal Doxorubicin in Ovarian Cancer Patients." BRIM is enthusiastic in working with you to further co-develop the JO recombinant protein series, as is demonstrated by the co-development agreement that was signed recently. BRIM is willing to provide financial support of up to \$1,000,000 to help with translating this work from the pre-clinical stage to clinical studies. This funding can help towards completing the requisite studies necessary through outsourced partners for producing cGMP material, conducting GLP toxicology studies, and the future clinical trial.

BRIM is a virtual drug development company established in 2013 with expertise in translational medicine. With a seasoned team having over 200 combined years of experience in the pharmaceutical industry in small and large molecules, BRIM brings a wealth of knowledge in various areas that are important in drug development, including discovery research, preclinical and clinical DMPK, biomarkers, toxicology and pathology, immune response, CMC, and statistics. BRIM is committed to working with you in bringing this research to the clinic and is excited to be moving this work forward.

We look forward to a successful partnership with you and wish you continued success.

Sincerely,

A handwritten signature in dark ink, appearing to read "Haishan Jang", is written over a horizontal line.

Haishan Jang, Ph. D., MBA  
Chief Executive Officer  
BRIM Biotechnology, Inc.

**BRIM Biotechnology, Inc.**

2F, No.36, Yuanqu St., Nan Gang Dist., Taipei 11560  
TEL: +886-2-2788-8090 FAX: +886-2-2788-6259





25 August, 2014

André M. Lieber, M.D., Ph.D.  
 Professor of Medicine, Adjunct Professor of  
 Pathology  
 University of Washington  
 K-240B Health Sciences Building  
 Medical Genetics, Box 357720  
 Seattle, WA 98195-7720  
 E-mail: [lieber00@u.washington.edu](mailto:lieber00@u.washington.edu)

BASi EVANSVILLE  
 10424 MIDDLE MT. VERNON RD  
 MT. VERNON, IN 47620 USA

812-985-3400, EXT. 1102  
 812-985-3403 (FAX)  
 JDEVINE@BASINC.COM

Dear André:

I have provided an informal cost estimate for the repeat dose studies in mice and monkeys. As time permits, please review the proposal and return any questions or comments. Once I receive your feedback, I can prepare formal cost estimates.

### **GENERAL TOXICOLOGY STUDIES**

<b>Description of Preclinical Toxicology Fees</b>	<b>Quantity</b>	<b>Subtotal</b>
GLP 16-Week IV Toxicity Study in DSG2 transgenic mice	1	170,500
GLP 16-Week IV Toxicity Study in Cynomolgus Monkeys	1	335,750

#### **GLP 16-Week IV Toxicity Study in DSG2 transgenic mice**

- This study will be designed to conform to the FDA Good Laboratory Practice for Nonclinical Studies regulations (CFR 21 Part 58).
- DSG2 transgenic mice will have DSG2 expressing tumors derived from the ID8 cells, a spontaneously transformed mouse ovarian surface epithelial cell (25, 35) – supplied by sponsor
- 10/sex/group main study animals (80 main study animals). An additional 5/sex/group will be assigned to the control and high-dose for recovery (20 recovery animals) and 9/sex/group will be assigned to Groups 2-4 for TK collections.
- Physical examinations, including ophthalmology, will be performed by a qualified veterinarian on all study animals prior to initiation and on all main study animals prior to their respective necropsy.

- Clinical observations will be performed at least twice-daily for main study animals during the dosing phase. Mortality observations will be performed twice daily for toxicokinetic study animals
- Body weights will be recorded once prior to treatment and weekly thereafter. Terminal body weights will be recorded for main study animals prior to necropsy following an overnight fast.
- Dosing solutions will be prepared once prior to study initiation, homogeneity assays (suspensions) and entrance assays will be performed on each dose level prior to its use. Samples will be collected and sent to a lab of the sponsor's choice for analysis. **(Cost of sample analysis not included)**
- Blood samples from the systemic exposure group will be collected from 3/rats/sex/group in Groups 2-4 only, on Days 1 and 28, at 6 time points. The samples will be spun down, the plasma separated, frozen and shipped to a lab of the sponsor's choice for analysis (N=216). **(Cost of sample analysis not included)**
- Terminal blood samples (hematology, serum chemistry, coagulation), will be collected from main study animals at their respective necropsy. At unscheduled necropsies of moribund animals, blood samples will be collected prior to euthanasia, when possible. BASi Evansville personnel will conduct the clinical pathology analyses.
- Following 4 cycles of dosing (1 time every four weeks for 16 weeks), all main study mice will be euthanized with carbon dioxide inhalation, exsanguinated and a gross necropsy performed. The remaining animals will be euthanized following a 4 week recovery period. A standard list of tissues will be collected and preserved in 10% NBF.
- All collected tissues from Groups 1 and 4, tissues from animals that die early, and any gross lesions will be embedded in paraffin, processed into blocks, sectioned, and stained. All slides from Group 1 & 4, slides from unscheduled deaths, and all gross lesions will be examined by a veterinary pathologist (ACVP). Target organs will be read in low and intermediate groups once identified and upon consultation with pathologist, study director and study monitor.
- An audited draft of the final report will be available 12 weeks following the final necropsy.
- The final report will be available 4 weeks after receipt of the sponsors edits to the audited draft and the applicable formulation analysis and TK reports generated from outside contract labs.

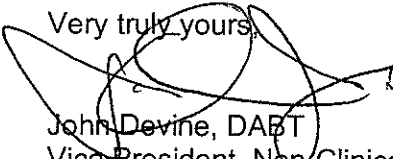
#### **GLP 16-Week IV Toxicity Study in Cynomolgus Monkeys**

- This study will be designed to conform to the FDA Good Laboratory Practice for Nonclinical Studies regulations (CFR 21 Part 58).

- The main study will consist of three dose groups and a control group of 3/sex/group in the main study and 2/sex/group in the control and high dose groups for recovery. Naïve cynomolgus monkeys (2-3 kgs), 30 days acclimation. N=32
- Blood samples will be collected from all treated animals (no controls) at each of 6 time points on days 1 and 28. Samples will be spun down, the plasma separated, frozen and shipped to the sponsor for analyses. N=384 plasma samples. **(Cost of sample analysis not included)**
- Dosing solutions will be prepared once prior to study initiation, homogeneity assays (suspensions) and entrance assays will be performed on each dose level prior to its use. Samples will be collected and sent to a lab of the sponsor's choice for analysis. **(Cost of sample analysis not included)**
- Food and water will be available *ad libitum*
- Body weight weekly
- Feed consumption daily
- Clinical observations twice-daily.
- Ophthalmology on all study animals prior to initiation and near the end of the dosing and recovery phase.
- ECGs recorded for all study animals prior to initiation and near the end of the dosing and recovery phases. N = 72 ECGs
- Hematology, serum chemistry, and coags pretest and near the end of the dosing and recovery phases. N=72 sets of each. BASi Evansville personnel will conduct the clinical pathology analyses.
- Following 4 cycles of dosing (1 time every four weeks for 16 weeks), the first 3 monkeys/sex/group will be euthanized with sodium pentobarbital, exsanguinated and a gross necropsy performed. The remaining monkeys will be euthanized following a 4 week recovery period. A standard list of tissues (~ 66/animal) will be collected and preserved in 10% NBF. N=2112 tissues.
- Tissues to be weighed include adrenals, brain, epididymides, heart, kidneys, liver, lungs, ovaries, spleen, thyroid/parathyroid, testes and uterus.
- All collected tissues will be trimmed, embedded in paraffin, sectioned, slides prepared and examined by a veterinary pathologist (ACVP). N=2112 tissues for examination.
- An audited draft of the final report will be available 12 weeks following the final necropsy.
- The final report will be available 4 weeks after receipt of the sponsors edits to the audited draft and the applicable formulation analysis and TK reports generated from outside contract labs.

I would like to thank you for considering BASi as your CRO partner for development of new drug candidate. If you have any questions, please do not hesitate to call me.

Very truly yours,

  
John Devine, DABT  
Vice President, Non-Clinical Services  
BASi Evansville



730 Daedeok-daero, Yuseong-gu, Daejeon, 305-717, Korea

Tel: +82-42-865-8020 Fax: +82-42-865-8499

August 29<sup>th</sup>, 2014

Andre M. Lieber, M.D., Ph.D.  
Professor of Medicine, Adjunct Professor of Pathology  
University of Washington  
K-240B Health Sciences Building  
Medical Genetics Box 357720  
Seattle, WA 98195-7720  
USA

Dear Professor Lieber,

We are excited to continue our work with you on your JO-4/OPUS therapeutic project as an adjunct therapy for cancer. Initial studies performed by us indicated that OPUS can increase the therapy of Samyang's chemotherapy drug platform.

Samyang pledges to continue to support your important ovarian cancer research. We will conduct additional tests with various formulation of OPUS to further evaluate its efficacy in improving our chemotherapeutic drug platform. Upon receipt of results acceptable to us, Samyang plans to license the JO-technology to be used in combination with Samyang's nanoparticle platform.

We wish you continued success in your research endeavors and look forward to productive future collaborations with you.

Yours sincerely

A handwritten signature in dark ink, appearing to read "Minhyo Seo", with a long horizontal stroke extending to the right.

Minhyo Seo  
Vice President  
Samyang Biopharmaceuticals Corporation



## UNIVERSITY OF WASHINGTON SCHOOL OF MEDICINE



*Department of  
Comparative Medicine*

T-142 Health Sciences Center  
Box 357190  
Seattle, WA 98195-7190  
Phone: 206-543-8047  
Fax: 206-685-3006

August 25, 2014

Andre Lieber, M.D., Ph.D.  
Professor  
Division of Medical Genetics  
University of Washington  
Seattle, WA 98195

Dear Andre,

I have read your Ovarian Cancer SPORE proposal entitled "A combination therapy of JO-1 and PEGylated liposomal doxorubicin in ovarian cancer patients". I would be pleased to collaborate with you on this proposal. In particular I will be able to assist you with the planning and performance of studies focused on selecting a safe dose of your therapeutics.

I have extensive experience in the planning and implementation of pre-clinical studies to support human clinical trials so I'm familiar with developing relevant biomarkers of injury/toxicity. In this regard I have contributed to several IND applications involving cancer therapeutics, including gene-based therapeutics, and I am familiar with the spectrum of pre-clinical studies and the process necessary to support clinical trials. Please let me know when you need assistance.

Sincerely,

A handwritten signature in cursive script, appearing to read "Denny Liggitt".

Denny Liggitt, DVM, PhD, DACVP  
Professor and Chair  
Department of Comparative Medicine  
School of Medicine

University of Washington



**UNIVERSITY OF WASHINGTON  
SCHOOL OF MEDICINE**  
Division of Medical Genetics, Department of Medicine  
University of Washington Medical Center  
Mailstop 357720 ♦ Seattle, WA 98195-7720  
Phone: 206-221-3974 ♦ Fax: 206-543-3050 ♦ Email: pair@uw.edu

**Gail Pairitz Jarvik, MD, PhD  
The Arno G. Motulsky Endowed Chair in Medicine  
Professor and Head, Division of Medical Genetics**

August 27, 2014

Andre Lieber, MD, PhD  
Professor  
Division of Medical Genetics, Adjunct Pathology  
University of Washington School of Medicine  
Box 357720  
K 240B Health Sciences  
Seattle, WA 98195

Dear Andre,

I am delighted to serve as a consultant on your Ovarian Cancer SPORE proposal  
*"Combination therapy of JO-1 and PEGylated liposomal doxorubicin in patients with ovarian cancer"*.

You can contact me in questions related to the statistical analysis of preclinical and clinical data.

I wish you the best of luck with your application.

Sincerely,

Gail P. Jarvik, M.D., Ph.D.  
The Arno G. Motulsky Chair Endowed in Medicine  
Professor and Head, Division of Medical Genetics



## **RESOURCE SHARING PLAN**

### **1. Data Sharing Plan**

Working as a team, comprising a single goal, we agree to adhere to all institutional, state and federal resource sharing guidelines and agree to share knowledge, research materials, and any other resources necessary and relevant in the particular focus of the grant, recognizing that final authorization will be cleared with all appropriate organizational parties. We will make all data gathered available to the public quickly and in an easy to interpret format, adhering to patient confidentiality regulations, provided that this does not conflict with our requirements.

This project will make available to the public results generated and any accompanying data that were supported by the NIH. The deliverables generated will be documented in an accessible form. Via a website and/or portal, we will join all project staff and representatives from the NCI into a cohesive team. We will be responsible for continuously updating the NCI to allow optimum transparency of our progress. This project team is committed to sharing results of data as soon as they are reportable through publication, conferences, and/or presentations so that new trials and research will be initiated based on our progress. The team will meet frequently, and at least monthly in a formal fashion to share progress results, accomplishments, pitfalls and progressive milestones.

### **2. Sharing Model Organisms**

N/A

### **3. Genome-Wide Association Studies (GWAS)**

N/A